Brookhaven National Laboratory

BNL-104771-2014-TECH

AGS/AD/Tech Note No. 355;BNL-104771-2014-IR

ANOTHER LOOK AT APERTURES IN THE AGS

P. Carolan

November 1991

Collider Accelerator Department

Brookhaven National Laboratory

U.S. Department of Energy

USDOE Office of Science (SC)

Notice: This technical note has been authored by employees of Brookhaven Science Associates, LLC under Contract No.DE-AC02-76CH00016 with the U.S. Department of Energy. The publisher by accepting the technical note for publication acknowledges that the United States Government retains a non-exclusive, paid-up, irrevocable, world-wide license to publish or reproduce the published form of this technical note, or allow others to do so, for United States Government purposes.

DISCLAIMER

This report was prepared as an account of work sponsored by an agency of the United States Government. Neither the United States Government nor any agency thereof, nor any of their employees, nor any of their contractors, subcontractors, or their employees, makes any warranty, express or implied, or assumes any legal liability or responsibility for the accuracy, completeness, or any third party's use or the results of such use of any information, apparatus, product, or process disclosed, or represents that its use would not infringe privately owned rights. Reference herein to any specific commercial product, process, or service by trade name, trademark, manufacturer, or otherwise, does not necessarily constitute or imply its endorsement, recommendation, or favoring by the United States Government or any agency thereof or its contractors or subcontractors. The views and opinions of authors expressed herein do not necessarily state or reflect those of the United States Government or any agency thereof.

Accelerator Division
Alternating Gradient Synchrotron Department
BROOKHAVEN NATIONAL LABORATORY
Upton, New York 11973

Accelerator Division
Technical Note

AGS/AD/Tech. Note No. 355

ANOTHER LOOK AT APERTURES IN THE AGS

P. Carolan, K.A. Brown, J. Zebuda, K.M. Brown

November 15, 1991

This note is a re-issue and update of TN #212 which described the maximum limiting horizontal and vertical apertures in the AGS. In TN #212 these apertures were determined with respect to a reference called the Beam Program Coordinate Axis. Since the issue of TN #212 E. Bleser, in TN #217, recommended the use of the Optimum Central Orbit (OCO) system in establishing the coordinates of all the ring devices. This note will define the various axes used in the AGS straight sections, and will determine the maximum limiting horizontal apertures with respect to the OCO axis for AGS devices. New horizontal and vertical maximum limiting apertures will be determined for the A10 Tune Meter (which has been modified), the IPM (which has been modified and moved), the E15 jump target,the C5 jump target, the F15 Current Transformer, the VHF Cavity, and the Booster Injection components (the L20 injection septum,A5 kicker and new vacuum chambers at A1,A2, and A3).

Defining the various axes

There are three main axes that comprise three distinct coordinate systems in the AGS straight sections. These three axes,the **Socket line**,the **Beam Program Coordinate line** and the **Optimium Central Orbit (OCO) line** are described by E. Bleser in TN #215,and 217. These descriptions will be reiterated here and references provided depicting the different axes in a typical 5 foot straight section. Two additional lines within a straight section will be described, the **Layout line** and the **Line Joining Vacuum Chamber Centerlines**.

In order to define the axes in a straight section, it is first necessary to define the *centerline of magnetic aperture* and the associated *magnet centerline*. Consider a cross-section of an AGS magnet taken in the vertical plane perpendicular to the long axis of the magnet (see figure 1 a or b). The *centerline of magnetic aperture* is a vertical line in this cross-section displaced a specified distance from an edge of the magnet iron. For a horizontally focussing magnet, the *centerline of magnetic aperture* is specified to be 5.25" from the inner edge (closest to the Ring center) of the magnet iron (see figure 1a). For a horizontally defocussing magnet, the specified distance is 7.25" from the inner edge of the magnet iron (see figure 1b). Note that the *centerline of magnetic aperture* is not at the physical center of the magnet pole tips (which is 6.25 " from either edge of a pole tip).

If this magnet cross-section is moved along the long magnet axis, the *centerline of magnetic aperture* will sweep out a vertical plane. The intersection of this vertical plane with the top surface of the magnet defines a horizontal line called the *magnet centerline* (see figure 1c). The *magnet centerline* is the starting point for the definitions given below. As an aside it is noted that in a main magnet the vacuum chamber is aligned such that the seam line of the chamber, which usually divides the

HORIZONTALLY FOCUSSING AGS MAGNET

HORIZONTALLY DE-FOCUSSING AGS MAGNET

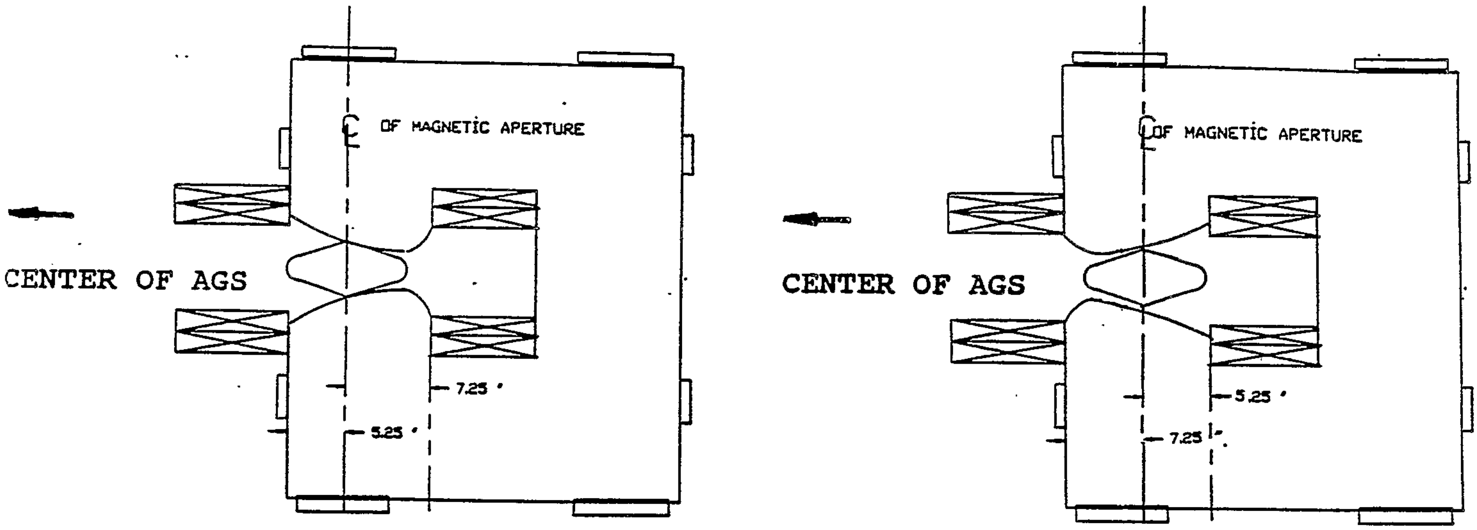

(a) (b)

Fig. 1

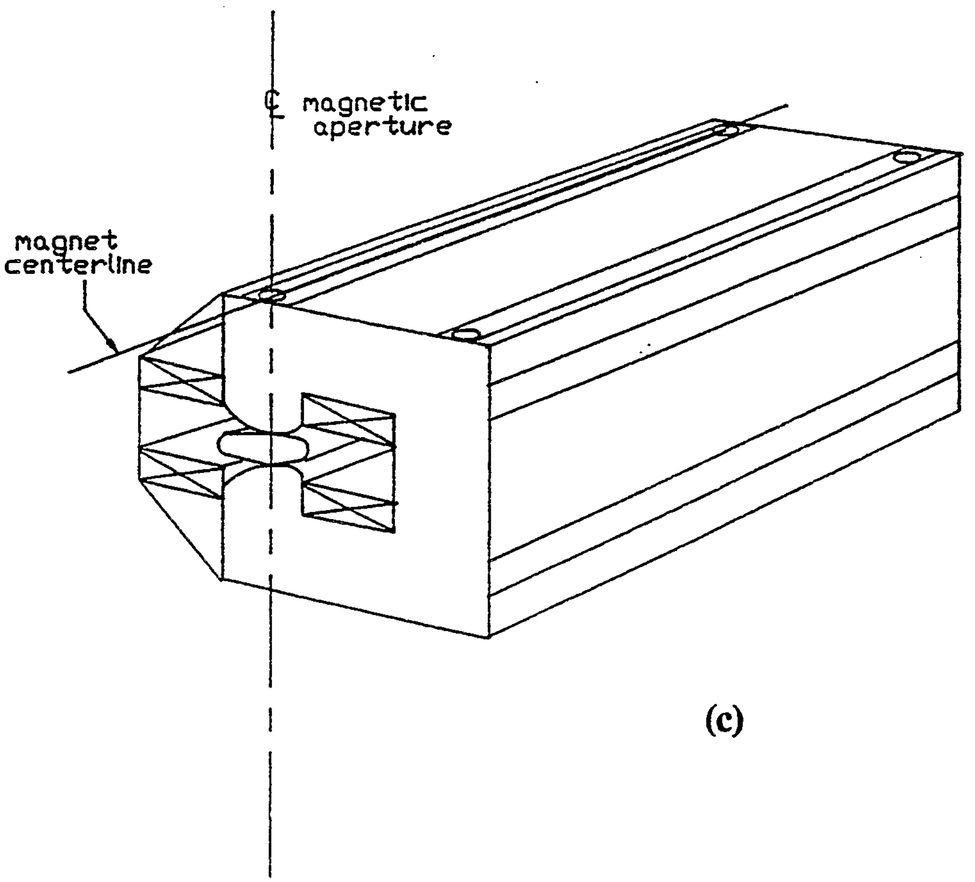

(c)

chamber into two symmetric halves, lies in the plane defined by the *centerline of magnetic aperture* and the *magnet centerline* (see figure 1).

The **Socket Axis** uses as reference points sockets located on top of each magnet, 3 " from either end of the magnet iron, along the magnet centerline (see figure 2). The socket axis of a straight section is the line joining the downstream socket of one magnet with the upstream socket of the next. This axis is used by surveyors to locate devices in straight sections.

The **Beam Program Coordinate Axis** uses as reference points the intersection of the magnet centerline with the edge of the magnet iron (see figure 2). The Beam Program Coordinate axis is the line connecting the points where the magnet centerlines of two successive magnets intersect the ends of the magnet iron. This axis is used in computer modelling programs.

The **OCO axis** is the axis along which an orbit at an appropriate momentum symmetrically traverses the main ring magnet vacuum chambers and makes optimal use of that aperture (see figure 3). This orbit has the characteristic that off-momentum orbits are symmetrically displaced from it. The OCO is the only axis here described along which an actual physical beam trajectory can occur and is displaced toward the center of the ring with respect to the other axes (see figure 2). The OCO was the subject of TN #217 and is also referred to as the **Theoretical Beam Center axis** or **R0**.

In addition to the three main axes above,figure 2 shows the **Layout axis**, which uses as reference points the intersection of the magnet centerline with the edge of the magnet fringe field. The magnet fringe field is defined to be along the magnet centerline at 2" from the end of the magnet iron. The Layout axis is the line connecting the points where the magnet centerlines of two successive magnets intersect the edges of the magnet fringe field. This axis was used to layout the AGS main magnets. In fig. 4, an additional line is shown and described as the **Line Joining Vacuum Chamber Centerlines.** This line uses as reference points the locations of the vacuum flanges where the main ring magnet vacuum chamber meets the straight section vacuum chamber. It is the line connecting these two points in a straight section.

Figure 4 shows the relative displacements of the Socket , Beam Program, OCO axes (and others) in a five foot straight section. All five foot straight sections are identical with respect to the relative locations of these axis within them. These various axes have different displacements in ten foot and two foot straight sections. This note is mainly concerned with the displacement between the Beam Program Coordinate (BPC) axis and the OCO axis in a given straight section. Table 1 gives the displacements for the different straight sections. These values for the displacements between the BPC axis and the OCO axis were established in ref. 4 (TN #217) and are taken from table A2 of that note.

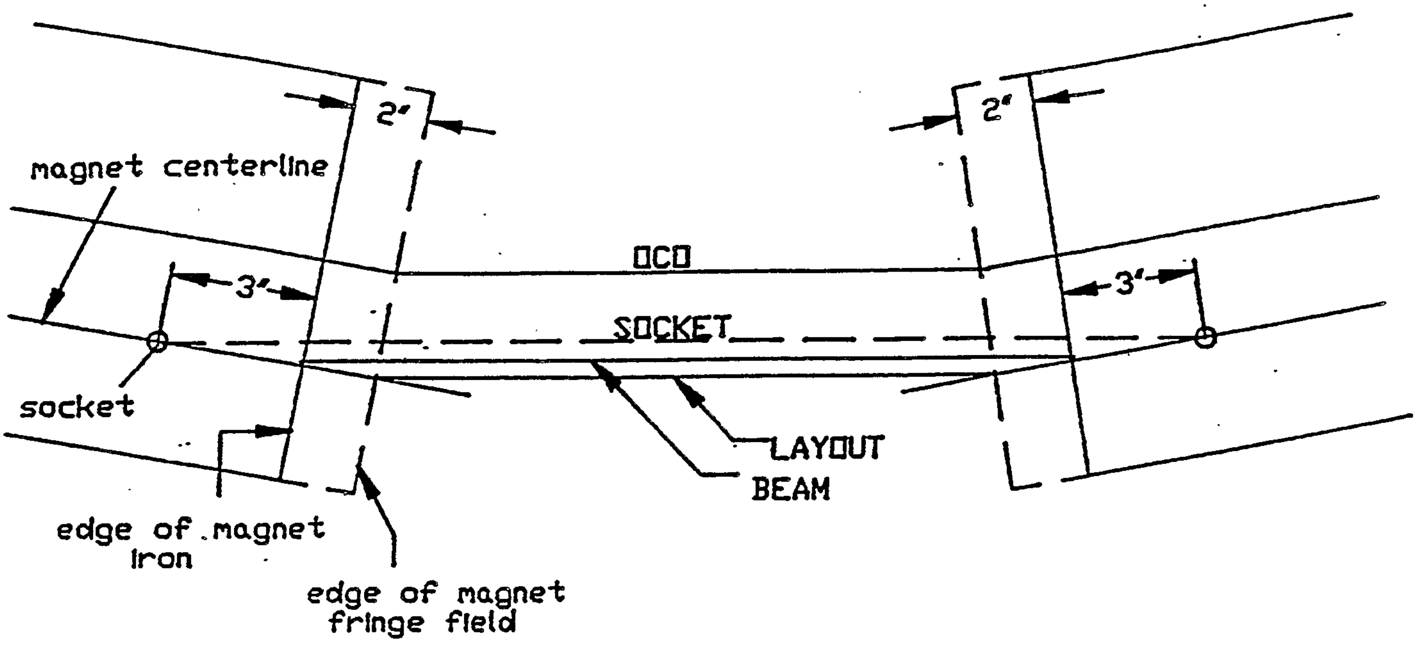
2"
2"
magnet centerline
OCO
3"
3"
SOCKET
socket
LAYOUT
BEAM
edge of magnet iron
edge of magnet fringe field

Fig. 2

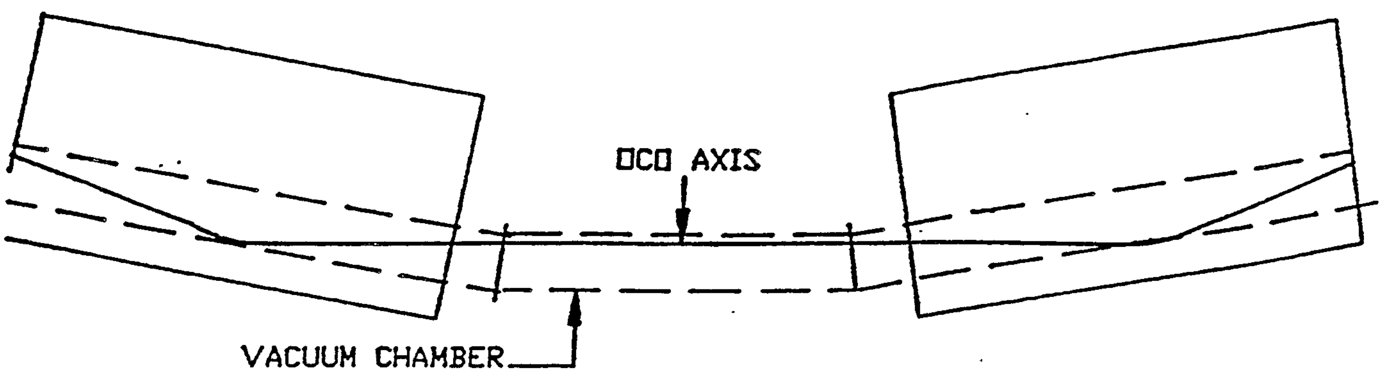
OCO AXIS
VACUUM CHAMBER

Fig. 3

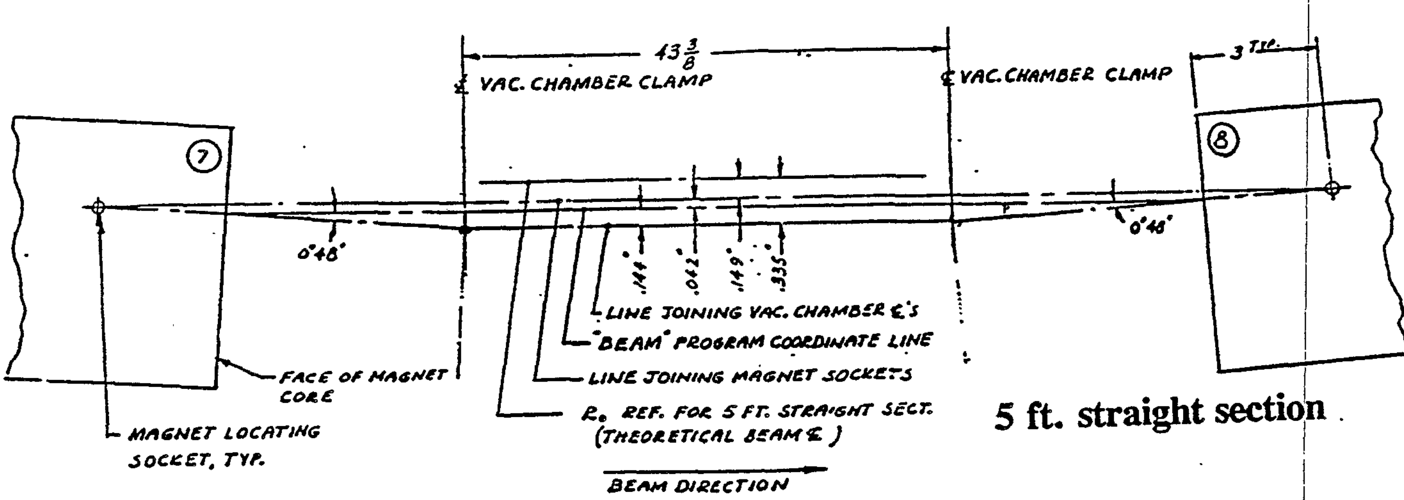

5 ft. straight section

Fig. 4

Table 1

Type of Straight Section	Displacment Between BPC Axis and OCO Axis (in.)
5 foot	.191
2 foot (between long magnets)	.191
10 foot	.131
2 foot (between short magnets)	.131

Effective and Limiting Apertures in the AGS

The physical aperture introduced by a device in a straight section can be considered with respect to different axes. TN # 212 used the convention shown below on the left. The direction in which the beam is travelling is into the paper. The direction to the center of the AGS is to the left of the page. The OCO is thought to be a desirable reference axis since it represents the path of an ideal beam orbit and thus this note uses the different convention shown below on the right to determine the inner and outer dimensions of the physical apertures.

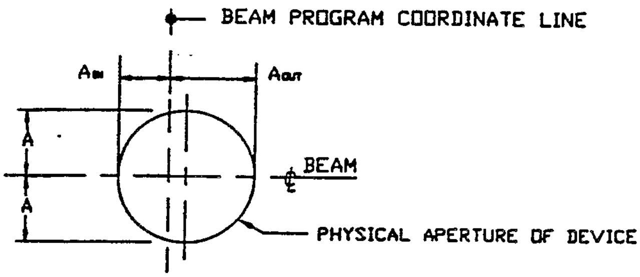

convention used in TN #212

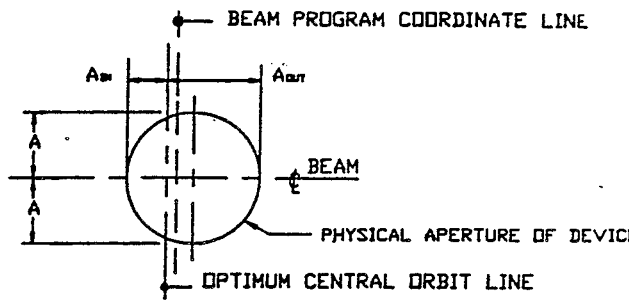

convention used here

The values for the displacements between the BPC axis and the OCO axis used to calculate new aperture data are taken from Table 1 of this note in most cases (see section on Errors and Uncertainty for noted exceptions).

Aside from coordinate system, when considering apertures in a synchrotron the beam size and its variation is important. In particular, for the AGS, the relative beam size is described by the Courant-Snyder Amplitude, or ß, function (shown in figure 5). The beam size at any point along its trajectory is proportional to the value of $\beta^{1/2}$ at that point. In considering apertures, then, it can be useful to define a quantity that is the physical aperture normalized to the size of the beam (or equivalently to the value of $\beta^{1/2}$ at the location of the aperture). This quantity can be defined so that the physical aperture, A, is normalized to $\beta^{1/2}$ in such a way that at a β_{max} (where beam size will be maximum) the quantity is equal to the physical aperture. If this quantity is called A_L then:

$$A_L \equiv A\sqrt{\frac{\beta_{max}}{\beta}}$$

where ß and β_{max} are taken from E.D. Courant's Internal Report EDC-28, "Precision Computation of AGS Orbit Parameters" (see also figure 5).

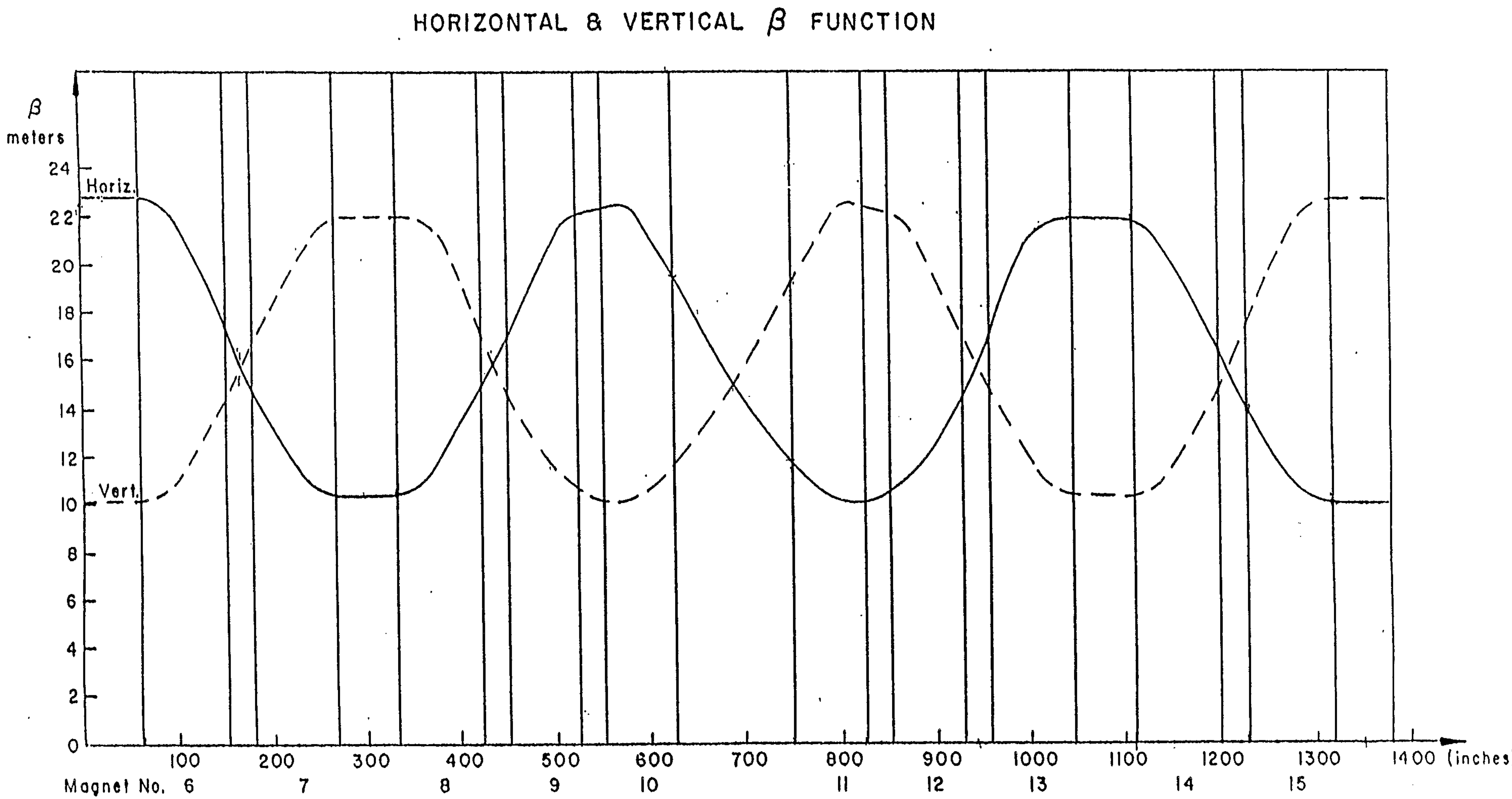
HORIZONTAL & VERTICAL β FUNCTION
β
meters
24
22
20
18
16
14
12
10
8
6
4
2
0
Horiz.
Vert.
100
200
300
400
500
600
700
800
900
1000
1100
1200
1300
1400 (inches)
Magnet No. 6
7
8
9
10
11
12
13
14
15

Fig. 5

In TN #212 this quantity, A_L, is referred to as "the maximum limiting aperture as seen by the beam" but here will be called the *effective aperture*. The notation is retained with the "L" subscript here signifying that this quantity takes on a particular value of interest when it denotes the *limiting aperture* in the AGS. The term *limiting aperture* as used here is not the same as the term maximum limiting aperture used in TN #212. The term maximum limiting aperture, as used in TN #212, refers to the minimum *effective aperture* introduced by a particular device. The *limiting aperture* is the physical aperture whose normalized (or effective) aperture is the minimum value of A_L for all devices considered. There is a limiting aperture in the horizontal and the vertical plane. It is the physical aperture that will, when encountered by a beam of sufficient size following the OCO trajectory, constrict the beam first - before any other aperture. If the beam always stayed on the OCO, then a complete discussion of limiting apertures would consist of determining the limiting (horizontal and vertical) apertures and listing where they occur around the ring (which could be one location or many, depending upon whether one device or a set of devices is producing the given limiting aperture).

Of course the beam does deviate from the OCO and this reality complicates the situation sufficiently to require a table of all apertures. Furthermore, this deviation changes during the acceleration cycle making the limiting aperture *time dependent*. Magnet errors, harmonic correction of these, and low field bumps move the orbit off of the OCO early; bumps and radial shifts have the same effect late in the acceleration cycle.

The beam itself shrinks during acceleration due to adiabatic damping of the betatron oscillation amplitude. By the end of the acceleration cycle, the beam can shrink in size (at high intensity) by up to 84%. This fact tends to reduce concerns about aperture once injection and capture are accomplished unless the orbit is moved significantly from the OCO, which happens if a radial shift is applied (e.g. before transition or extraction) and/or if an orbit bump is applied (e.g. the 3/2 λ bumps). Note that most of these orbit distortions are in the horizontal plane. For these cases, an inspection of the effective apertures off of the OCO is necessary.

Nevertheless, it is very useful to have a listing of the "on OCO" (perfect orbit, perfect survey, no bumps) limiting apertures, which is the purpose of this note. It is desireable not to produce a physical aperture in the AGS whose effective aperture, A_L, is less than the value of the present "on OCO" limiting aperture (i.e. the present minimum value of A_L as calculated here).

When considering these "on OCO" effective apertures it is important to note the proximity in value of the different effective apertures. For example, Drawing # 2 shows the vertical effective apertures less than 2.50 " , with the E20 D/S aperture shown as the vertical limiting aperture. Within 20 mils there are the (A-L) ferrite quad apertures. The error in determining A_L (introduced by possible errors in the physical size of the aperture or positioning of the device as well as uncertainty in ß --see later section on errors) could well lead to a ± 20 mil error in the value of either the E20 or ferrite quad effective apertures, and the absolute determination of the limiting aperture is subject to these errors.

Values of ß

As noted above, EDC-28 provides values of ß at the entrance to a magnet (at the beginning edge of the fringe field --see figure 2), the end of a magnet (at the edge of the fringe field), and the center of a straight section. Since the release of TN #212 E. Auerbach, in TN #297, has compiled MAD generated values of ß. These values of ß were calculated for different AGS energies (see figure 6). As seen from figure 6, the value of ß varies with energy and for a given five-foot straight section can be from 0.5 - 1.5 % higher than the minimum value of ß in that straight section for an energy range of 15-29 Gev/c. In addition, the machine lattice itself and thus the ß-function may be intentionally distorted at different times during the acceleration cycle (e.g. during transition using the gamma - transition jump scheme).

The EDC-28 values of ß will be used in this note to maintain consistency with TN #212. Here, as in TN #212, the ß-function is assumed to be linear in a straight section. The physical aperture and the location of a device in a straight section is determined from the survey data. Using the linear estimation the value of ß at that location is determined. For devices that run along a significant portion of a straight section (such as the L20 injection septum) the values of ß at the upstream and downstream ends of the device are used to obtain values of A_L at each end of the device, since ß varies significantly across a 10 foot straight section.

Tn # 212 determined the effective apertures, A_L, according to the convention shown below left, while this note determines the effective apertures, A_L, according to the following different convention shown below right:

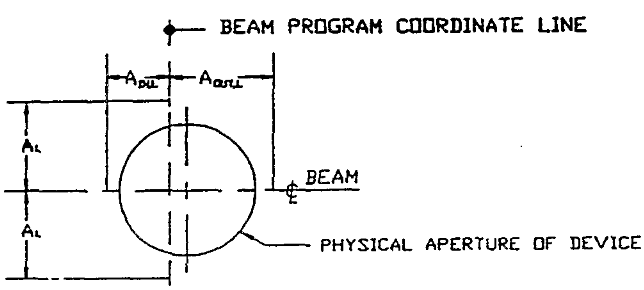

convention used in TN #212

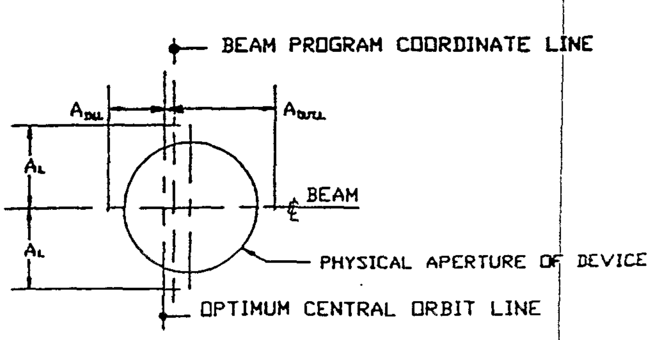

convention used here

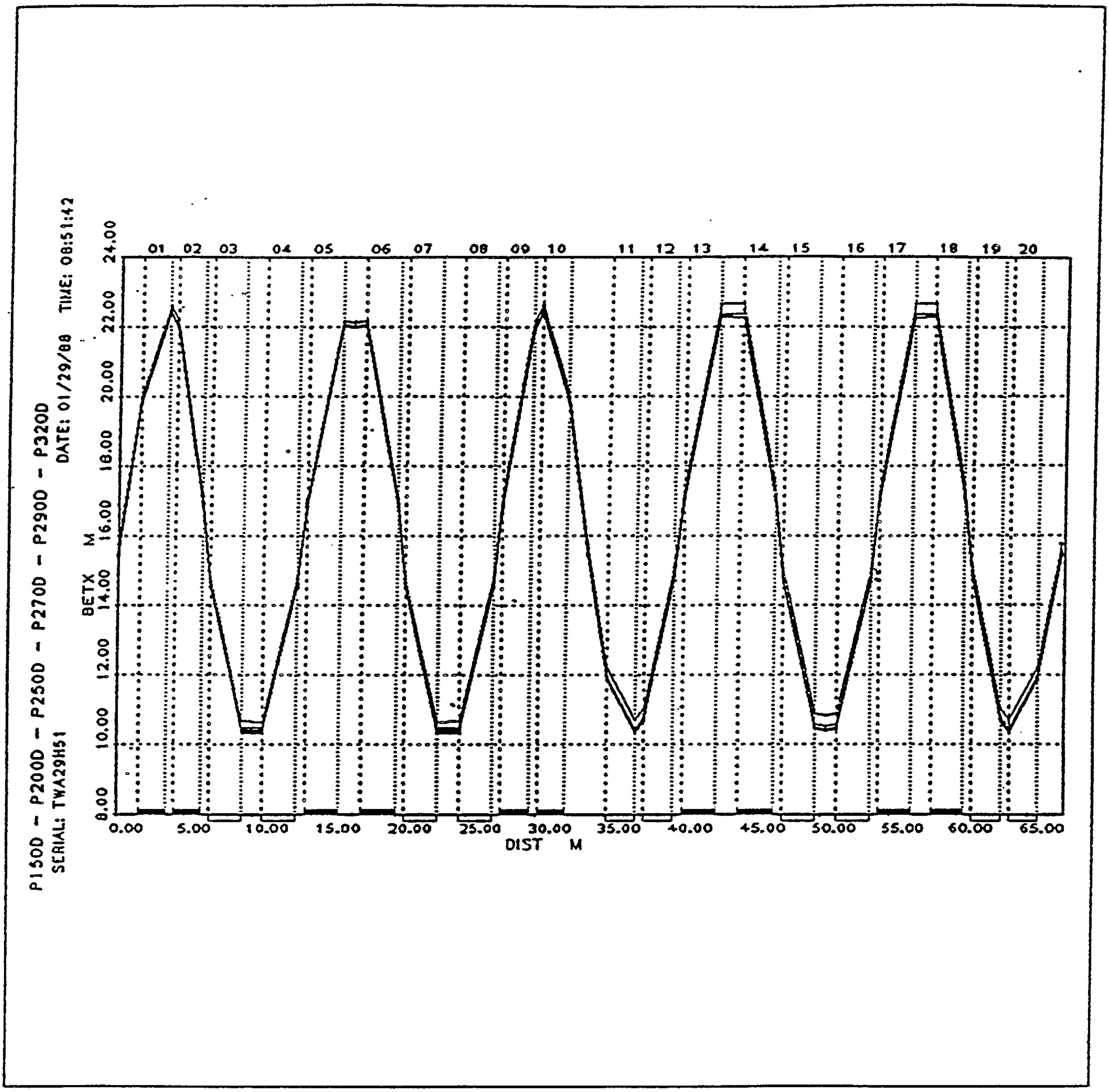

Courant-Snyder Parameter Beta-x (in meters) for the D.C. "Bare" Machine (main magnets only) at high fields: 15-32 GeV/c, given for one superperiod.

Fig. 6

Uncertainty and Errors in A_L

The equation for A_L is

$$A_L \equiv A\sqrt{\frac{\beta_{max}}{\beta}}$$

where A, again, is determined from the chamber size and chamber placement (with respect to R0) given on the survey drawings. It follows, using a standard deviation approach, that the dependence of the uncertainty in A_L on A (the physical aperture), β_{max} and β is given by:

$$\frac{\delta A_L}{A_L} = \left[\left(\frac{\delta A}{A}\right)^2 + \frac{1}{2}\left(\frac{\delta \beta_{max}}{\beta_{max}}\right)^2 + \frac{1}{2}\left(\frac{\delta \beta}{\beta}\right)^2\right]^{1/2}$$

An error in β_{max} will not affect the relative scaling when comparing different values of A_L. Roughly equal errors in $\delta A_L/A_L$ of about 1% would result from a 1/32" error in an aperture, A, with a value of 2.9 inches (inner or outer dimension) and a .1 m error in β (due to an error in determining the exact location of the aperture in a device, and thus the value of β at the aperture, due to using the linear estimation for β, or due to taking into account the variation of β with energy).

This uncertainty is going to vary depending on many parameters. For example, the main magnet vacuum chambers will have a large uncertainty for the following reasons:

1. When thay are positioned into place there is a likelihood (from PUE measurements) of as much as 1/8 of an inch uncertainty in their position.

2. They are measured while at atmospheric pressure. How much this changes while they are under vacuum is unknown.

3. The thickness of the walls of the chambers may vary considerably.

Therefore, for the vacuum chambers, this uncertainty could be on the order of 5%. On the other hand, many devices are surveyed in very precisely and constructed very precisely, and the uncertainty will then be less.

The extraction equipment (E5, H5, F5, F10, and H10) has been taken to be positioned in the normal operating position according to the blueprints. This is not the actual normal operating position. A valuable reference for finding the actual positions are the STORE data books in the Main Control Room.

All the device drawings show the minimum effective apertures, A_L, at the postion in the ring where the device is located. Exceptions are the drawings of the vacuum chambers. The drawing for a typical vacuum chamber (Drawing #50) shows the minimum effective apertures for the horizontal and vertical apertures, which do not lie in the same place in the ring. The drawings for A1, A2, and A3 vacuum chambers (Drawing #'s 7-9) show apertures that were determined as described in Appendix A.

The original aperture drawings for certain devices in ten foot straight sections (G10, I10, E20, F10, and H10) show the displacement between the BPC and the OCO to be .135 ". The value of .135 " appears as the separation between the BPC and the OCO on many AGS survey and device drawings, rather than the value of .131" established in ref. 4 of this note. Thus the value of .135 " was used to translate the aperture data from the BPC to the OCO in these cases.

Other devices may not be positioned as shown. This depends on how they were placed initially and then may have changed. An example is the E20 beam catcher which is a moveable device and whose vertical and horizontal apertures are changed when it is moved.

Tables and Drawings

Table 2 shows new values of A_L (for inner and outer dimensions) calculated with respect to the OCO for all of the horizontal apertures given. Table 3 shows values of A_L in the vertical plane, unchanged from TN #212. At the end of tables 2 & 3 are the values of A_L (calculated with respect to the OCO in the horizontal plane) for certain new or modified devices.

A Table of Contents has been added listing the drawings of the apertures by number. Drawings of apertures (beginning with Drawing #5) have been ordered to reflect as much as possible the order in which the particle beam would first encounter an aperture in the AGS. Drawings made to reflect data for the new or modified devices listed at the end of tables 2 & 3 are indicated in the Table of Contents. Drawings of the RF Cavity Upstream and Downstream Flange Apertures have been corrected to illustrate that they are centered on the OCO (R0) and not the centerline of the vacuum chamber. All other drawings attatched to this note were carried over unchanged from TN #212.

I (P.C.) would like to acknowledge the contribution of Paul Montanez, a summer student who initiated work on many of the new drawings.

References

1.Precision Computation of AGS Orbit Parameters, E.D. Courant, BNL Internal Report edc-28, December 4, 1958.

2.BNL Memorandum, "Devices in AGS Ring", from M. Zguris/K.A. Brown, November 13,1984.

3.Reference Drawings:
   i. AGS Component Layout, D05-m-1224-5.
   ii. AGS Vacuum System Typical 5 Ft. Straight Section, C-D95-M-864-2.

4. The Optimum Central Orbit in the AGS, E. Bleser, Acc. Div. Tech. Note # 217, July 22, 1985.

5. Where are the AGS Magnets ?, E. Bleser, Acc. Div. Tech. Note # 215, May 20, 1985.

6. Computer Models of the AGS, I: The D.C. "Bare" Machine at High Fields, E. Auerbach, Acc. Div. Tech Note # 297, March 7, 1988.

APPENDIX A .Notes on A1, A2 A3 Vacuum Chambers

Effective apertures relative to R0 were determined for the new A1, A2, A3 vacuum chambers. Because the vacuum chambers are not located in straight sections, the values of A_L for these chambers are subject to particular sources of uncertainty arising from the behavior of R0 and the β-function in regions that are not straight sections (i.e. regions within the main magnets). As figure 3 suggests, the OCO axis (R0) is curved within the vacuum chamber in the main magnet region. Also, as figure 3 and 4 show, the vacuum chamber is deflected a certain angle from the straight section at the connecting flange. Thus R0 within the vacuum chamber, in the region between the connecting flange and the face of the magnet, is not parallel to the edge of the vacuum chamber defining the aperture. These two realities lead to uncertainty in determining any absolute value for A, the physical aperture of the vacuum chamber relative to R0.

In addition , β in the main magnet region (and thus within the vacuum chamber) is not linear, as seen in figure 5. This leads to uncertainty in determining what β is at the loacation of the smallest physical aperture relative to R0 (which could lie within the main magnet region of the vacuum chamber).

Fortunately, and not suprisingly, even given these uncertainties, the horizontal apertures introduced by the A1, A2, or A3 vacuum chambers are not close to limiting apertures, and thus are not of general concern. For the purpose of Table 2, the values of β were taken at the fringe field points (magnet entrance or exit) for A1, A2, and A3 vacuum chambers, where β is assumed known, to minimize error in β. The physical aperture with respect to R0, A, was determined using the known seperation between R0 and the vacuum chamber seamline at the vacuum chamber clamp (flange).

Vertical effective apertures, A_L, for these vacuum chambers were determined at whichever end of the vacuum chamber where β_y is maximum.

Table 2

EFFECTIVE APERTURES WITH RESPECT TO R-0
THE OPTIMUM CENTRAL ORBIT (OCO) LINE

HORIZONTAL APERTURES

β_{max} = 22.745 ± 0.0005 meters

Devices	β ± 0.1 (meters)	A_{out} (in.)	A_{in} (in.)	$(\beta_{max}/\beta)^{1/2}$	$A_{out,L}$ (in.)	$A_{in,L}$ (in.)
B1 foil	21.9	2.460	3.291	1.02	2.51	3.35
B2 graphite	22.0	3.641	3.422	1.02	3.70	3.48
(A,I,K) 3 US	10.4	2.585	2.585	1.48	3.82	3.82
(A,I,K) 3 DS	10.4	2.398	2.398	1.48	3.55	3.55
(B-H,J,L) 3	10.4	2.873	2.873	1.48	4.25	4.25
L5	22.7	3.924	3.326	1.00	3.93	3.33
(A-E,G,J-K) 5	22.7	2.873	2.873	1.00	2.88	2.88
(G,J,L) 7 US	10.4	2.585	2.585	1.48	3.82	3.82
(G,J,L) 7 DS	10.4	2.398	2.398	1.48	3.55	3.55
(A-F,H,I,K) 7	10.4	2.873	2.873	1.48	4.25	4.25
G10 POLARIMETER	17.4	3.438	3.420	1.14	3.92	3.90
I10 DAMPER	14.9	3.010	2.740	1.24	3.73	3.40
A13	21.9	2.873	2.873	1.02	2.93	2.93
(B-L) 13	21.9	2.873	2.873	1.02	2.93	2.93
FERRITE QUADS @15	10.1	2.219	2.219	1.50	3.33	3.33
(A-L) 17	21.9	2.873	2.873	1.02	2.93	2.93
E20 US	12.7	3.108	1.738	1.34	4.15	2.33
E20 DS	18.2	3.258	1.988	1.12	3.64	2.23
MAG VAC CHAMB	22.7	3.406	3.406	1.00	3.41	3.41
E5 US	22.7	2.209	3.290	1.00	2.21	3.29
E5 DS	22.7	2.259	3.290	1.00	2.26	3.29
H5 US	22.7	2.209	3.290	1.00	2.21	3.29
H5 DS	22.7	2.259	3.290	1.00	2.26	3.29
F5 NOMINAL	22.7	2.540	3.290	1.00	2.54	3.29
F10 NOMINAL US	18.5	2.237	3.171	1.11	2.48	3.52
F10 MIDDLE	16.1	1.928	3.171	1.19	2.29	3.77
F10 DS	15.7	1.978	3.179	1.20	2.37	3.82
H10 NOMINAL US	18.3	2.777	3.171	1.11	3.08	3.52
H10 DS	12.6	2.385	3.179	1.34	3.20	4.26
F15 IX	10.0	2.465	2.847	1.51	3.72	4.30
RF CAV. 10 US	18.5	2.844	2.844	1.11	3.15	3.15
RF CAV. 20 DS	18.5	2.844	2.844	1.11	3.15	3.15
A1 VAC CHAMB•	22.3	3.159	4.685	1.01	3.19	4.73
A2 VAC CHAMB•	21.9	3.159	3.904	1.02	3.22	3.98
A3 VAC CHAMB•	14.5	2.309	2.979	1.25	2.89	3.73
A5 KICKER	22.7	2.532	2.532	1.00	2.53	2.53
L20 SEPT US	12.5*/12.2+	3.288	2.000	1.37	4.49	2.70
L20 SEPT DS	18.5*/19.3+	3.135	2.000	1.09	3.40	2.22
C5 IPM	22.7	2.852	3.523	1.00	2.85	3.52
E15 IPM	10.0	2.665	3.335	1.51	4.03	5.04
C5 JUMP TGT	22.7	2.915	3.585	1.00	2.92	3.59
E15 JUMP TGT	10.0	1.978	2.648	1.51	2.98	3.99
VHF CAVITY US	12.2	2.750	2.750	1.36	3.75	3.75
VHF CAVITY DS	14.8	2.750	2.750	1.24	3.42	3.42
A10 TUNE METER US	18.7	2.728	2.990	1.10	3.01	3.30
A10 TUNE METER DS	15.5	2.786	3.048	1.21	3.38	3.69

• see Appendix A

* at location of A_{in} (see drawing)
\+ at location of A_{out} (see drawing)

Table 3

EFFECTIVE APERTURES WITH RESPECT TO BEAM CENTERLINE VERTICAL APERTURES β_{max} = 22.745 ± 0.0005 meters Devices	β ± 0.1 (meters)	A (in.)	$(\beta_{max}/\beta)^{1/2}$	A_L (in.)
B1 foil	10.4	1.488	1.48	2.20
B2 graphite	14.5	1.547	1.25	1.94
(A,I,K) 3 US	21.9	1.960	1.02	2.00
(A,I,K) 3 DS	21.9	1.835	1.02	1.87
(B-H,J,L) 3	21.9	2.973	1.02	2.93
L5	10.1	3.625	1.50	5.44
(A-E,G,J-K) 5	10.1	2.973	1.50	4.31
(G,J,L) 7 US	21.9	1.960	1.20	2.00
(G,J,L) 7 DS	21.9	1.835	1.20	1.87
(A-F,H,I,K) 7	21.9	2.973	1.20	2.93
G10 POLARIMETER	13.5	1.88	1.30	2.44
I10 DAMPER	19.1	1.500	1.19	1.64
A13	10.4	2.973	1.48	4.25
(B-L) 13	10.4	2.873	1.48	4.25
FERRITE QUADS @15	22.7	1.469	1.00	1.47
(A-L) 17	10.4	2.873	1.48	4.25
E20 US	18.5	1.435	1.11	1.59
E20 DS	12.9	1.091	1.33	1.45
MAG VAC CHAMB	22.7	1.531	1.00	1.53
E5 US	10.1	0.283	1.50	0.43
E5 DS	10.1	0.283	1.50	0.43
H5 US	10.1	0.283	1.50	0.43
H5 DS	10.1	0.283	1.50	0.43
F5 NOMINAL	10.1	0.35	1.50	0.53
F10 NOMINAL US	14.5	0.39	1.25	0.488
F10 MIDDLE	14.8	0.39	1.24	0.484
F10 DS	18.3	0.39	1.11	0.433
H10 NOMINAL US	12.8	0.49	1.33	0.652
H10 DS	18.9	0.49	1.10	0.539
F15 IX	22.7	2.656	1.00	2.66
RF CAV. 10 US	12.7	2.844	1.34	3.81
RF CAV. 20 DS	12.7	2.844	1.34	3.81
A1 VAC CHAMB	11.7	1.469	1.40	2.06
A2 VAC CHAMB	14.4	1.469	1.26	1.85
A3 VAC CHAMB	21.9	1.563	1.02	1.59
A5 KICKER	10.0	1.094	1.51	1.64
L20 SEPT US	19.2	3.062	1.09	3.33
L20 SEPT DS	12.1	3.063	1.37	4.20
C5 IPM	10.0	3.000	1.51	4.50
E15 IPM	22.7	3.188	1.00	3.19
C5 JUMP TGT (A[illegible])	10.0	3.125	1.51	4.72
C5 JUMP TGT (A_{down})	10.0	1.75	1.51	2.64
E15 JUMP TGT	22.7	1.75	1.00	1.75
VHF CAVITY US	19.2	2.750	1.09	2.99
VHF CAVITY DS	16.7	2.750	1.17	3.21
A10 TUNE METER US	15.0	1.25	1.23	1.54
A10 TUNE METER DS	18.2	1.281	1.12	1.44

Table of Contents for Drawings

Drawing is new or updated with this release [shaded box]

Table of Contents for Drawings

Drawing is new or updated with this release (shaded)

Table of Contents for Drawings

Drawing is new or updated with this release

HORIZONTAL LIMITING APERTURES OF DEVICES WITH APERTURES LESS THAN 3.15

← DIRECTION TO CENTER OF RING

R_0

A_{IN_L}	A_{OUT_L}	Device
2.53	2.53	A5 KICKER
3.29	2.21	E5 U/S
3.29	2.21	H5 U/S
3.29	2.26	E5 D/S
3.29	2.26	H5 D/S
3.40	2.22	L20 SEPTUM D/S
2.88	2.88	(A–E,G,J–K) 5
3.29	2.54	F5 NOMINAL
3.35	2.51	B1 FOIL
2.93	2.93	A13
2.93	2.93	(B–L) 13
2.93	2.93	(A–L) 17
2.23	3.64	E20 D/S
3.52	2.48	F10 NOMINAL U/S
3.77	2.29	F10 MIDDLE
3.82	2.37	F10 D/S
3.30	3.01	A10 TUNE METER U/S
3.15	3.15	RF CAV. 10 U/S
3.15	3.15	RF CAV. 20 D/S
3.52	2.85	C5 IPM
2.33	4.15	E20 U/S
3.59	2.92	C5 JUMP TARGET
3.73	2.89	A3 VAC. CHAMBER
3.52	3.08	H10 NOMINAL U/S
3.99	2.98	E15 JUMP TARGET
4.49	2.70	L20 SEPTUM U/S

VERTICAL LIMITING APERTURES OF DEVICES WITH APERTURES LESS THAN 2.50

DIRECTION TO CENTER OF RING ↑

	A_L ℄ BEAM	A_L	
E20 D/S	1.45	1.45	
A10 TUNE METER D/S	1.47	1.40	(CONSIDERED AT CORNERS OF BOX)
(A-L)15 (FERRITE QUADS)	1.47	1.47	
A10 TUNE METER D/S	1.54	1.50	(CONSIDERED AT CENTER OF BOX)
MAGNET VACUUM CHAMBERS	1.53	1.53	
A10 TUNE METER U/S	1.54	1.54	
E20 U/S	1.59	1.59	
I10 DAMPER	1.64	1.64	
A5 KICKER	1.64	1.64	
E15 JUMP TARGET	1.75	1.75	
(A,I,K)3 D/S	1.87	1.87	
(G,J,L)7 D/S	1.87	1.87	
B2 (GRAPHITE)	1.94	1.94	
(A,I,K)3 U/S	2.00	2.00	
(G,J,L)7 U/S	2.00	2.00	
B1 (FOIL)	2.20	2.20	
G10 POLARIMETER	2.4	2.4	

11-12-9

2

4-10-85

VERTICAL LIMITING APERTURES AT EXTRACTION

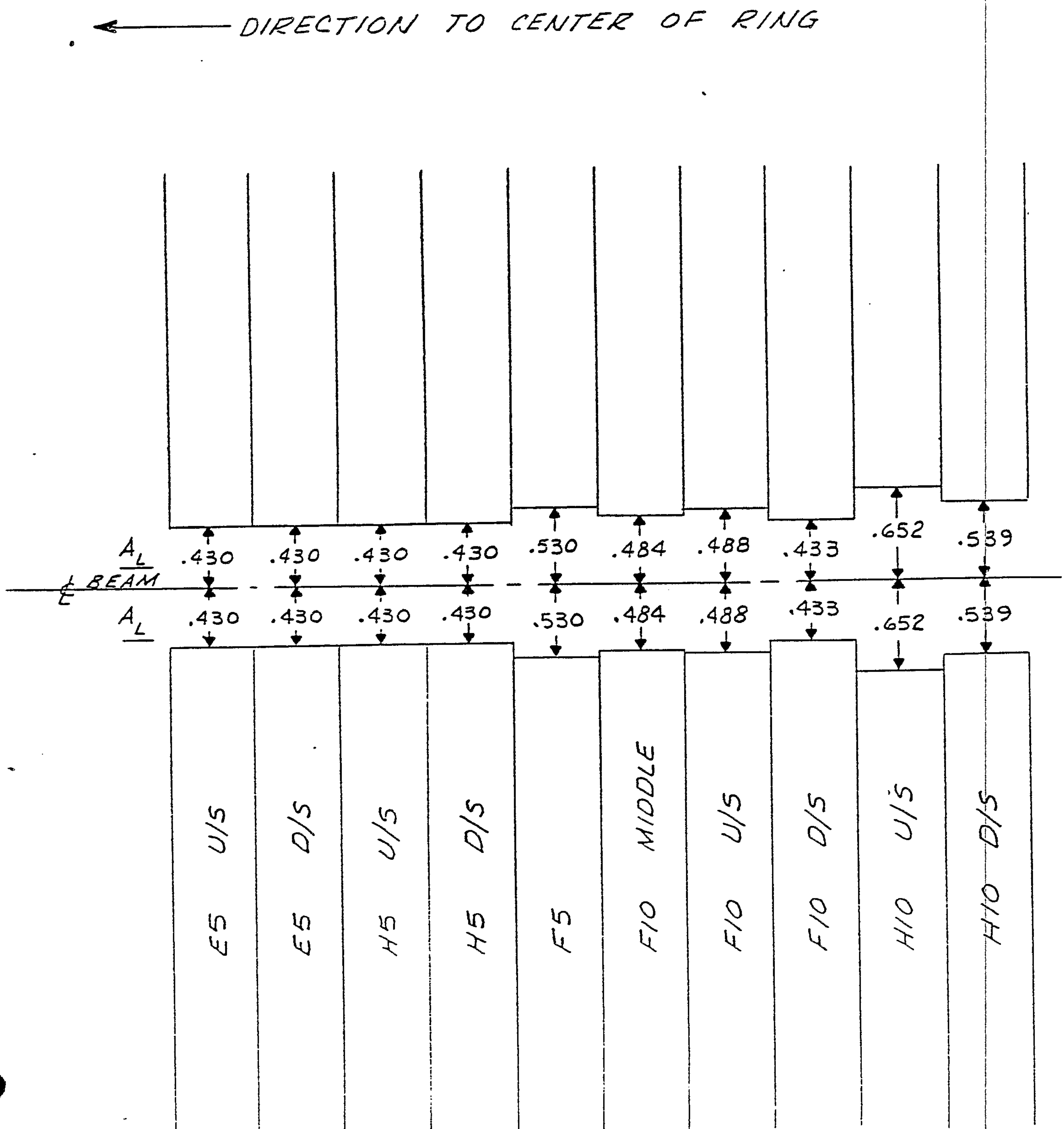

DISTANCE ALONG #10 & #20 STRAIGHT SECTIONS TO LIMITING APERTURES

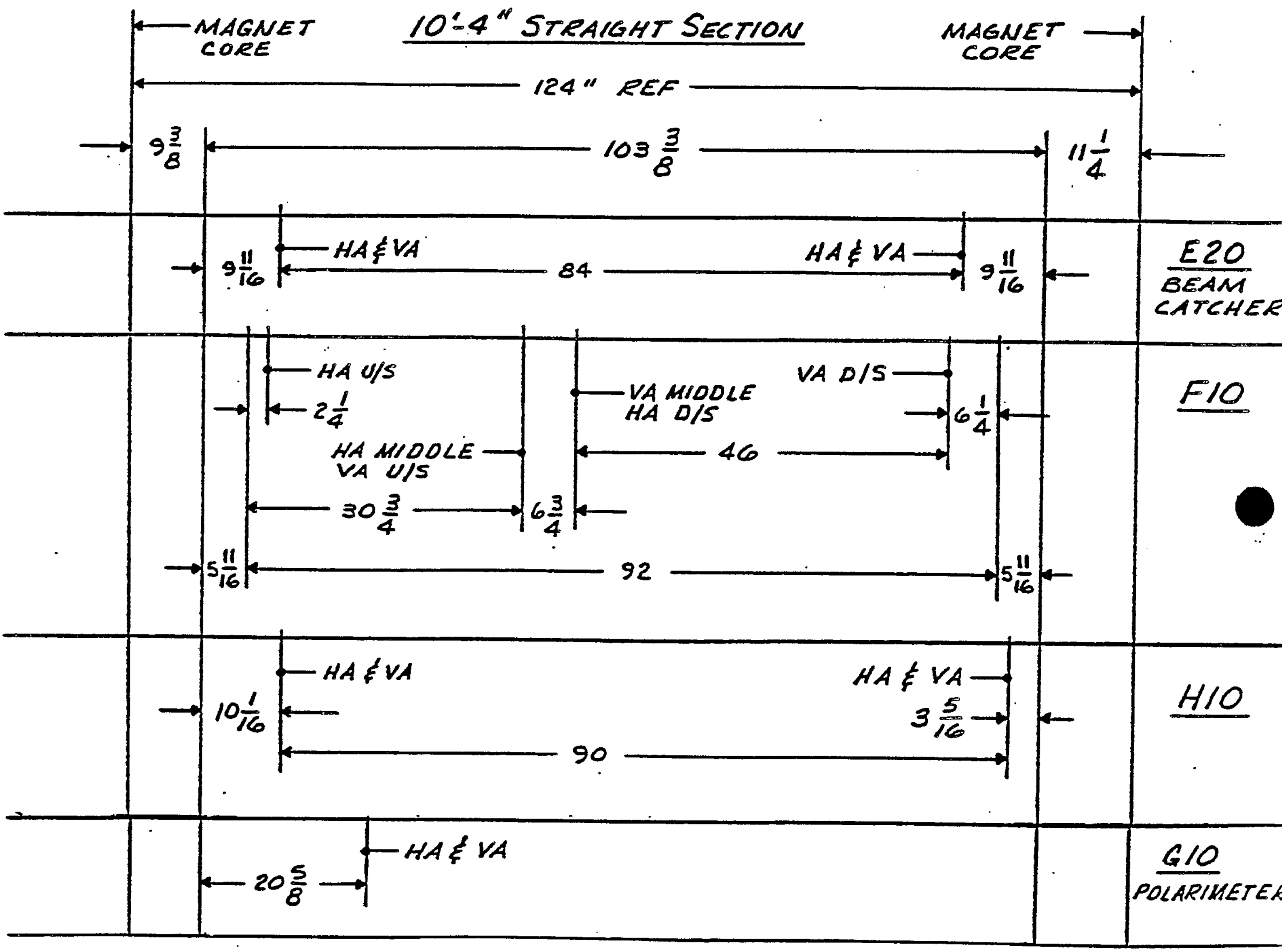

DISTANCE ALONG #10 & #20 STRAIGHT SECTIONS TO LIMITING APERTURES

10'-4" STRAIGHT SECTION

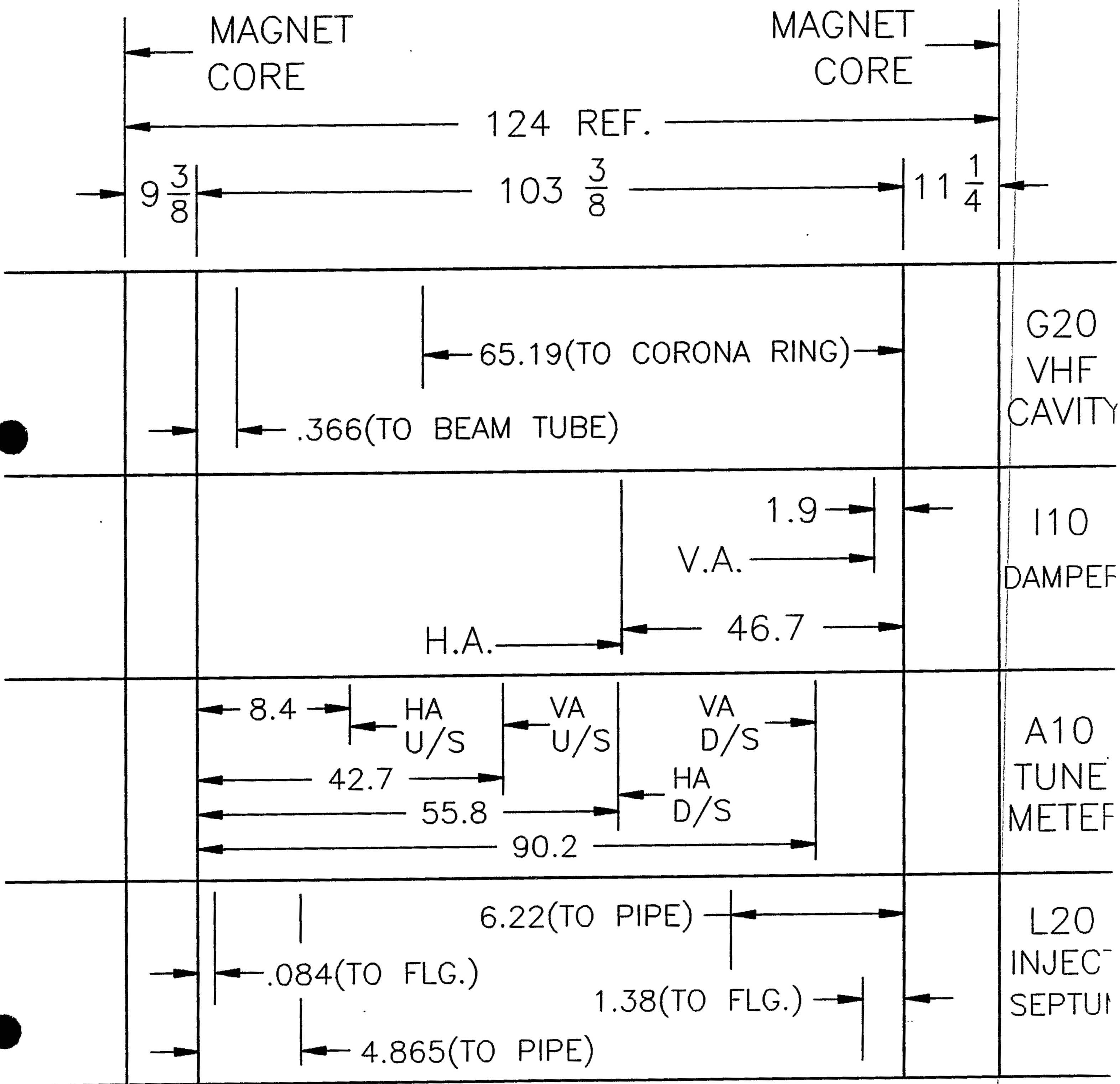

NOTE:
FOR L20, VALUES ARE FOR BOTH H.A. & V.A..

UPSTREAM (VIEW LOOKING DOWNSTREAM)

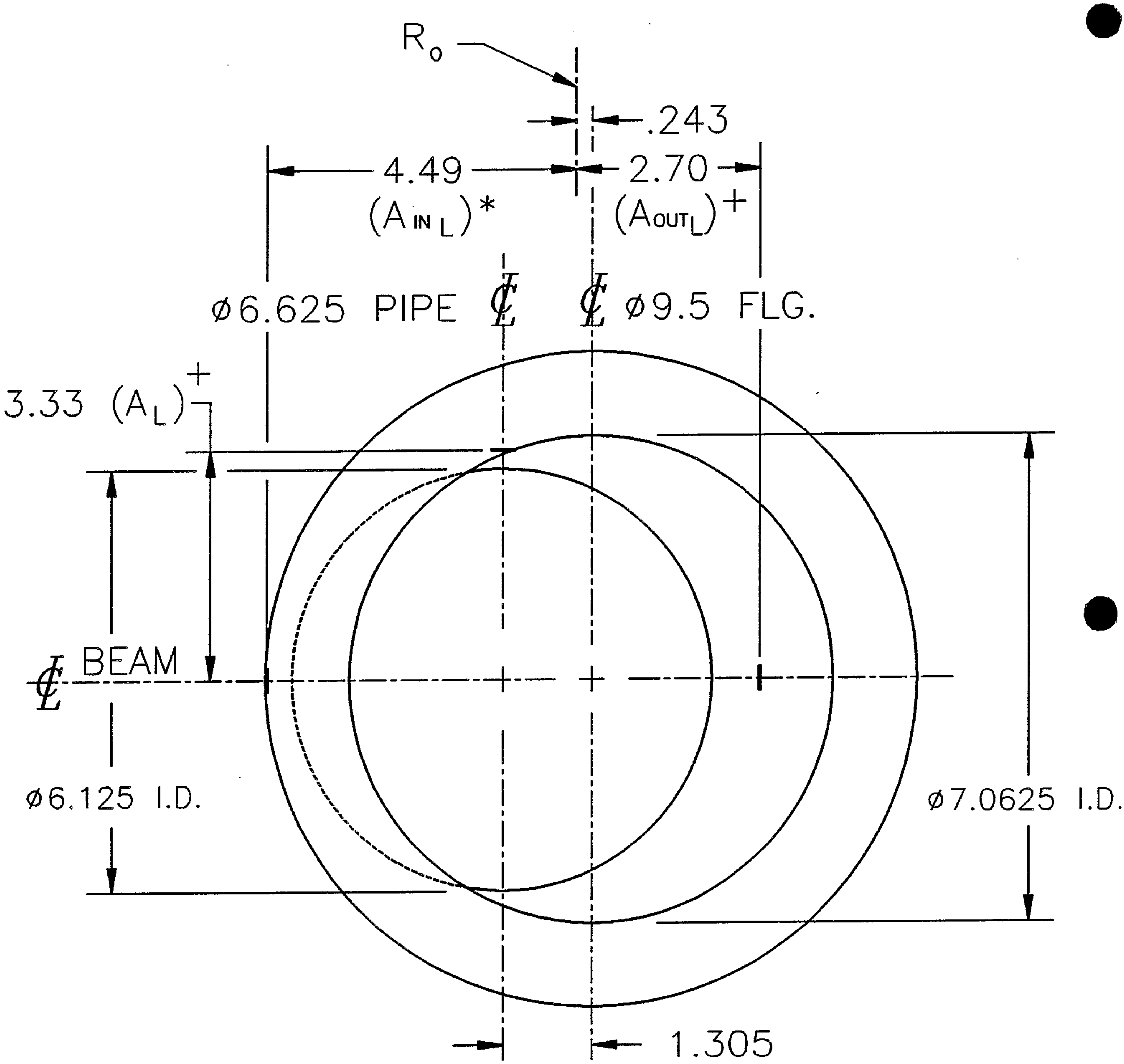

* $A_{IN\,L}$ DETERMINED AT ENTRANCE TO 9.5" FLANGE
\+ $A_{OUT\,L}$, A_L DETERMINED AT ENTRANCE TO 6.625" PIPE

L20 INJECTION SEPTUM

REF. DWGS.: D37-M-0429-4, D37-M-0430-4, D37-M-0431-5
D37-M-0515-4, D37-M-0432-5

DOWNSTREAM (VIEW LOOKING DOWNSTREAM)
(VIEW SHOWN IS NORMAL OPERATING POSITION)

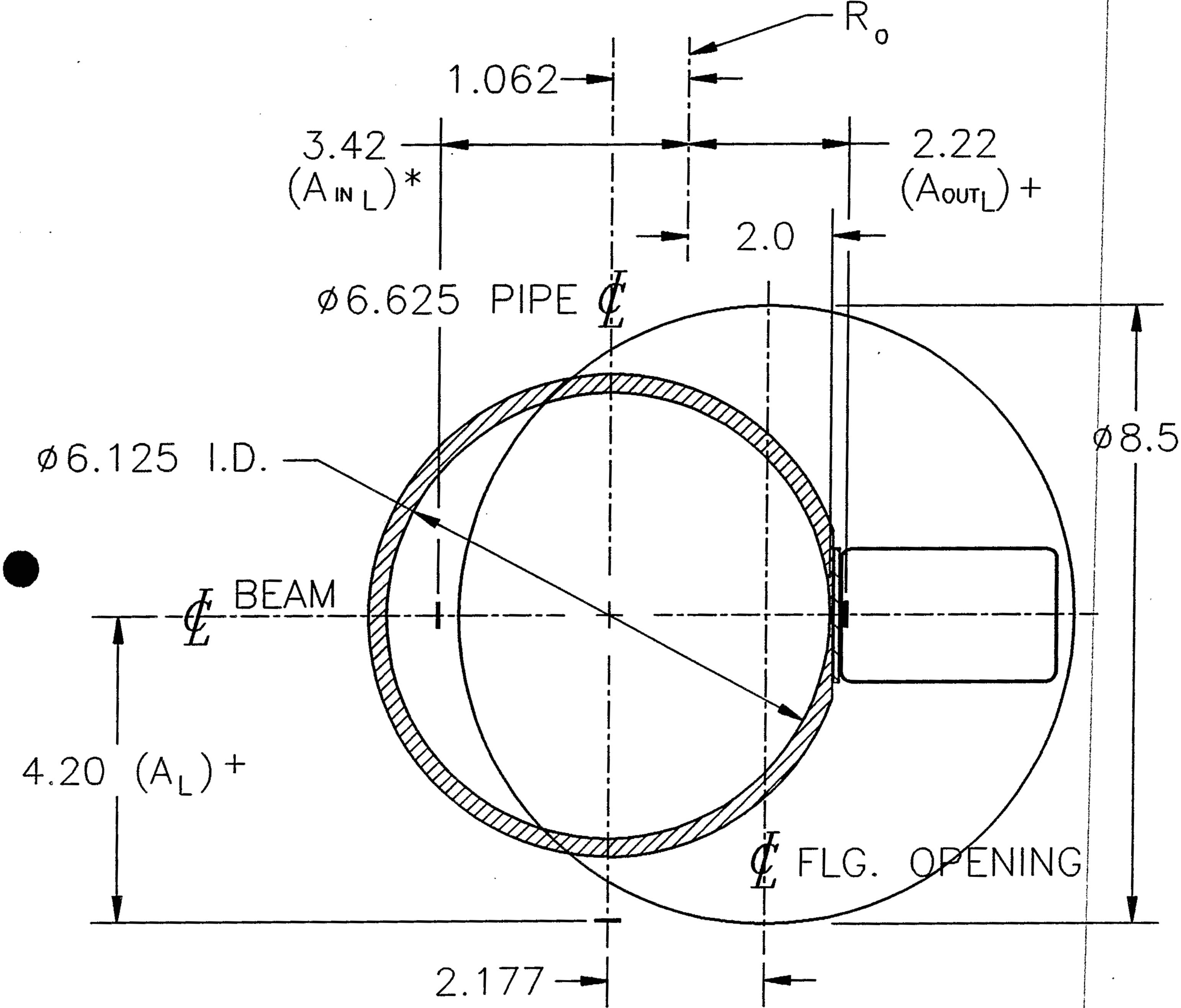

NOTE:

(LIMITS OF TRAVEL: 9/16 TOWARD CENTER
1/16 AWAY FROM CENTER)

* A_{IN_L} DETERMINED AT ENTRANCE TO DOWNSTREAM FLANGE

+ A_{OUT_L}, A_L DETERMINED AT EXIT OF 6.625" PIPE

L20 INJECTION SEPTUM

REF. DWGS.: D37-M-0431-5(SHTS. 1-3) & D37-M-0432-5

UPSTREAM (VIEW LOOKING DOWNSTREAM)

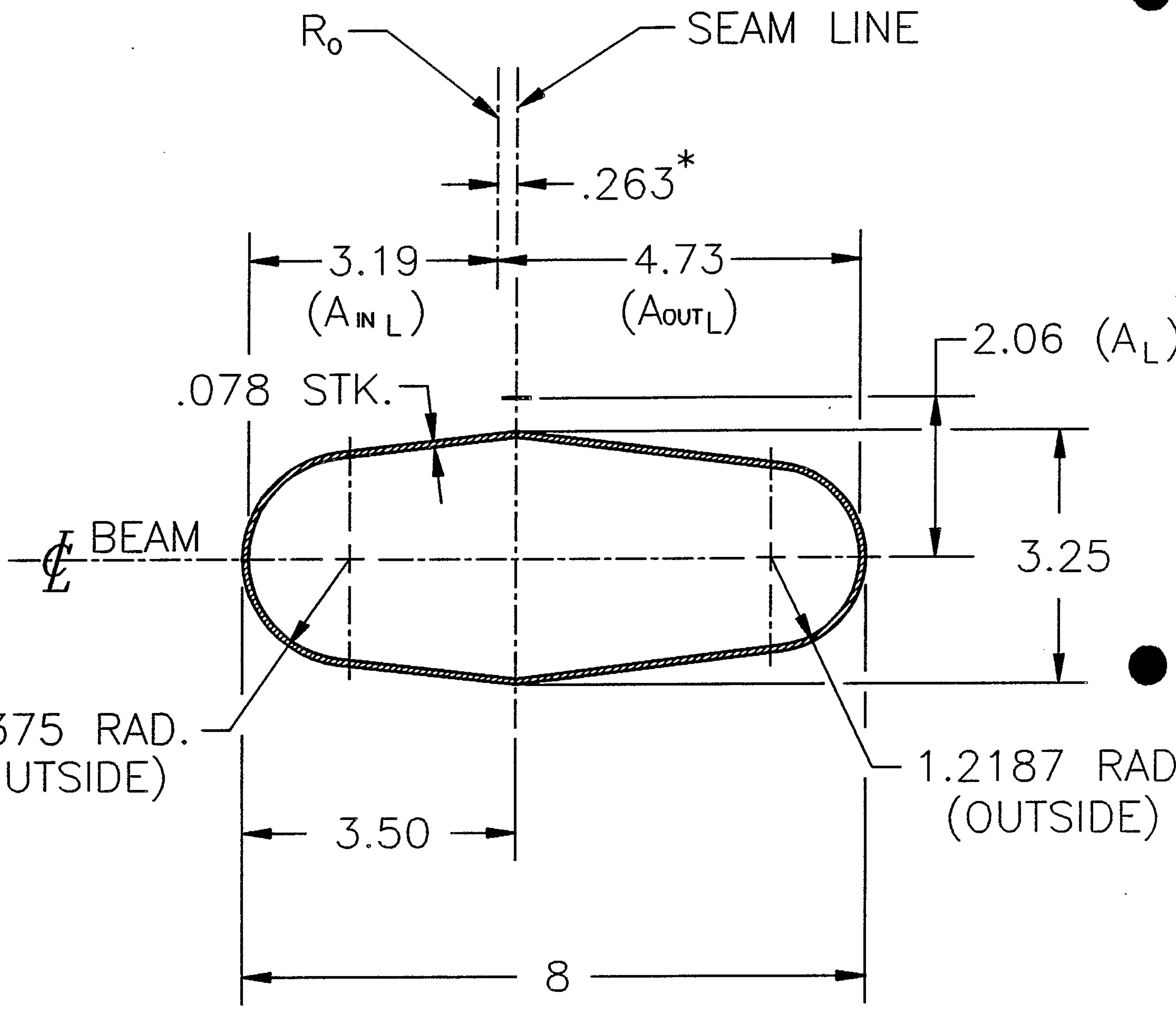

* SEPARATION BETWEEN Ro AND SEAMLINE AT DOWNSTREAM END OF A1 VACUUM CHAMBER.

A1 VACUUM CHAMBER

REF. DWGS.: D05-M-2620-5, D05-M-2624-5 & D25-M-2108-5

UPSTREAM (VIEW LOOKING DOWNSTREAM)

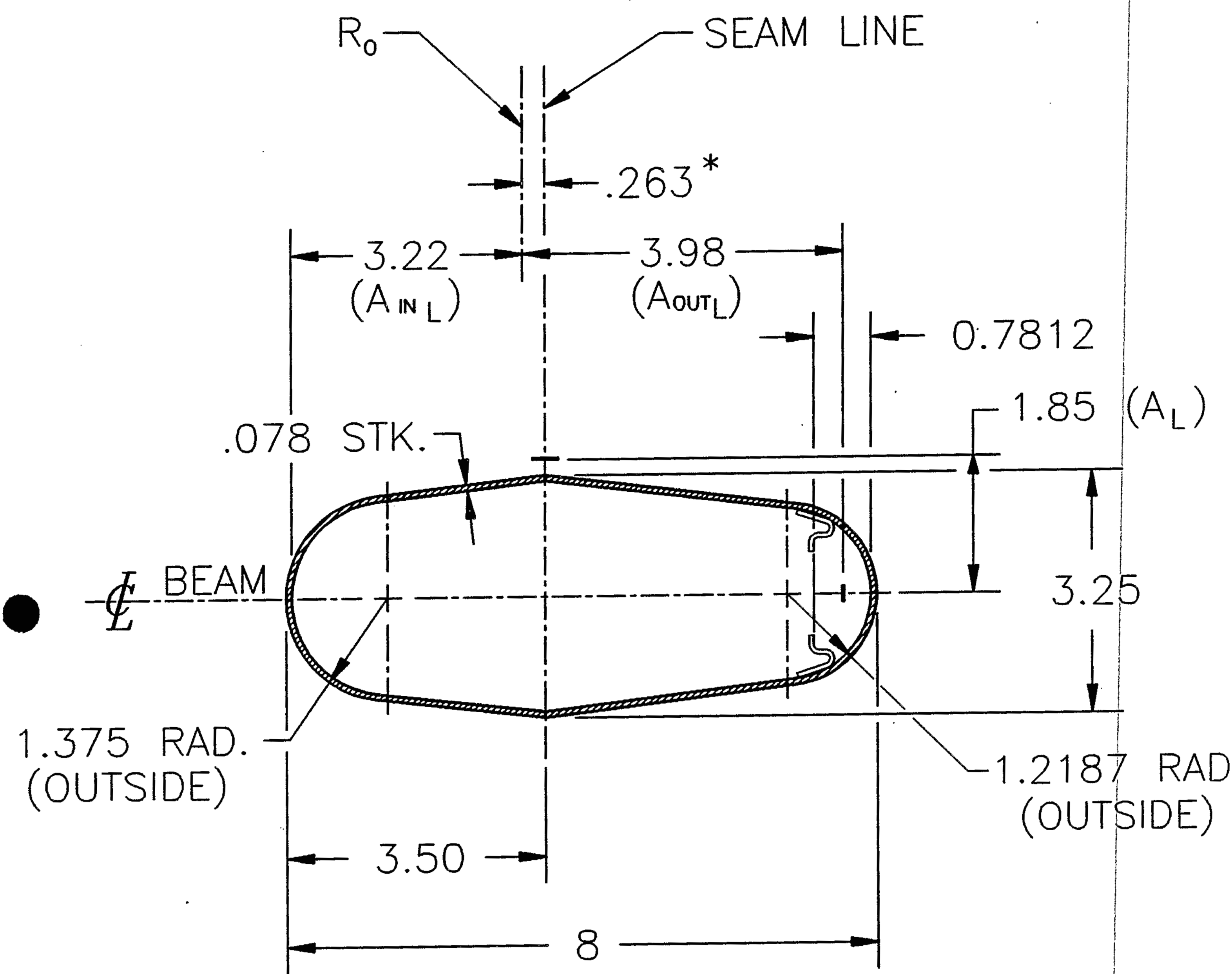

* SEPARATION BETWEEN Ro AND SEAMLINE AT UPSTREAM END OF A2 VACUUM CHAMBER.

A2 VACUUM CHAMBER

REF. DWGS.: D05-M-2621-5, D05-M-2623-5 & D25-M-2108-5

UPSTREAM (VIEW LOOKING DOWNSTREAM)

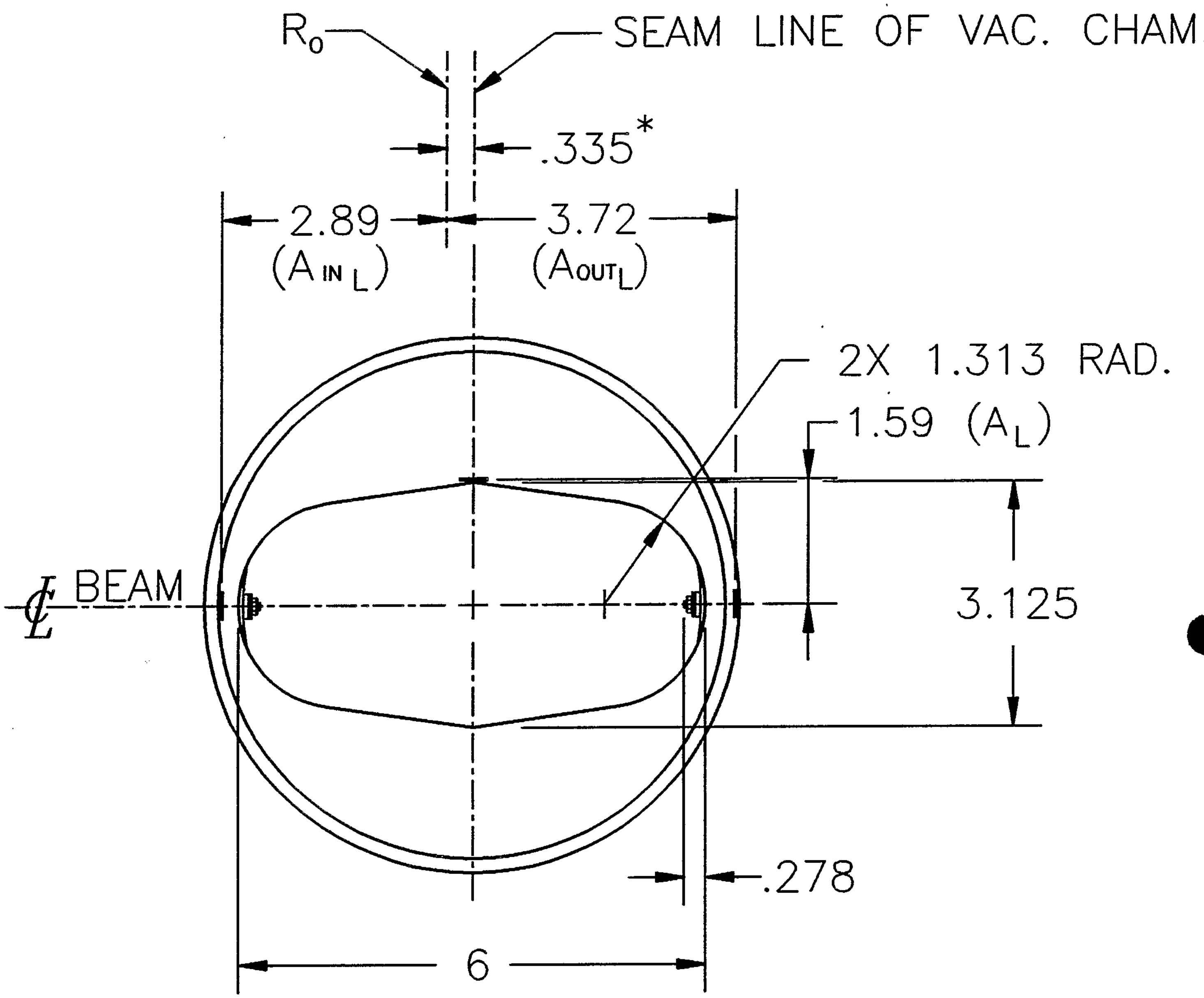

* SEPARATION BETWEEN Ro AND SEAMLINE AT UPSTREAM END OF A3 VACUUM CHAMBER.

A3 VACUUM CHAMBER

REF. DWGS.: D05-M-2622-5, D05-M-2618-5 & D06-M-1524-4

3-20-85

SECTION THRU UPSTREAM END
VIEW LOOKING DOWNSTREAM

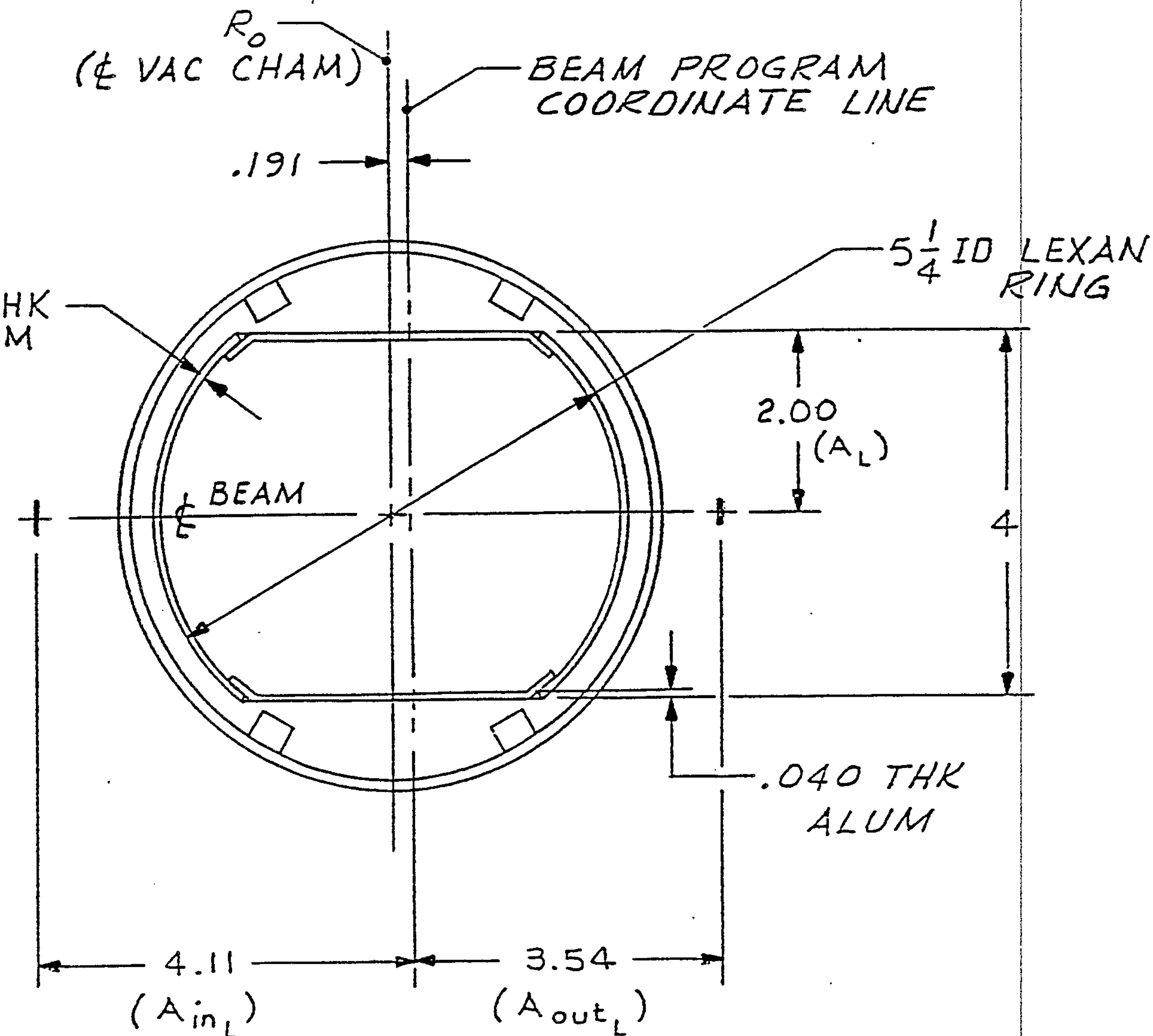

A3, I3, K3

VERTICAL PICK-UP ELECTRODE

REF DWGS: D06-M-165-4 & D06-M-254-4

SECTION THRU DOWNSTREAM END

VIEW LOOKING DOWNSTREAM

3-20-85

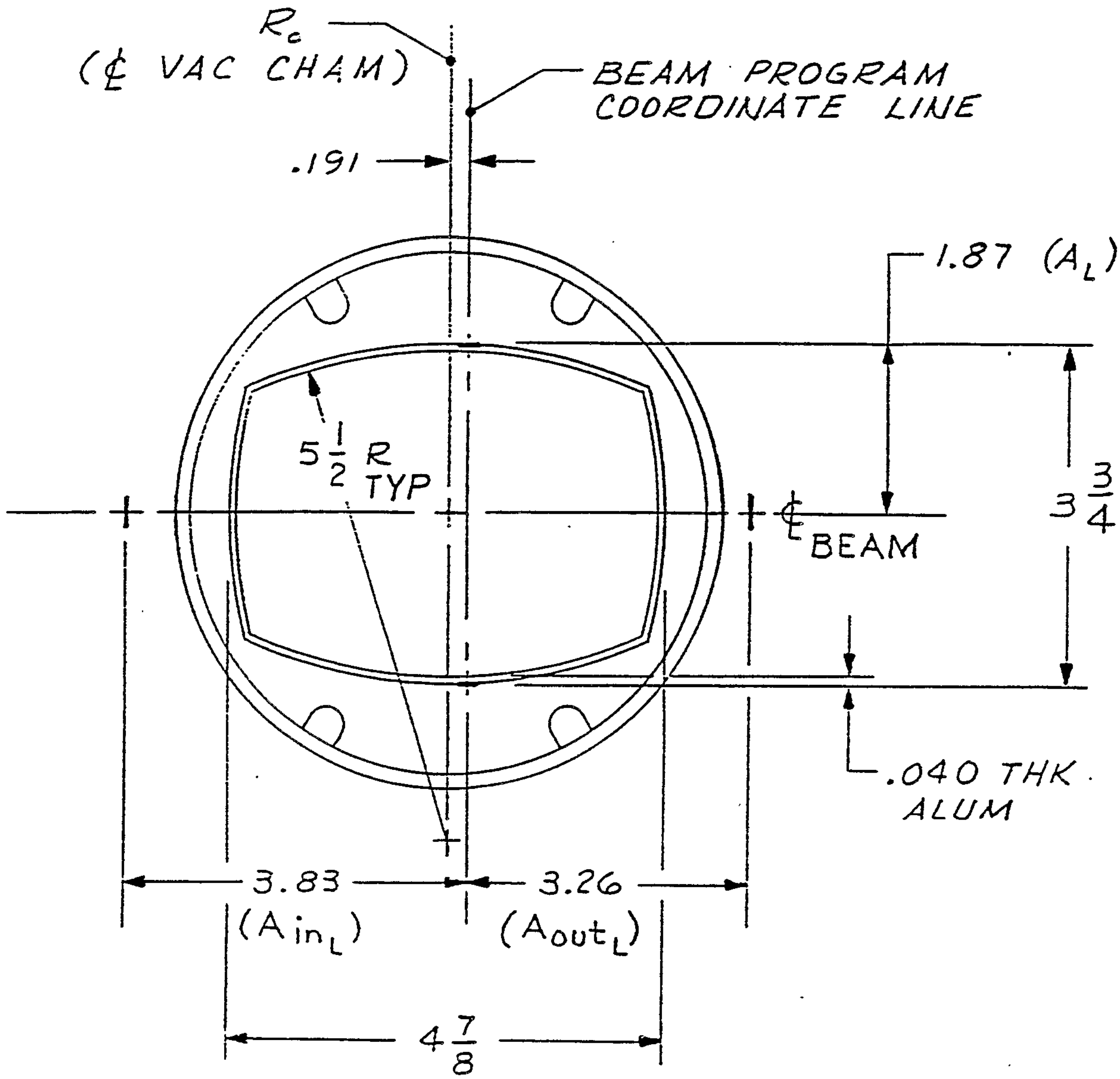

A3, I3, K3

HORIZONTAL PICK-UP ELECTRODE

REF DWGS: D06-M-254-4 & D06-M-165-4

UPSTREAM (VIEW LOOKING DOWNSTREAM)

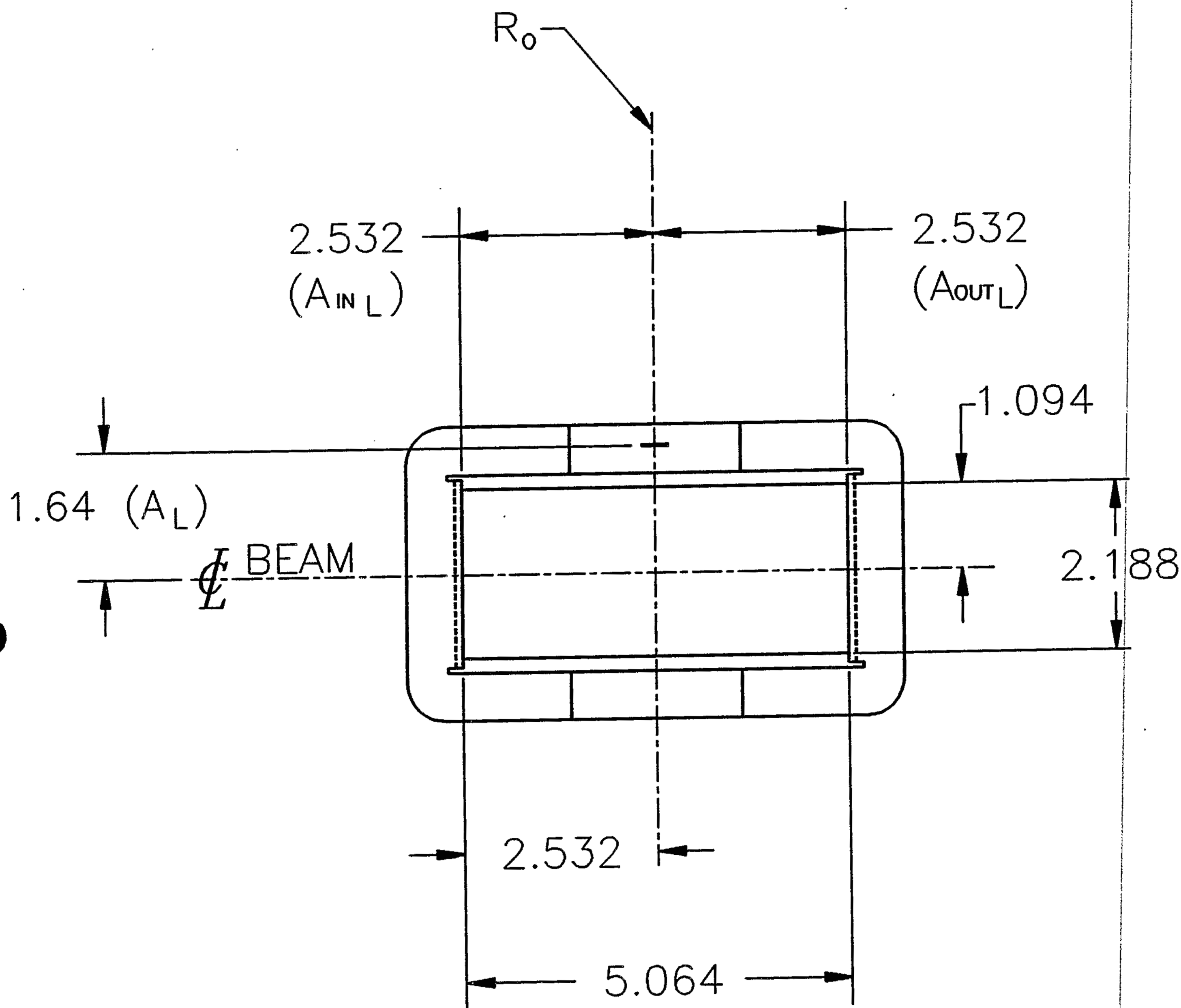

A5 KICKER

REF. DWGS.: D11-M-11985 & D36-M-1185-2

VIEW LOOKING DOWNSTREAM

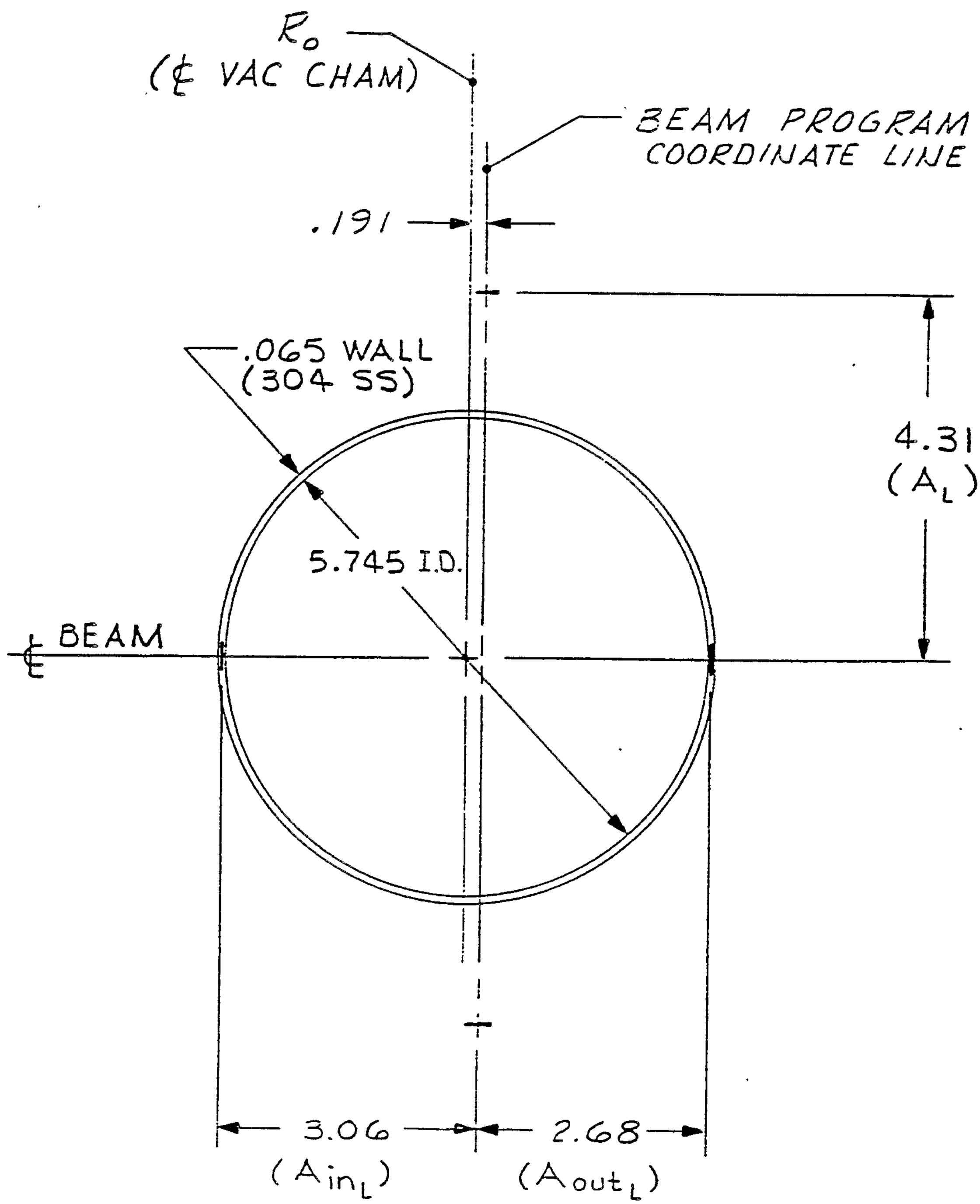

A5 THRU E5, G5, I5 THRU K5

REF DWGS: D05-M-960-5

3-19-85

VIEW LOOKING DOWNSTREAM

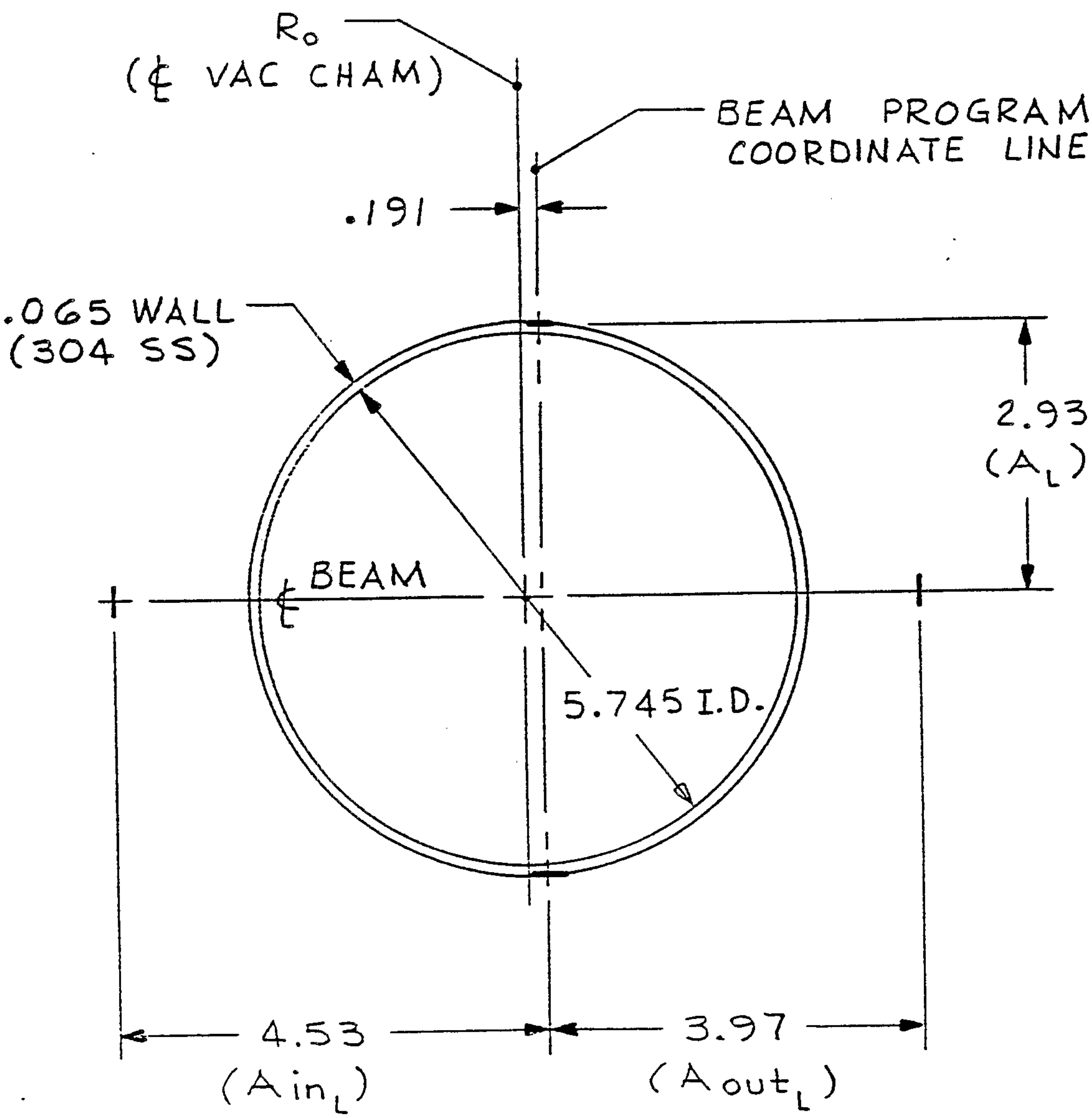

A7 THRU F7, H7, I7, K7

REF DWGS: D05-M-960-5

UPSTREAM BOX ASSEMBLY

VIEW LOOKING DOWNSTREAM

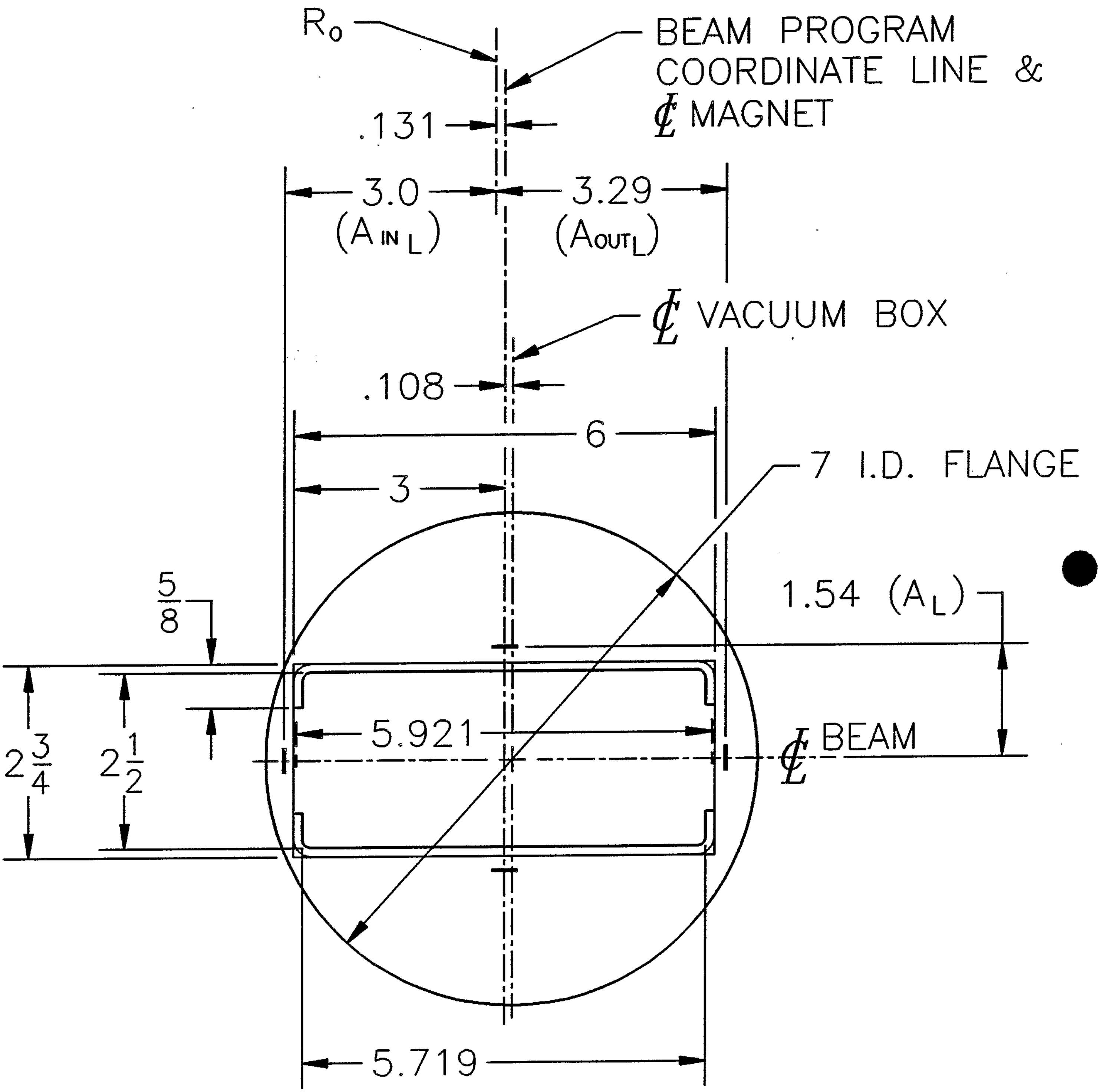

A10

BEAM TUNE METER

REF. DWGS.: D11-M-11455-5, D11-M-11454-5 & D11-M-11453-5

DOWNSTREAM BOX ASSEMBLY

VIEW LOOKING DOWNSTREAM

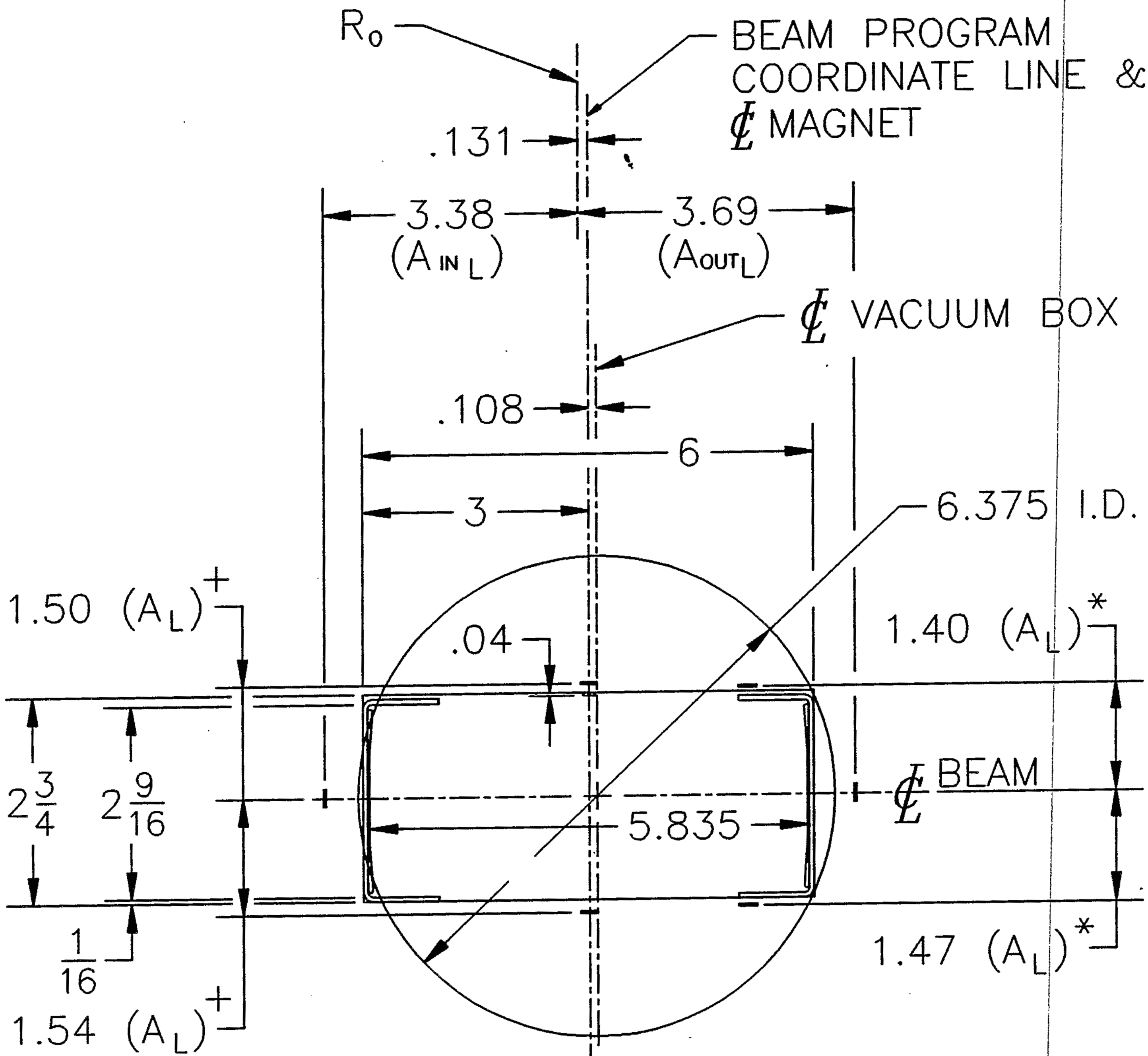

* DETERMINED AT CORNERS OF BOX ASSEMBLY
\+ DETERMINED AT CENTER OF BOX ASSEMBLY

A10

BEAM TUNE METER

REF. DWGS.: D11-M-11455-5, D11-M-11454-5 & D11-M-11453-5

VIEW LOOKING DOWNSTREAM

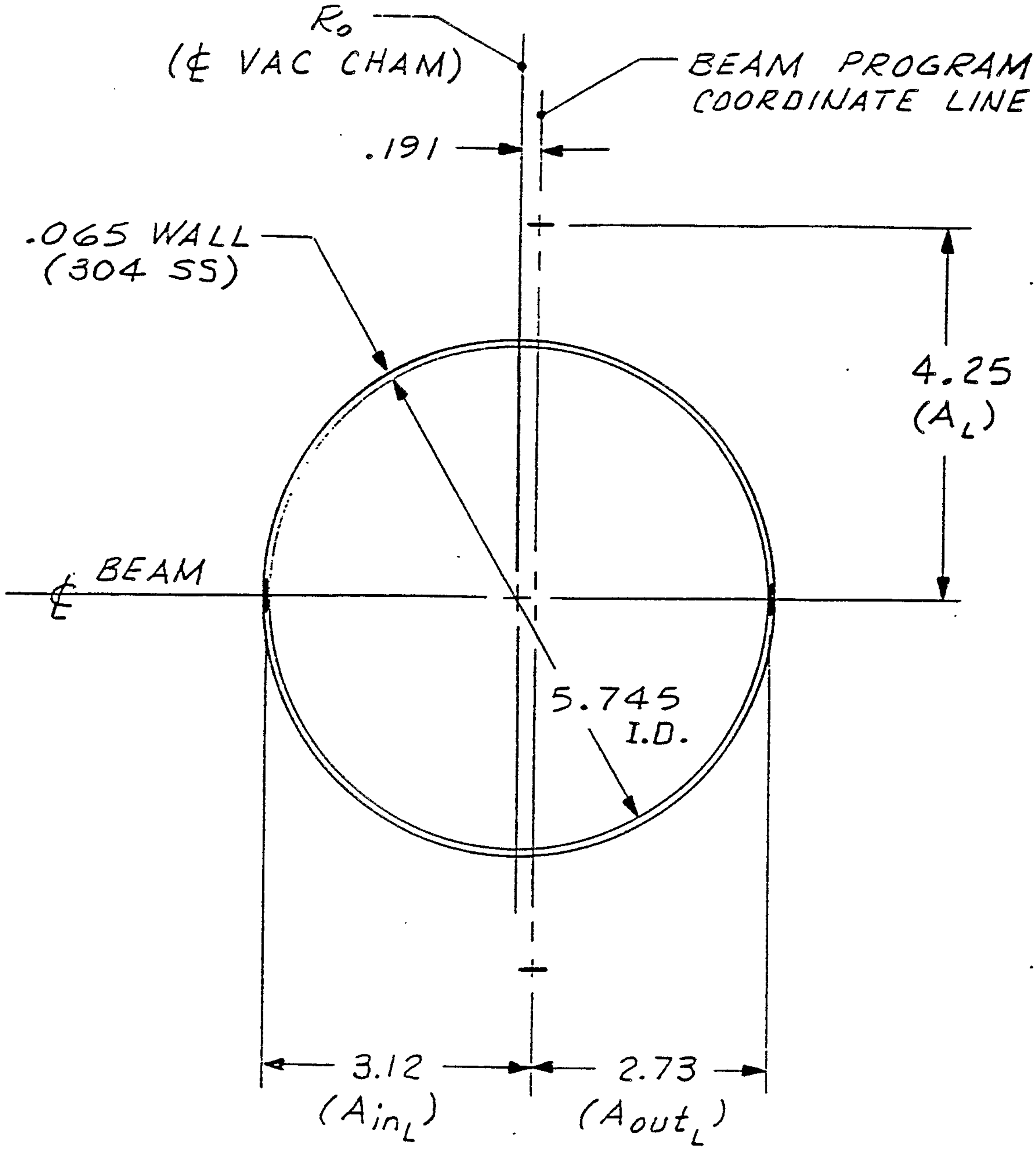

A13

REF DWG: D05-M-960-5

3-20-85

VIEW LOOKING DOWNSTREAM

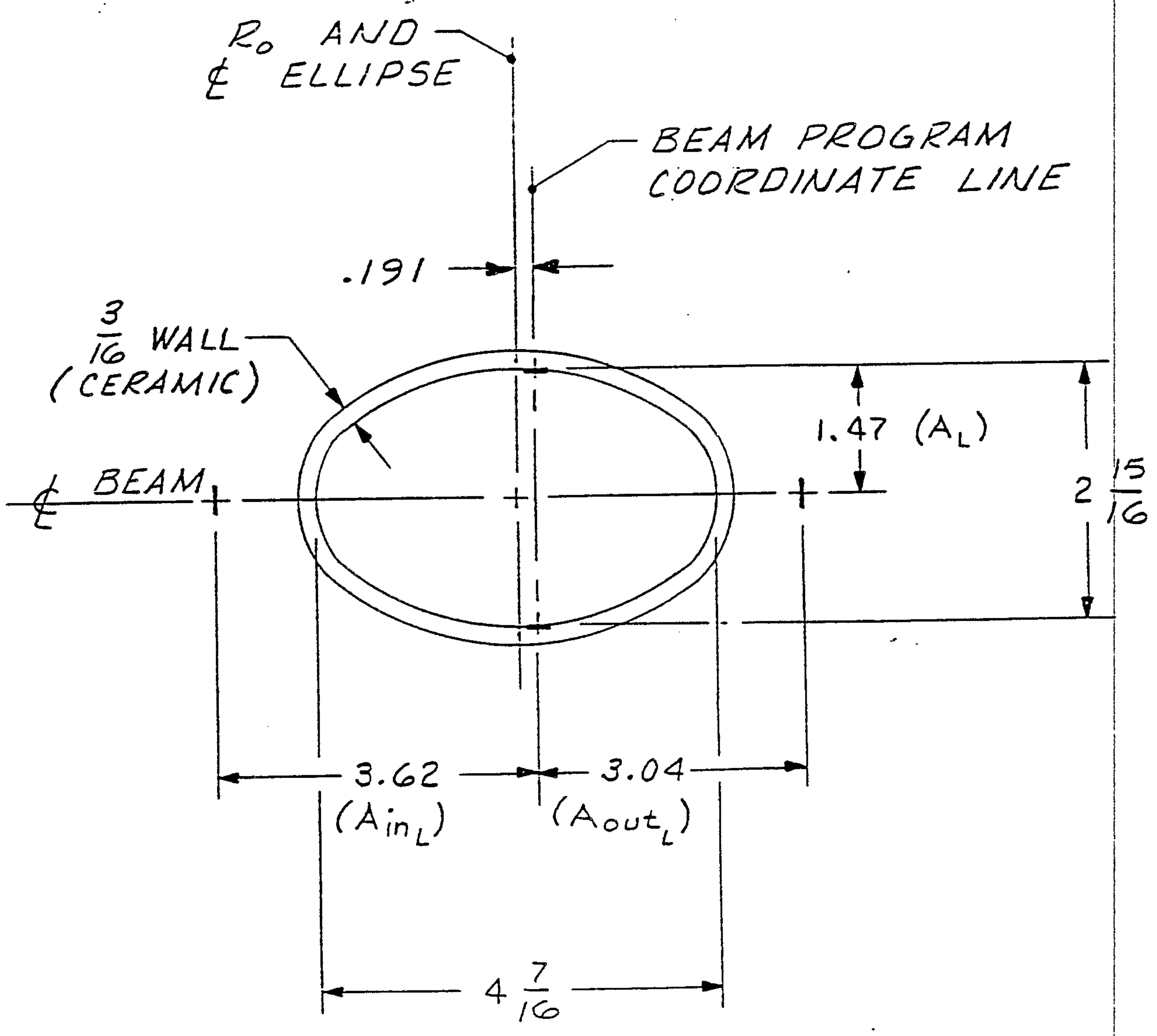

A15 THRU L15
FERRITE QUADS

REF DWGS: 005-M-2160-5 & 005-M-2170-4

VIEW LOOKING DOWNSTREAM

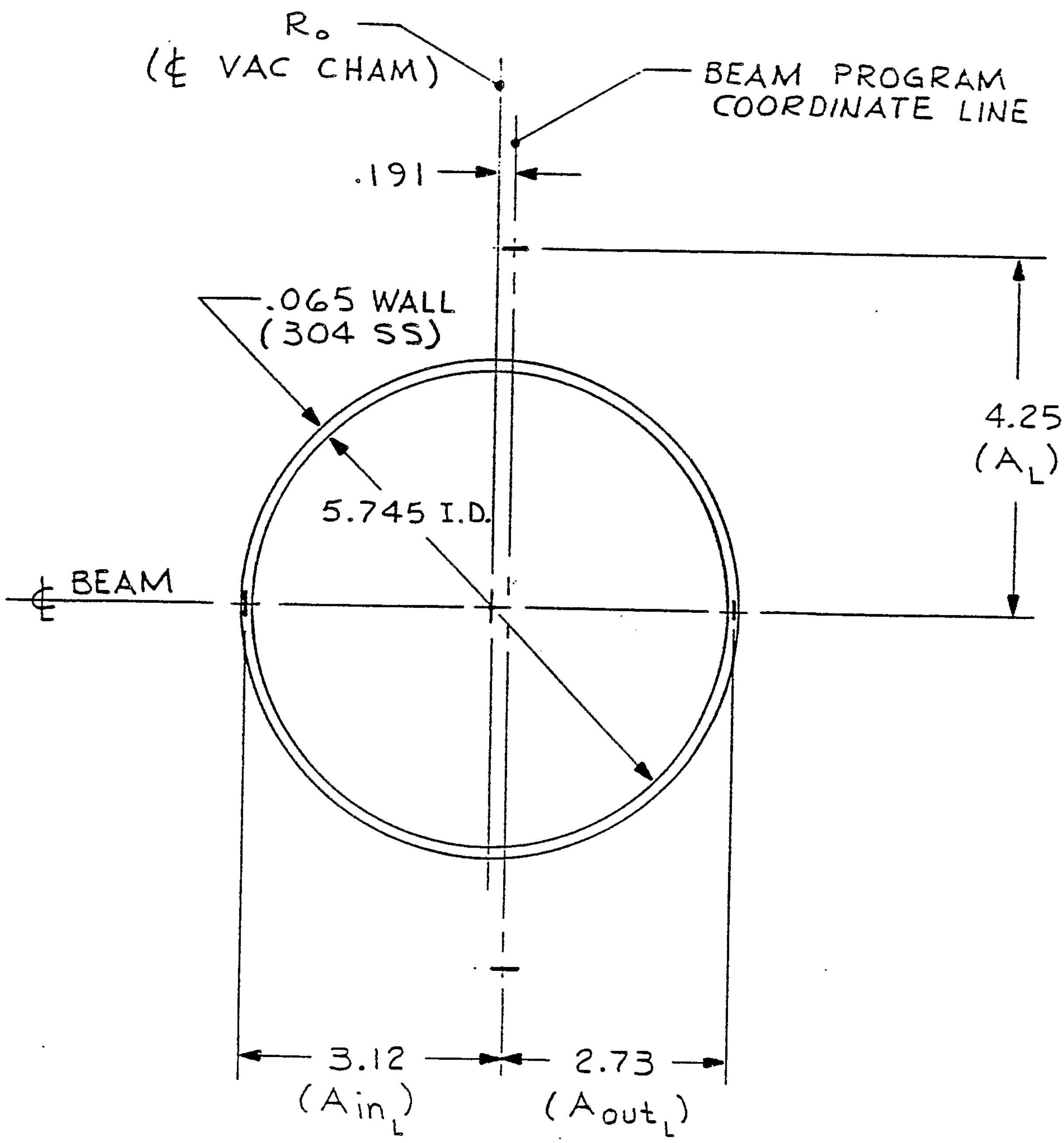

A17 THRU L17

REF DWGS: D05-M-960-5

VIEW LOOKING DOWNSTREAM

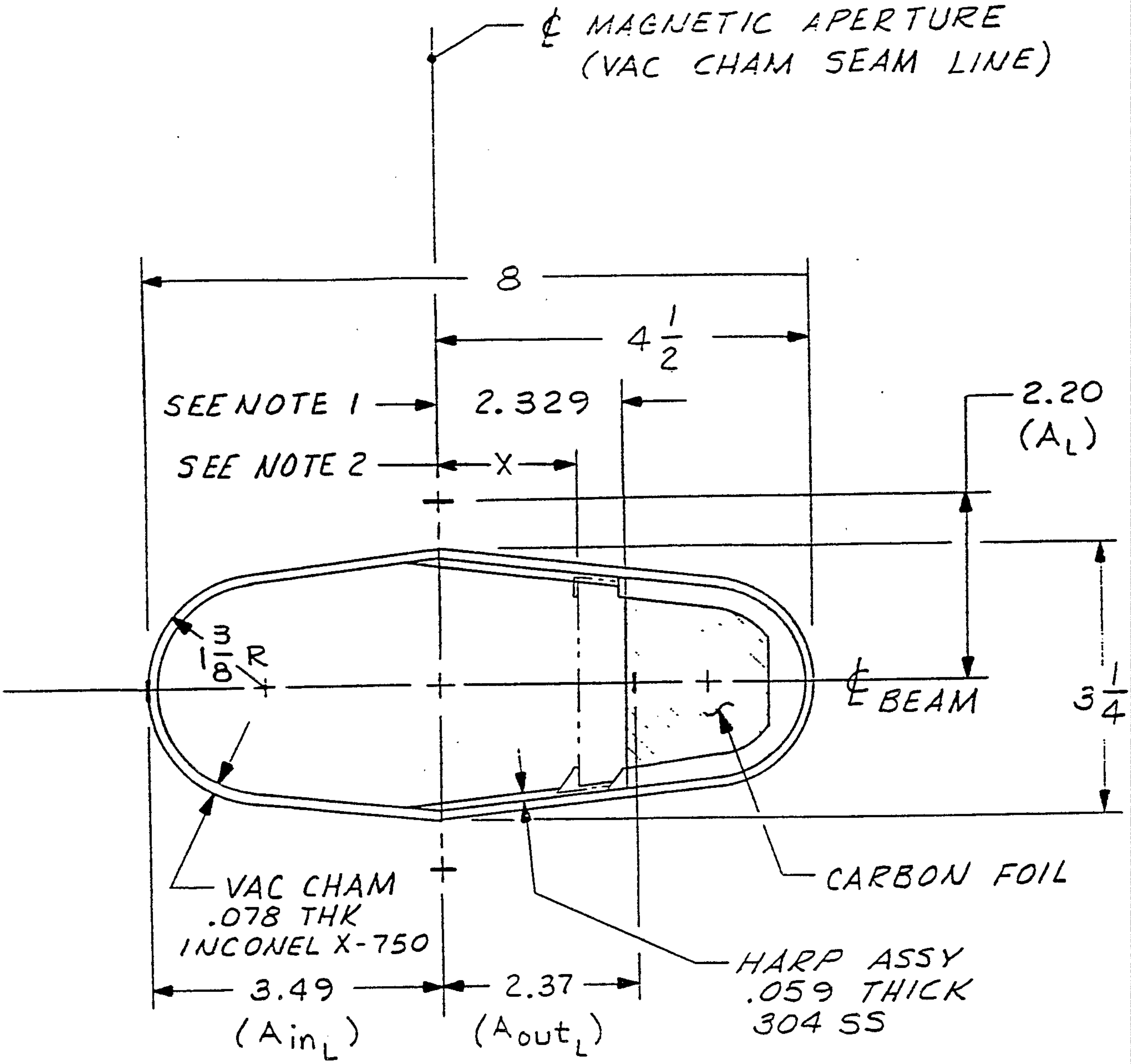

NOTES:

1. FULLY INSERTED - DVM READING 9.515
2. PARTIALLY INSERTED - FOR DVM READING (V) DISTANCE (X) FOUND BY: $X = 2.329 - 3(9.515 - V)$ FOR $V = 9.321$, $X = 1.747$

B1
$H^{(-)}$ CARBON FOIL MECHANISM

REF DWGS: D25-M-2178-5 & D25-M-2091-5

VIEW LOOKING DOWNSTREAM

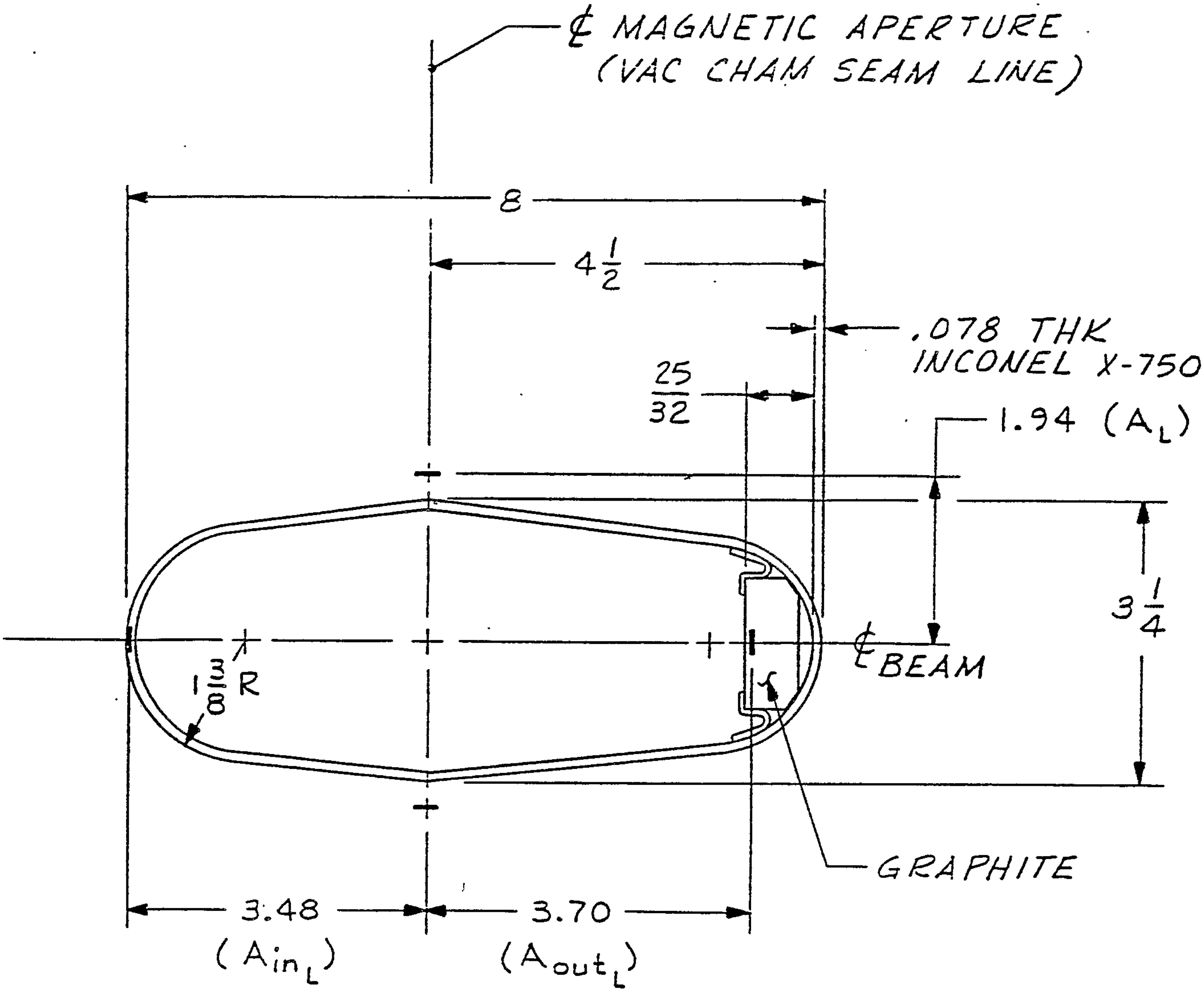

B2

REF: D25-M-2108-5 & D11-M-7212-5

VIEW LOOKING DOWNSTREAM

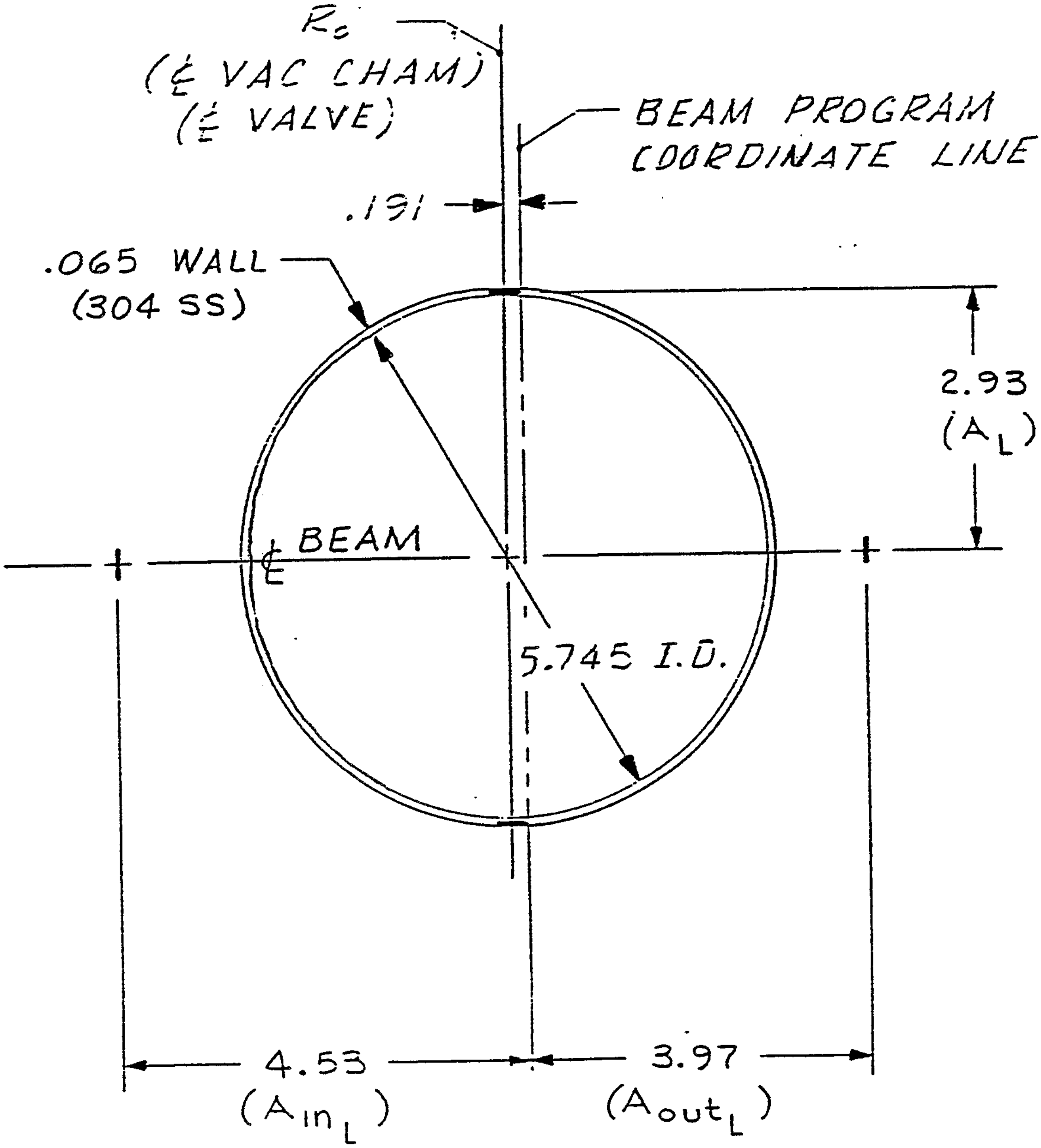

B3 THRU H3, J3, L3

REF DWGS: D05-M-959-4 & D05-M-962

UPSTREAM FLANGE (VIEW LOOKING DOWNSTREAM)

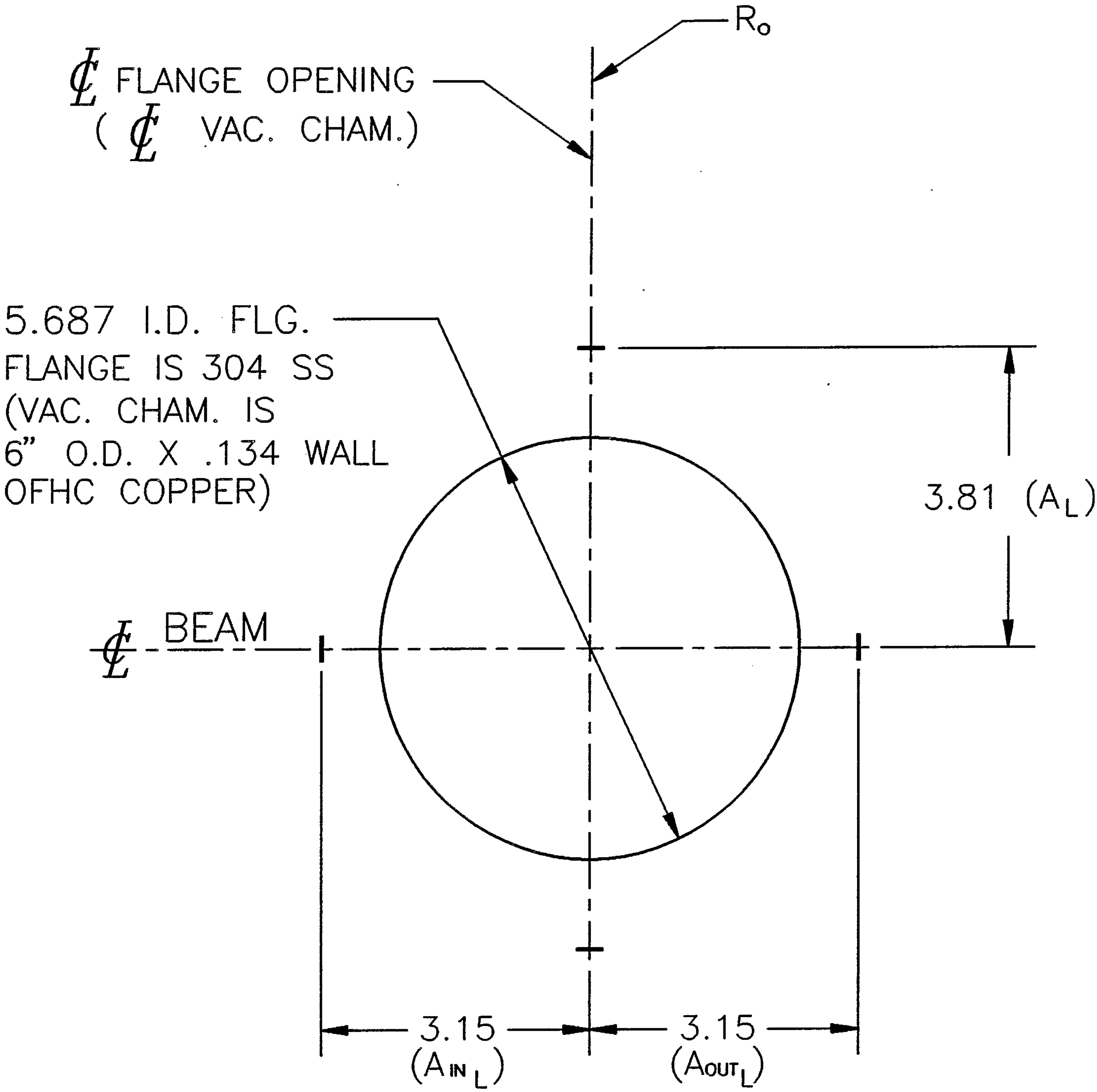

B10, C10, D10, J10, K10

RF CAVITIES

REF. DWGS.: D06-M-879-6 & D06-M-670-3

VIEW LOOKING DOWNSTREAM

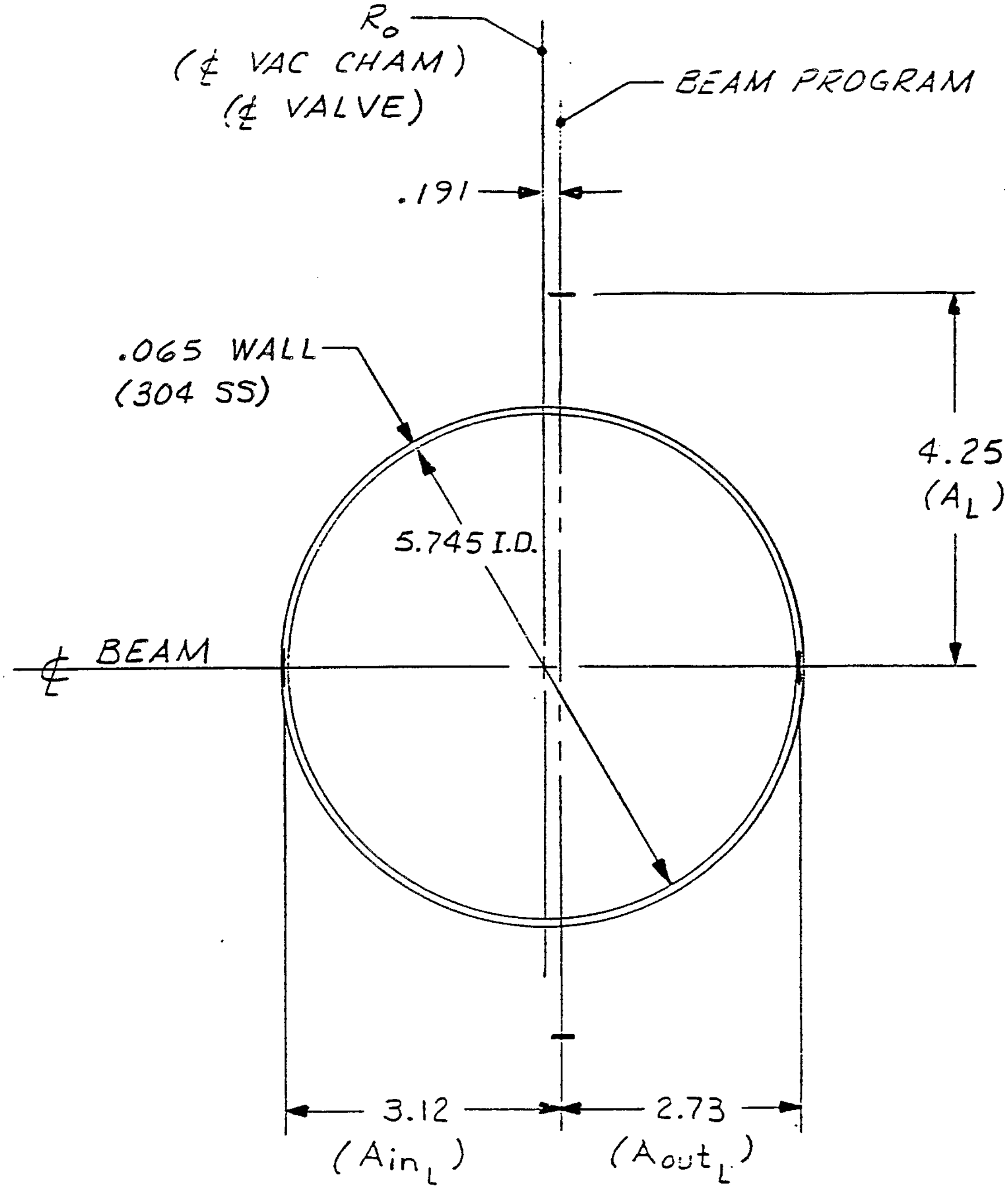

B13 THRU L13

REF DWGS: D05-M-959-4 & D05-M-962

DOWNSTREAM FLANGE (VIEW LOOKING DOWNSTREAM)

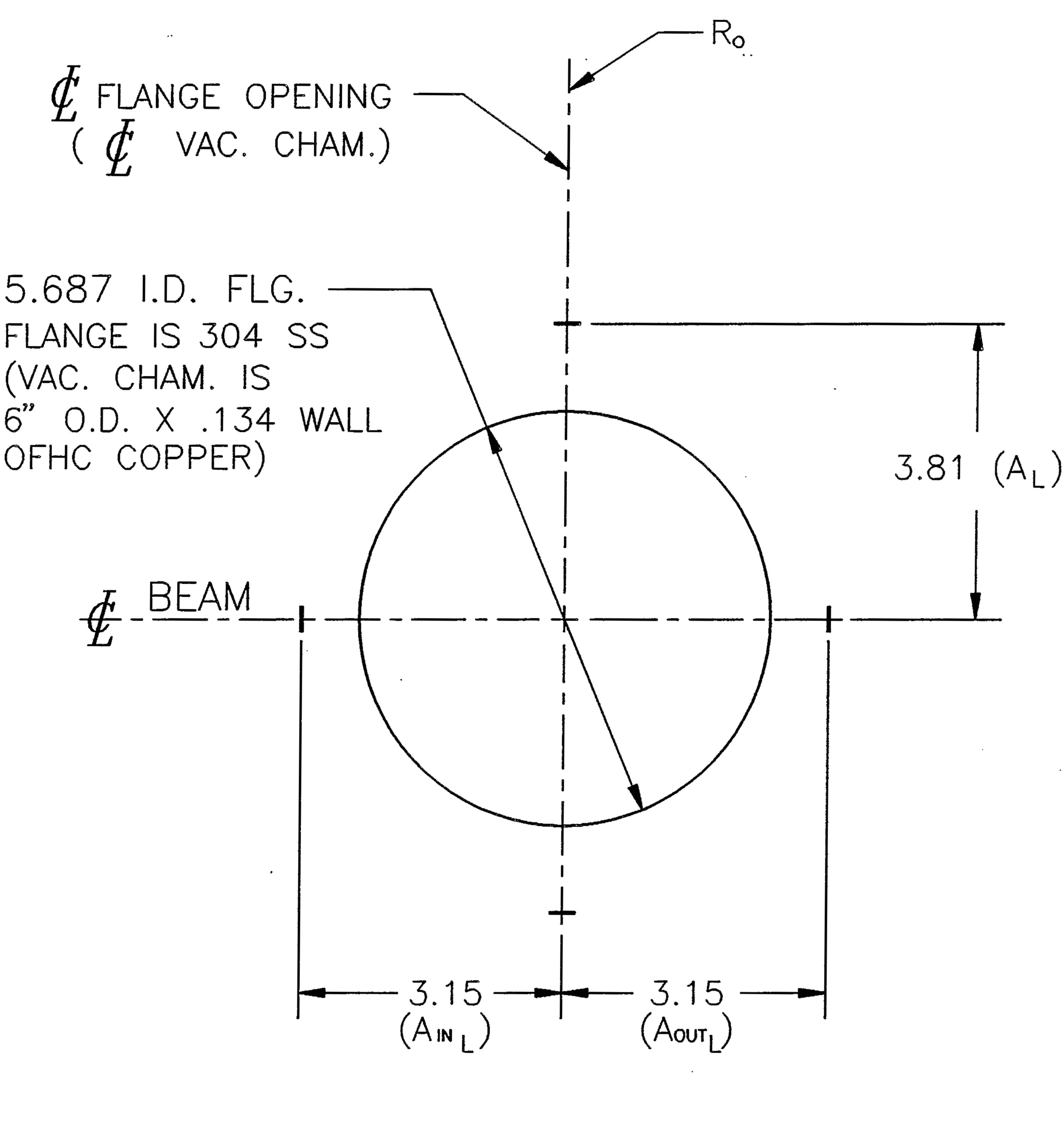

B20, C20, D20, I20, J20, K20

RF CAVITIES

REF. DWGS.: D06-M-879-6 & D06-M-669-3

UPSTREAM (VIEW LOOKING DOWNSTREAM)

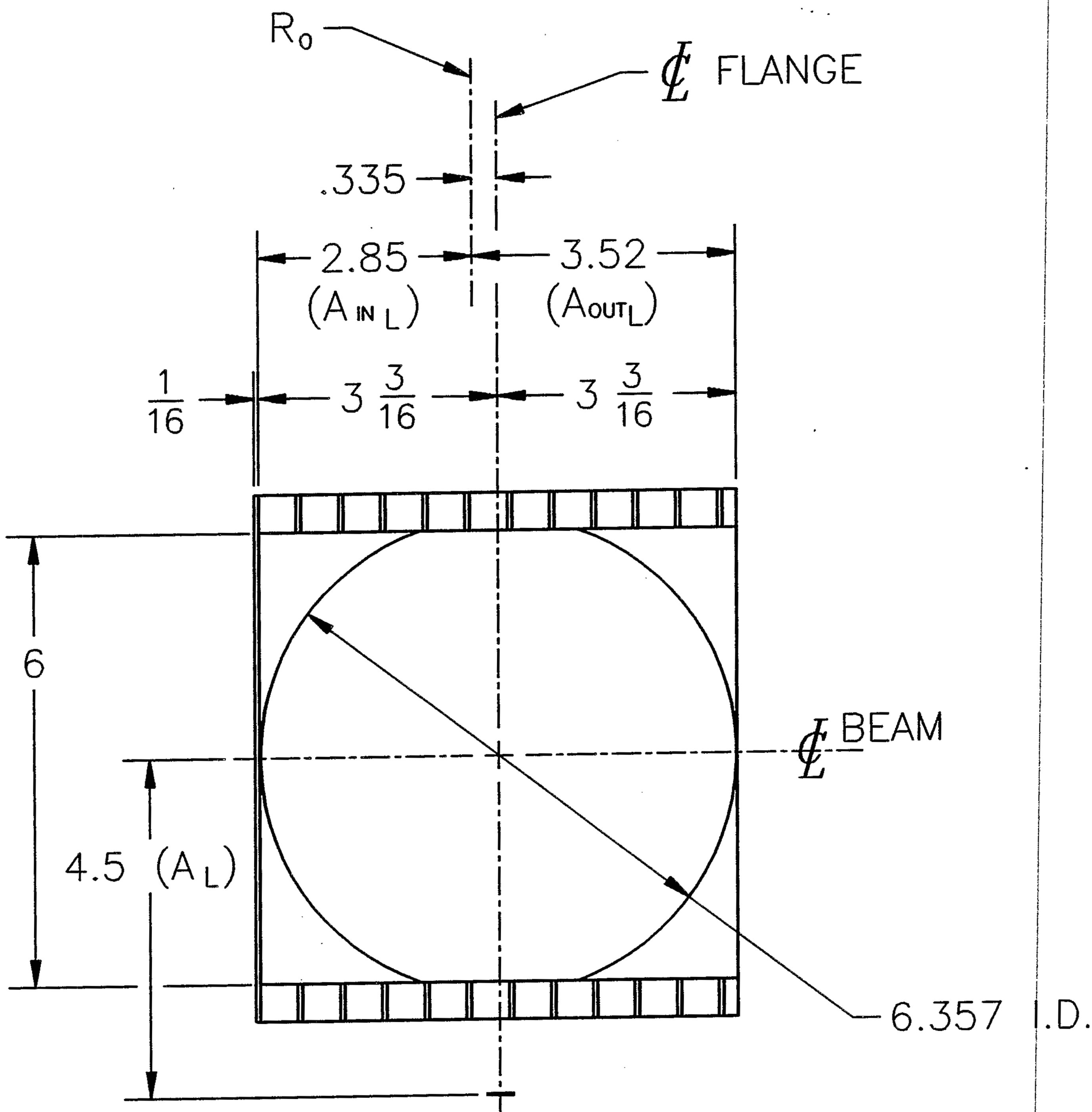

C5

IONIZATION PROFILE MONITOR

REF. DWGS.: D11-M-11926-5 & D11-M-11908-5

UPSTREAM (VIEW LOOKING DOWNSTREAM)

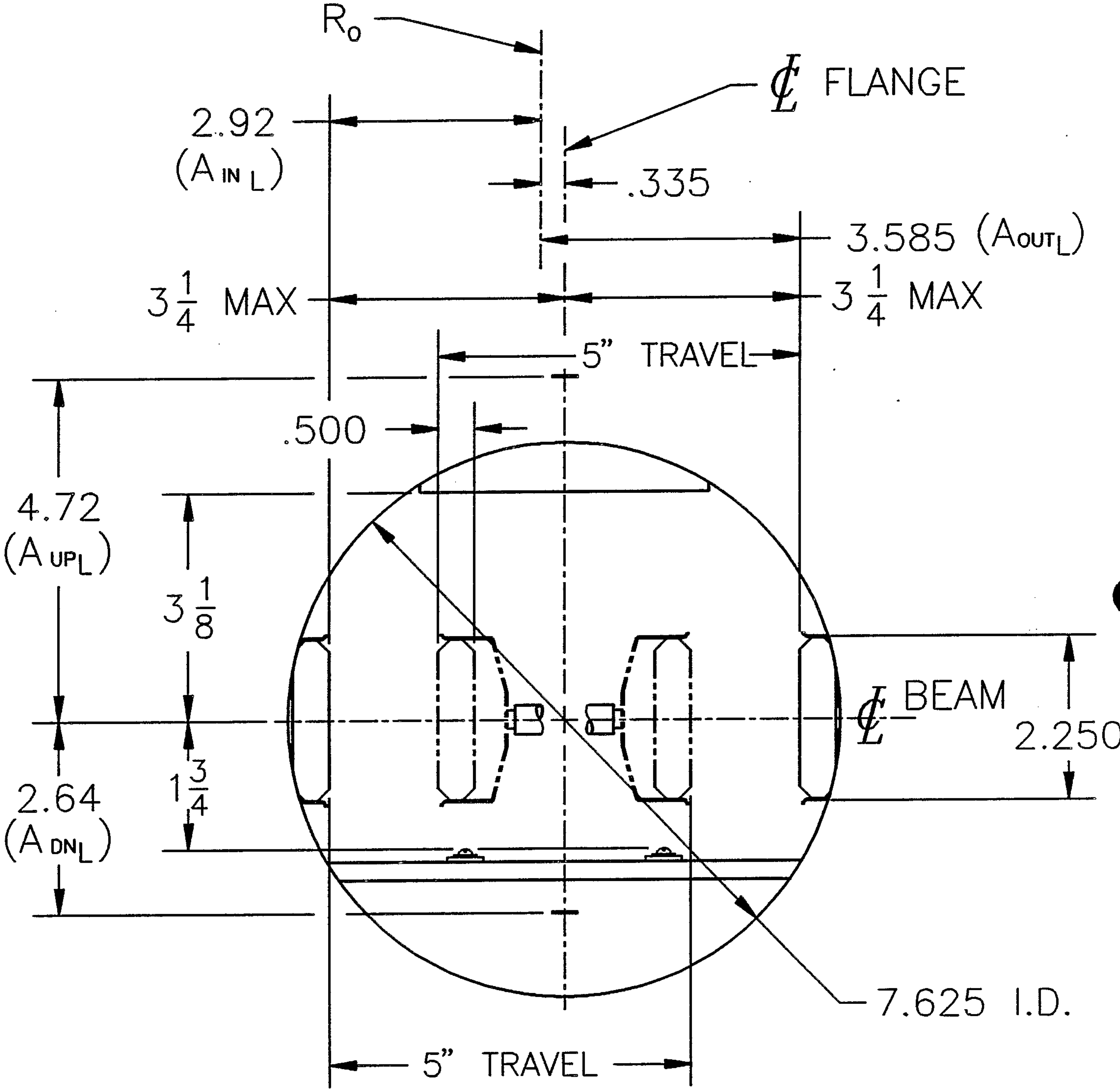

C5

JUMP TARGET

REF. DWGS.: D11-M-11812-5

SECTION THRU UPSTREAM END
VIEW LOOKING DOWNSTREAM

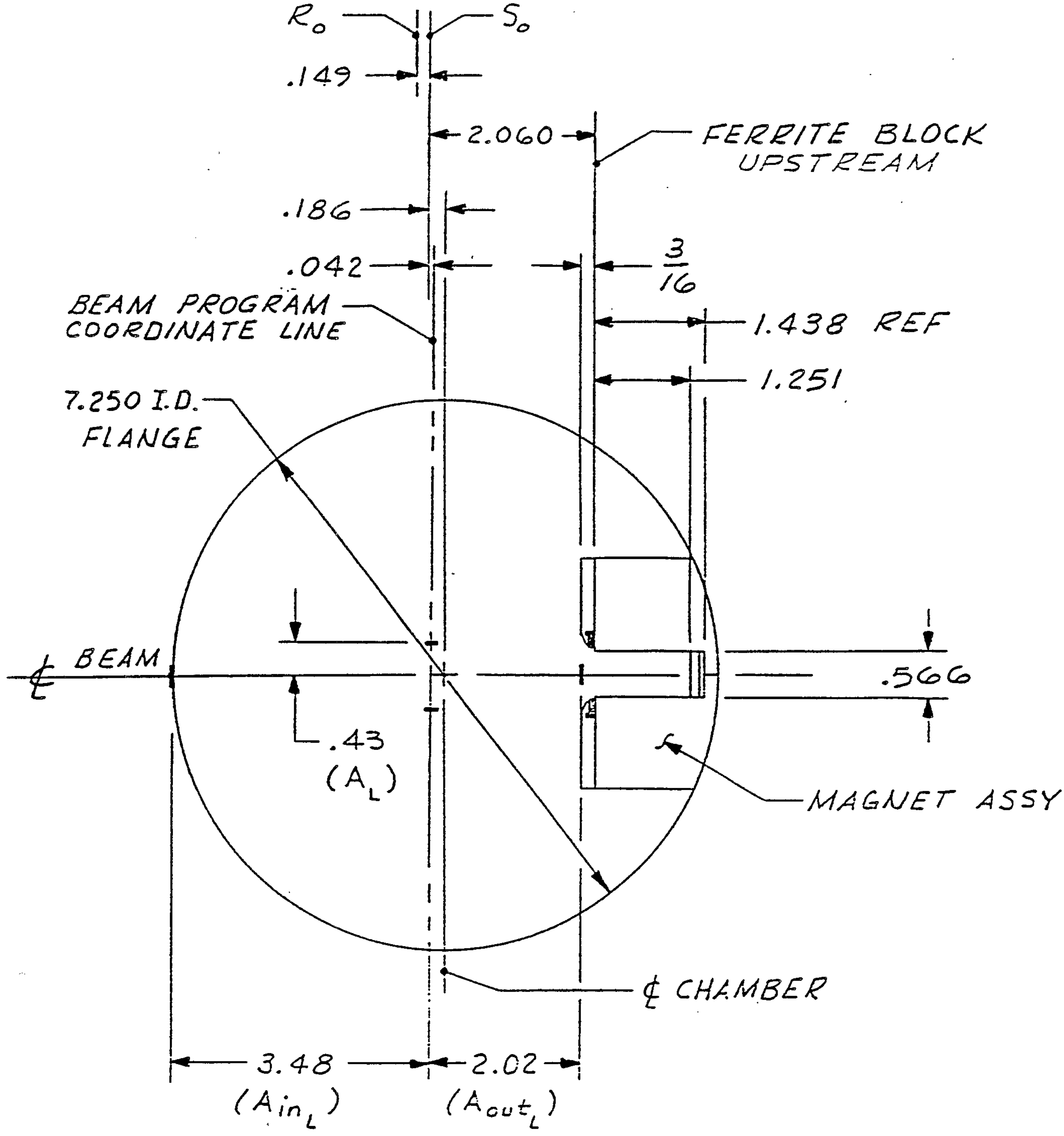

E5
CONVERTIBLE KICKER

REF DWGS: D11-M-11272-5, D11-M-11350-5 & D11-M-11271-5

SECTION THRU DOWNSTREAM END

VIEW LOOKING DOWNSTREAM

3-20-85

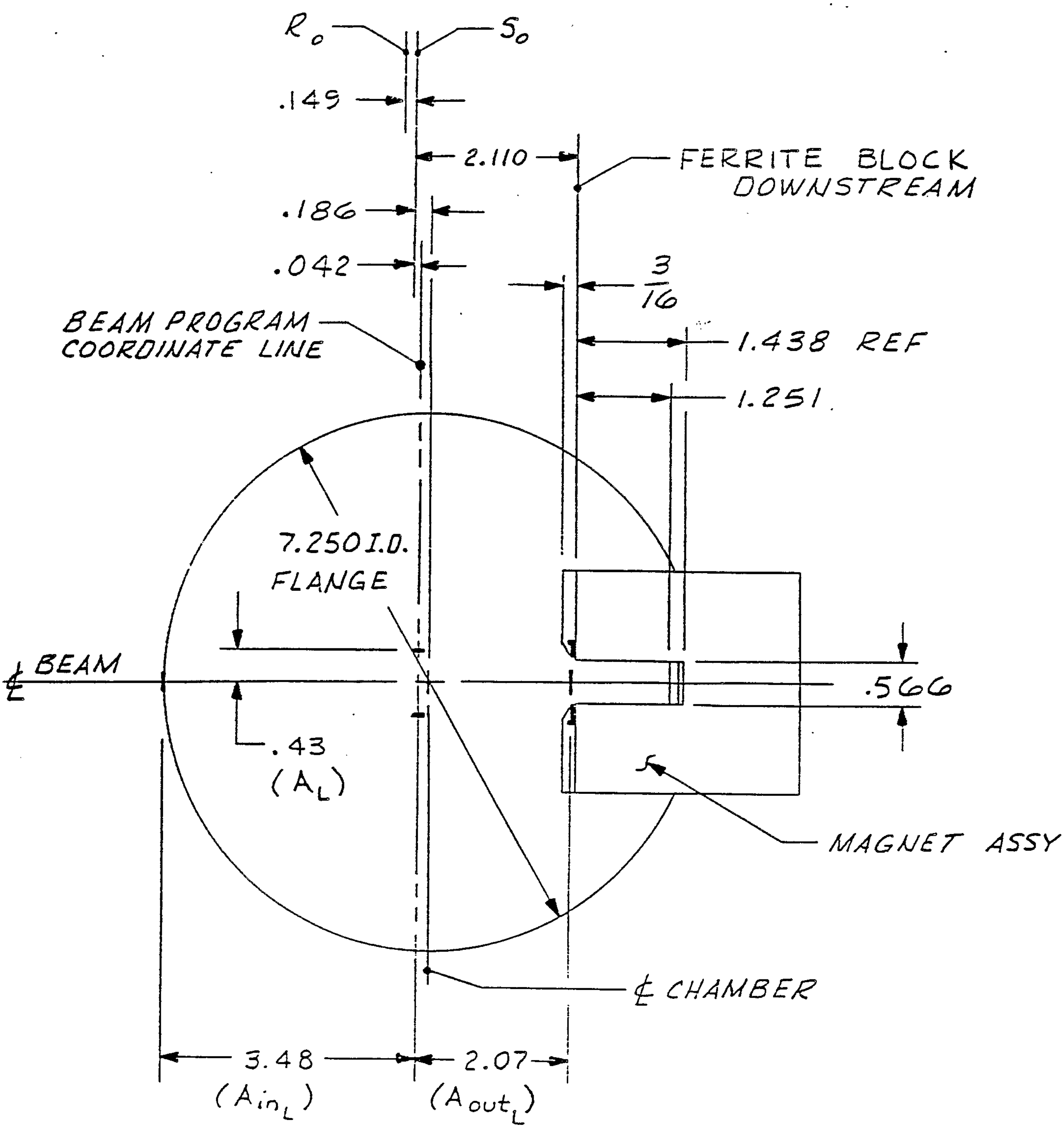

E5

CONVERTIBLE KICKER

REF DWGS: D11-M-11272-5, D11-M-11350-5 & D11-M-11271-5

UPSTREAM (VIEW LOOKING DOWNSTREAM)

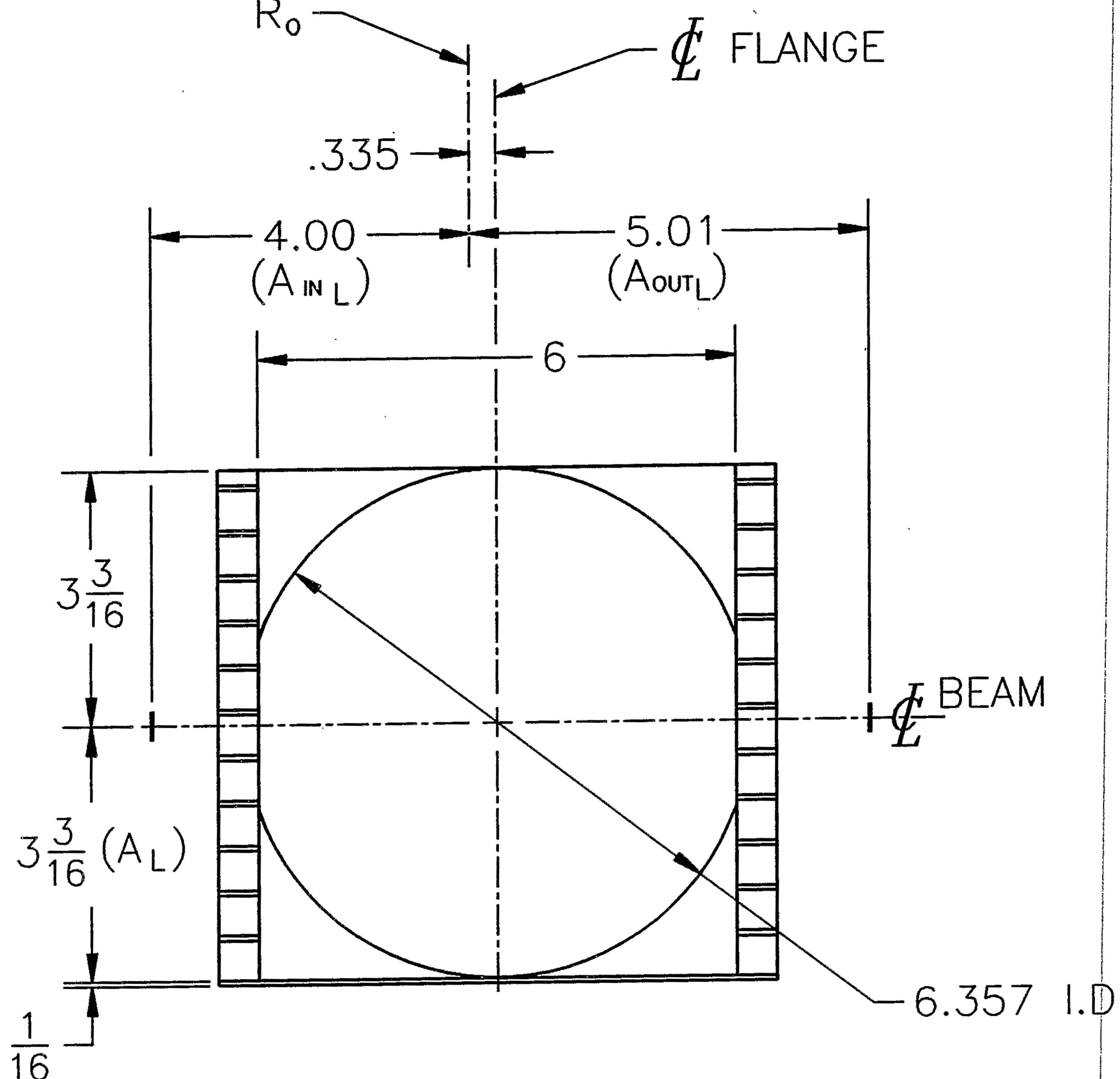

E15

IONIZATION PROFILE MONITOR

REF. DWGS.: D11-M-11925-5 & D11-M-11907-5

UPSTREAM (VIEW LOOKING DOWNSTREAM)

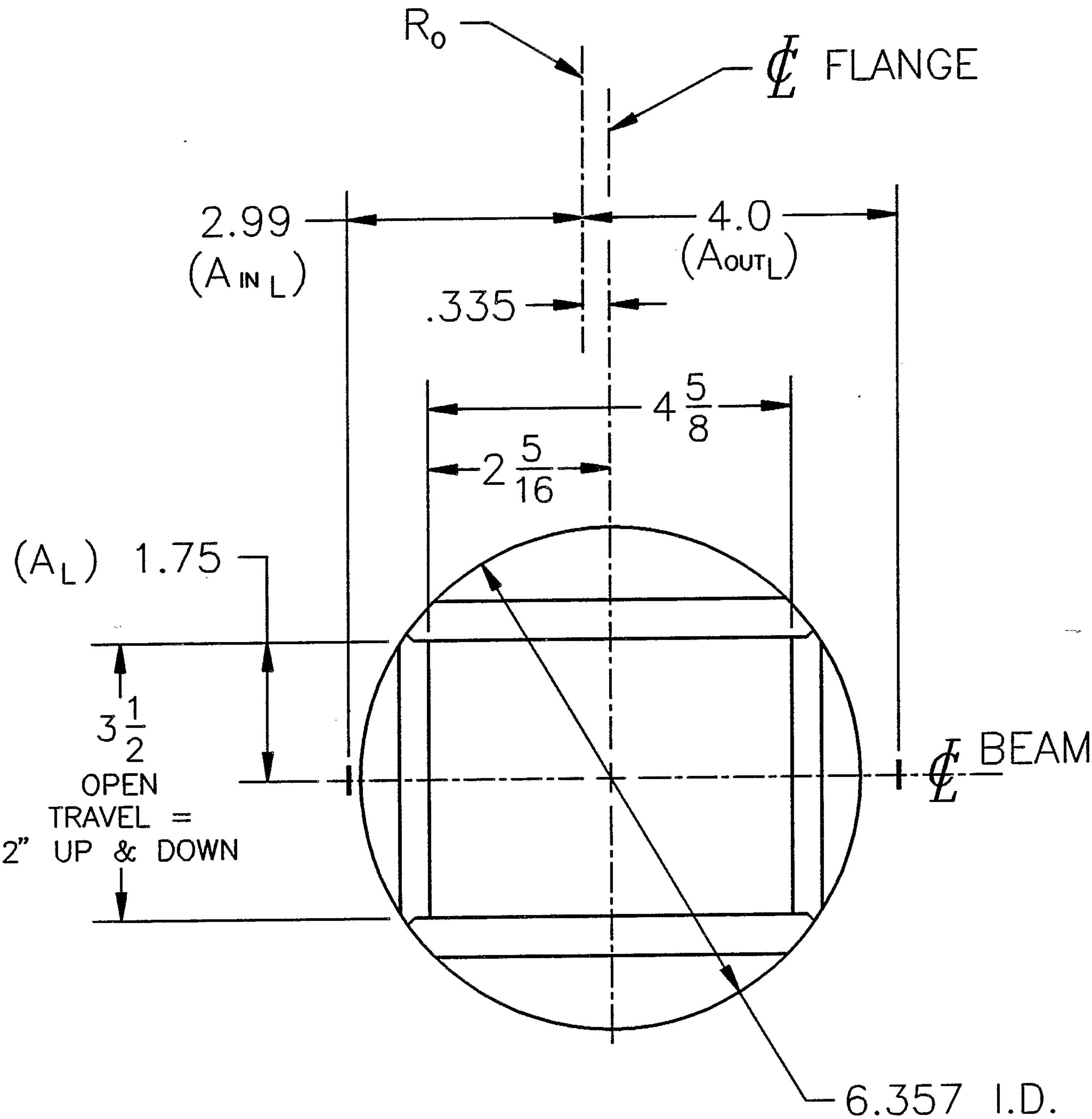

E15

JUMP TARGET

REF. DWGS.: D11-M-11838-5

SECTION THRU UPSTREAM END
VIEW LOOKING DOWNSTREAM

3-20-85

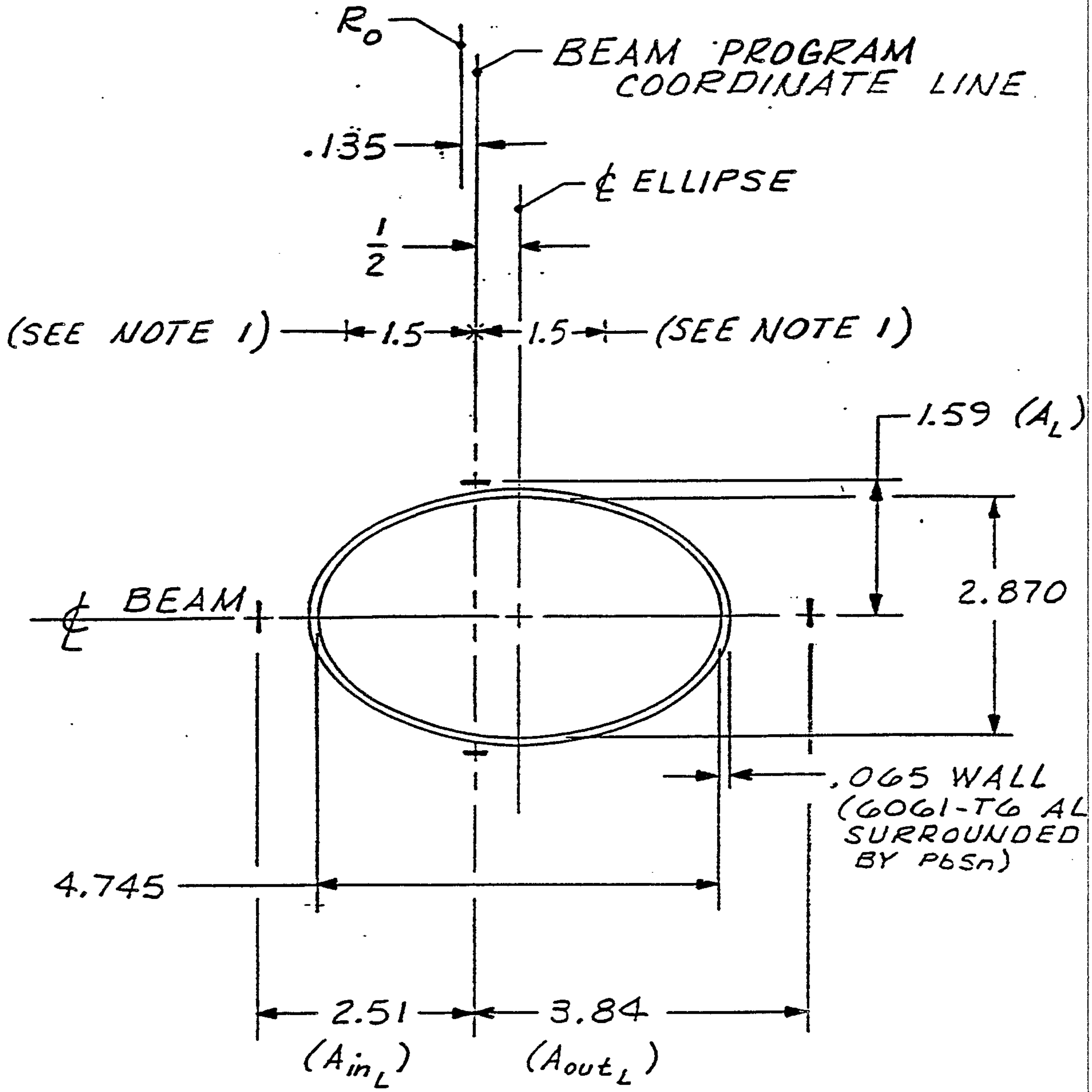

NOTE :

1. BEAM CATCHER SHOWN IN NOMINAL OPERATING POSITION. MOVEMENT IS ± 1.5". (LIMITING SWITCH HAS BEEN TEMPORARILY DISABLED)

E-20
BEAM CATCHER

REF DWGS : D08-M-124-5 & D08-M-118-5

3-22-135

SECTION THRU DOWNSTREAM END
VIEW LOOKING DOWNSTREAM

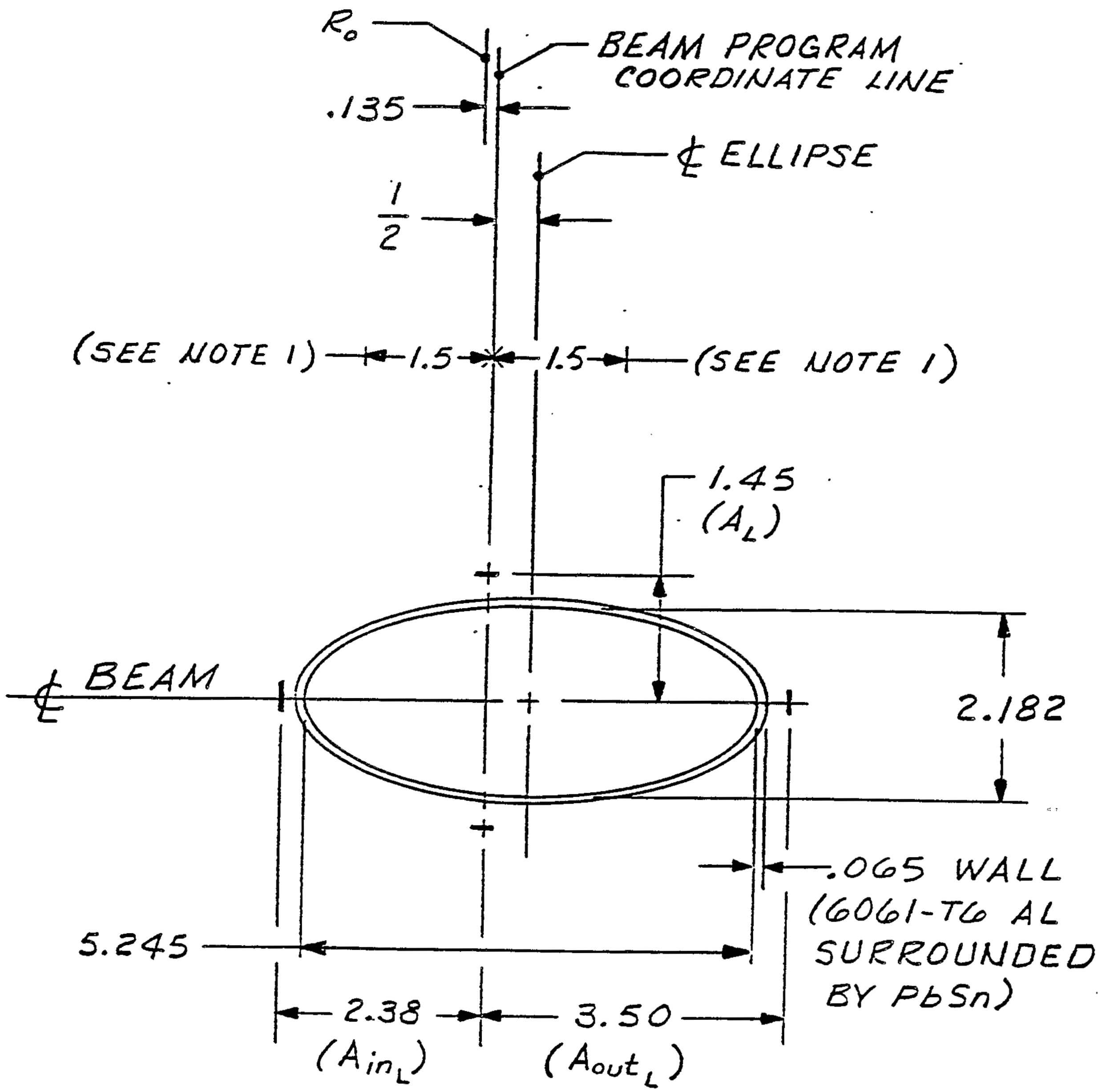

NOTES:

1. BEAM CATCHER SHOWN IN NOMINAL OPERATING POSITION. MOVEMENT IS ± 1.5. (LIMITING SWITCH HAS BEEN TEMPORARILY DISABLED)

E-20
BEAM CATCHER

REF DWGS: D08-M-124-5 & D08-M-118-5

VIEW LOOKING DOWNSTREAM

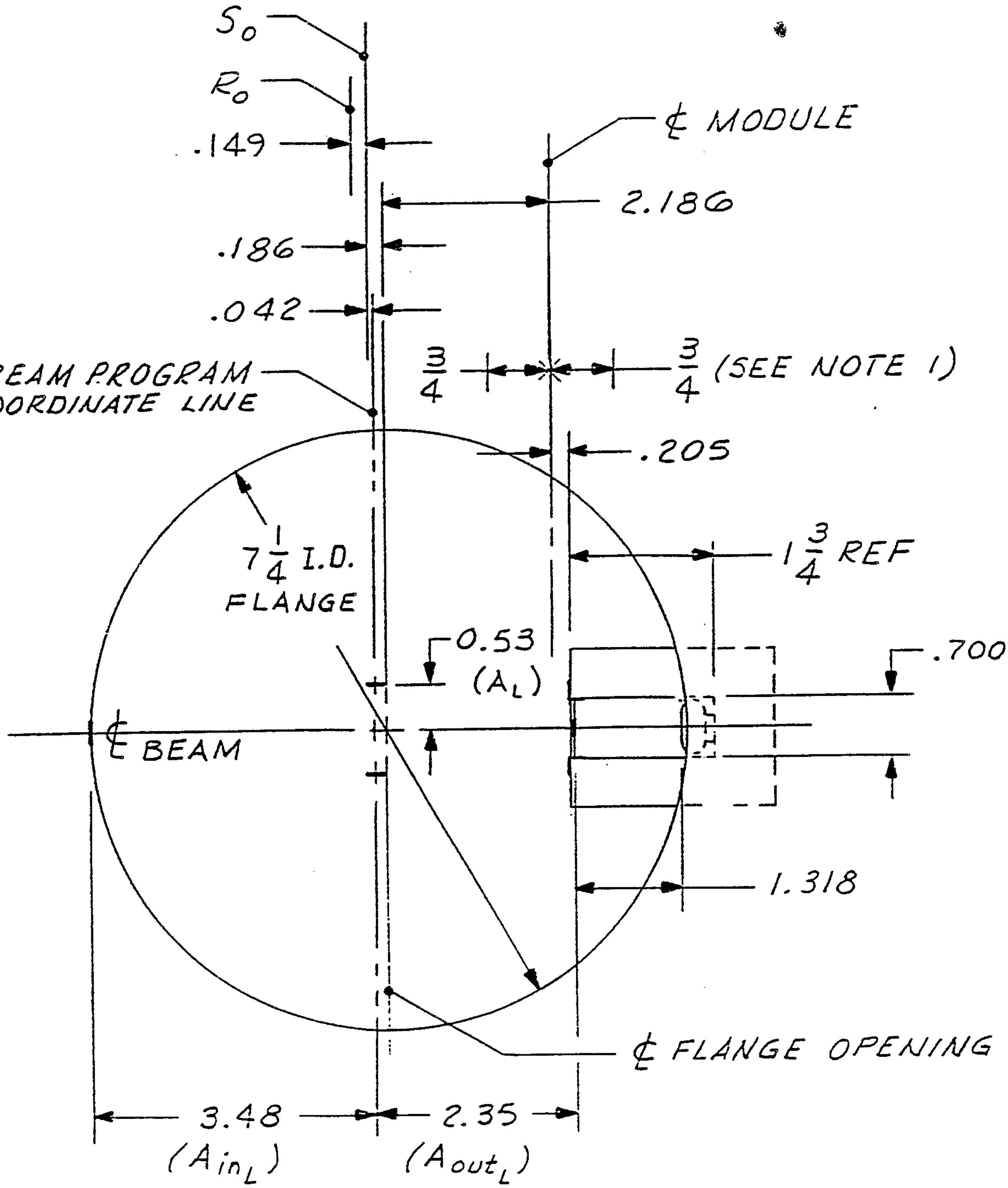

NOTES:

1. MAGNET SHOWN IN NOMINAL OPERATING POSITION. MOVEMENT IS ± 3/4"

F5

REF DWGS: DII-M-9313-5 DII-M-10909-4 & DII-M-9414-4

UPSTREAM END CORE #1

VIEW LOOKING DOWNSTREAM

4-5-85

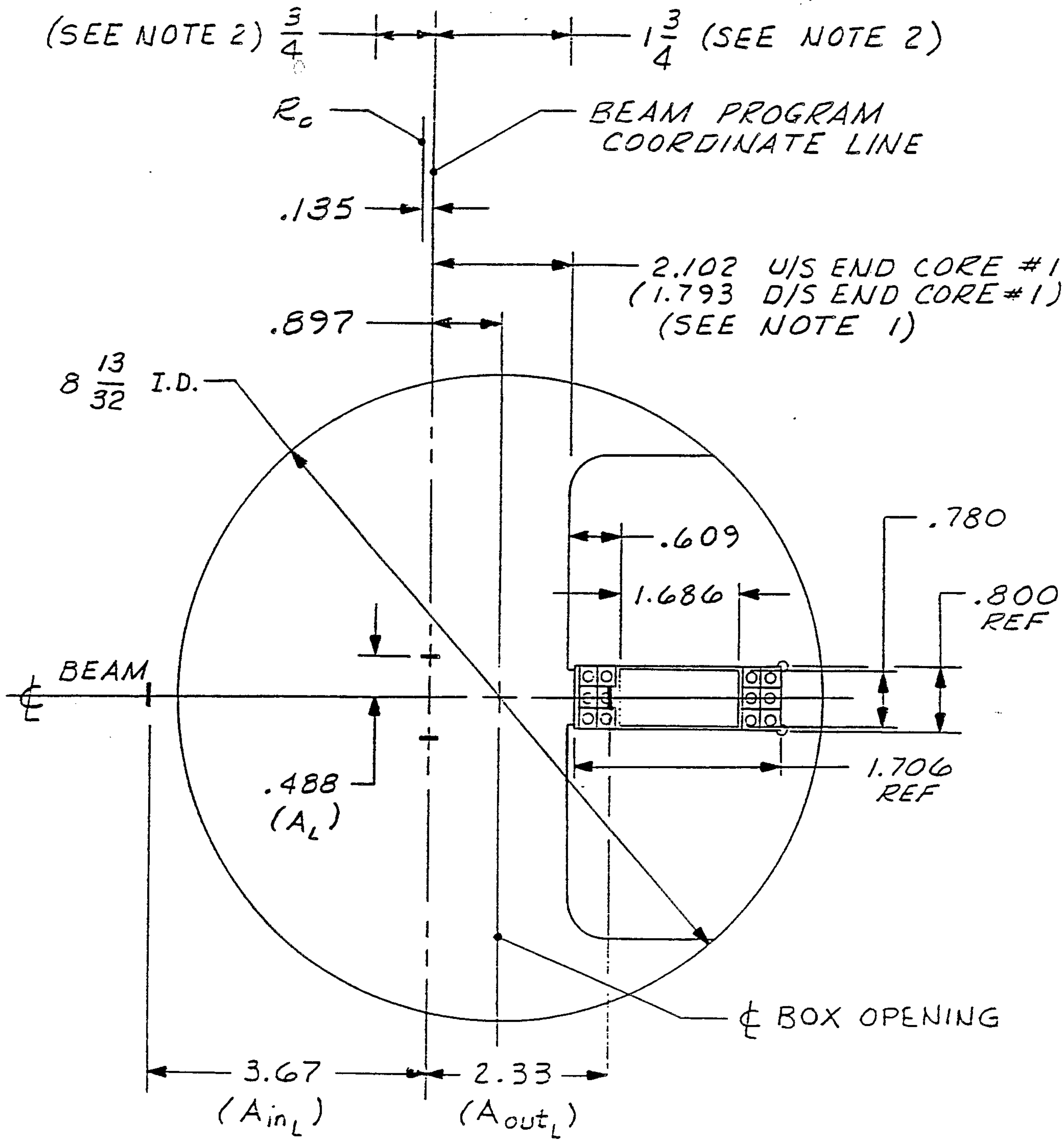

NOTES:

1. CORE #1 (D11-M-2339-5) IS LOCATED IN UPSTREAM END OF F-10 MAGNET ASSEMBLY.
2. MAGNET SHOWN IN NOMINAL OPERATING POSITION. MOVEMENT IS 3/4" TO BEAM; 1 3/4" FROM BEAM.

F10

REF DWGS: D11-M-8701-5 & D11-M-8711-5

4-5-85

DOWNSTREAM END CORE #1
VIEW LOOKING DOWNSTREAM

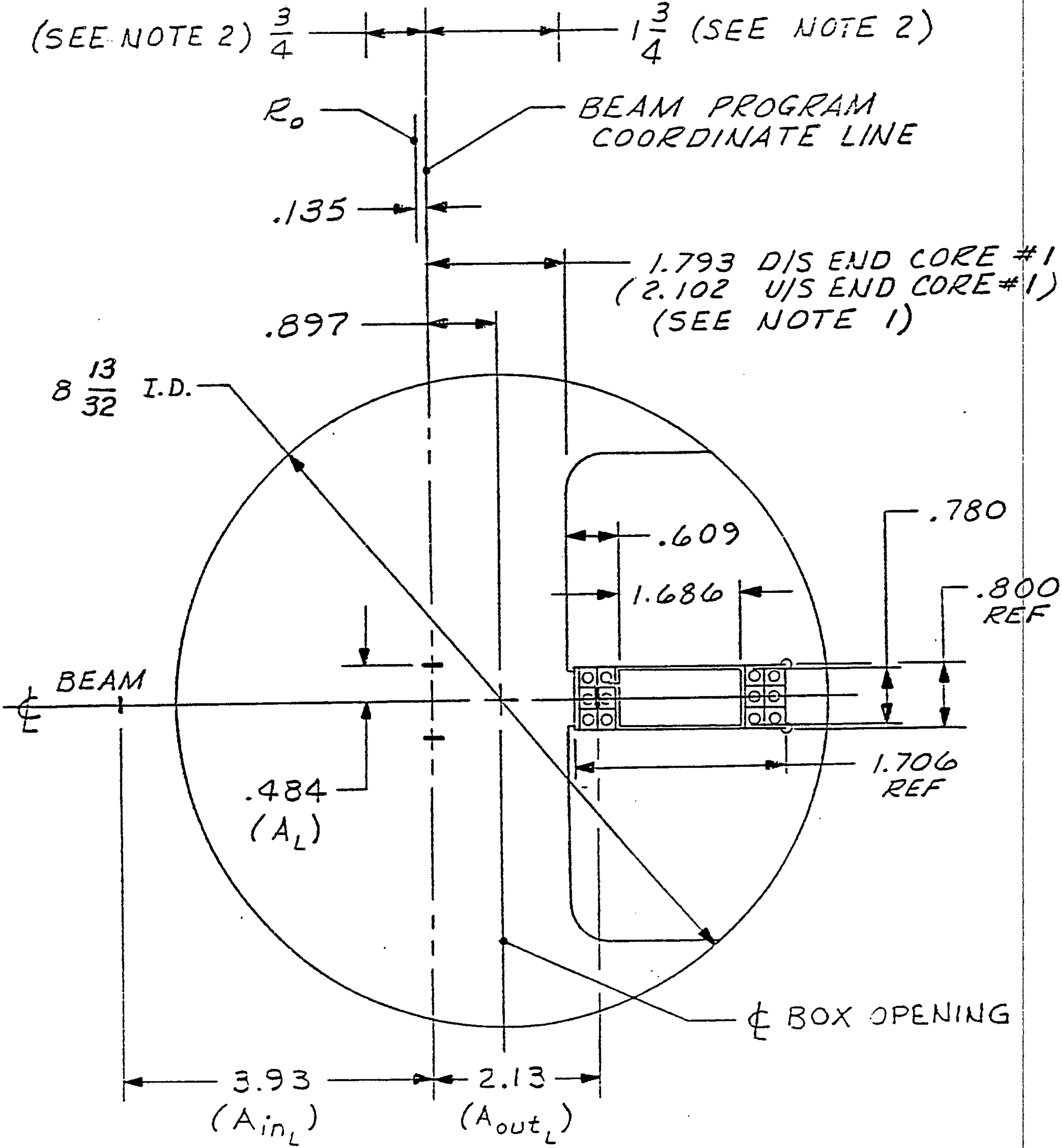

NOTES:

1. CORE #1 (D11-M-2339-5) IS LOCATED IN UPSTREAM END OF F-10 MAGNET ASSEMBLY.
2. MAGNET SHOWN IN NOMINAL OPERATING POSITION. MOVEMENT IS 3/4" TO BEAM; 1 3/4" FROM BEAM.

F10

REF DWGS: D11-M-8701-5 & D11-M-8711-5

DOWNSTREAM END CORE #2 4-5-85

VIEW LOOKING DOWNSTREAM

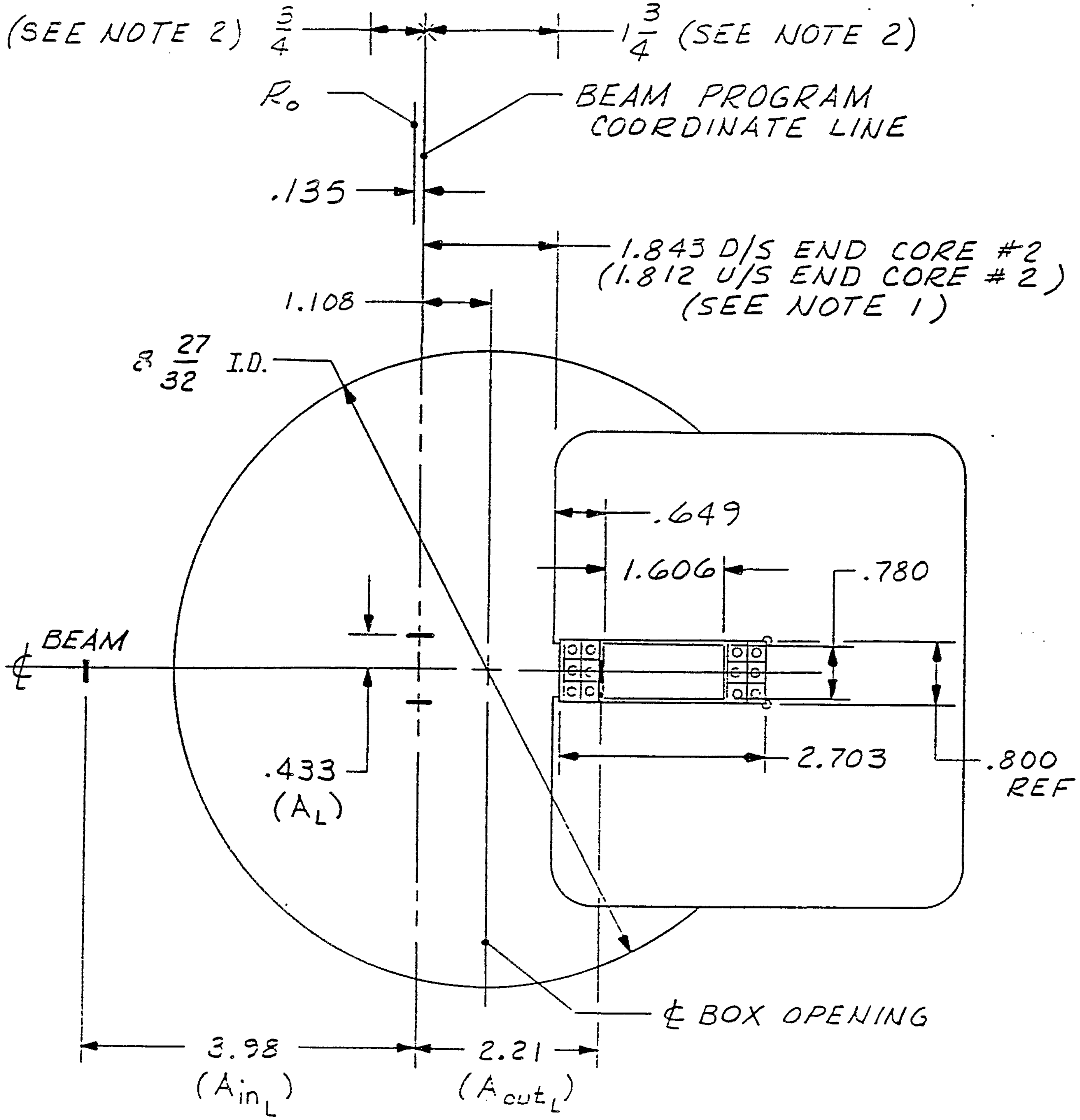

NOTES:

1. CORE #2 (D11-M-2338-5) IS LOCATED IN DOWNSTREAM END OF F-10 MAGNET ASSEMBLY.
2. MAGNET SHOWN IN NOMINAL OPERATING POSITION. MOVEMENT IS 3/4" TO BEAM; 1 3/4" FROM BEAM.

F10

REF DWGS: D11-M-8701-5 & D11-M-8711-5

VIEW LOOKING DOWNSTREAM

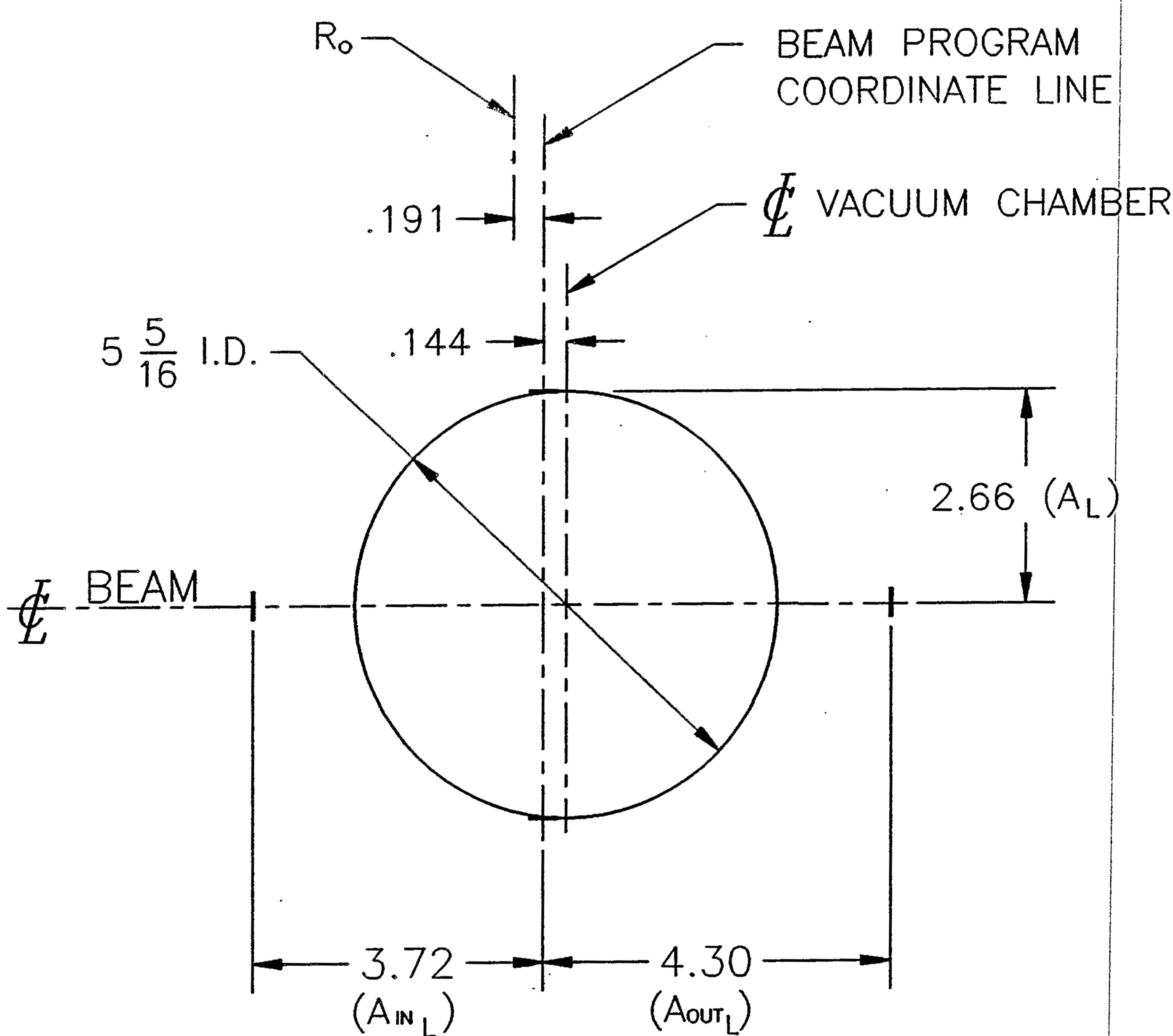

F15

BEAM CURRENT TRANSFORMER

REF. DWGS.: D09-M-372-5

SECTION THRU UPSTREAM END

VIEW LOOKING DOWNSTREAM

3-20-85

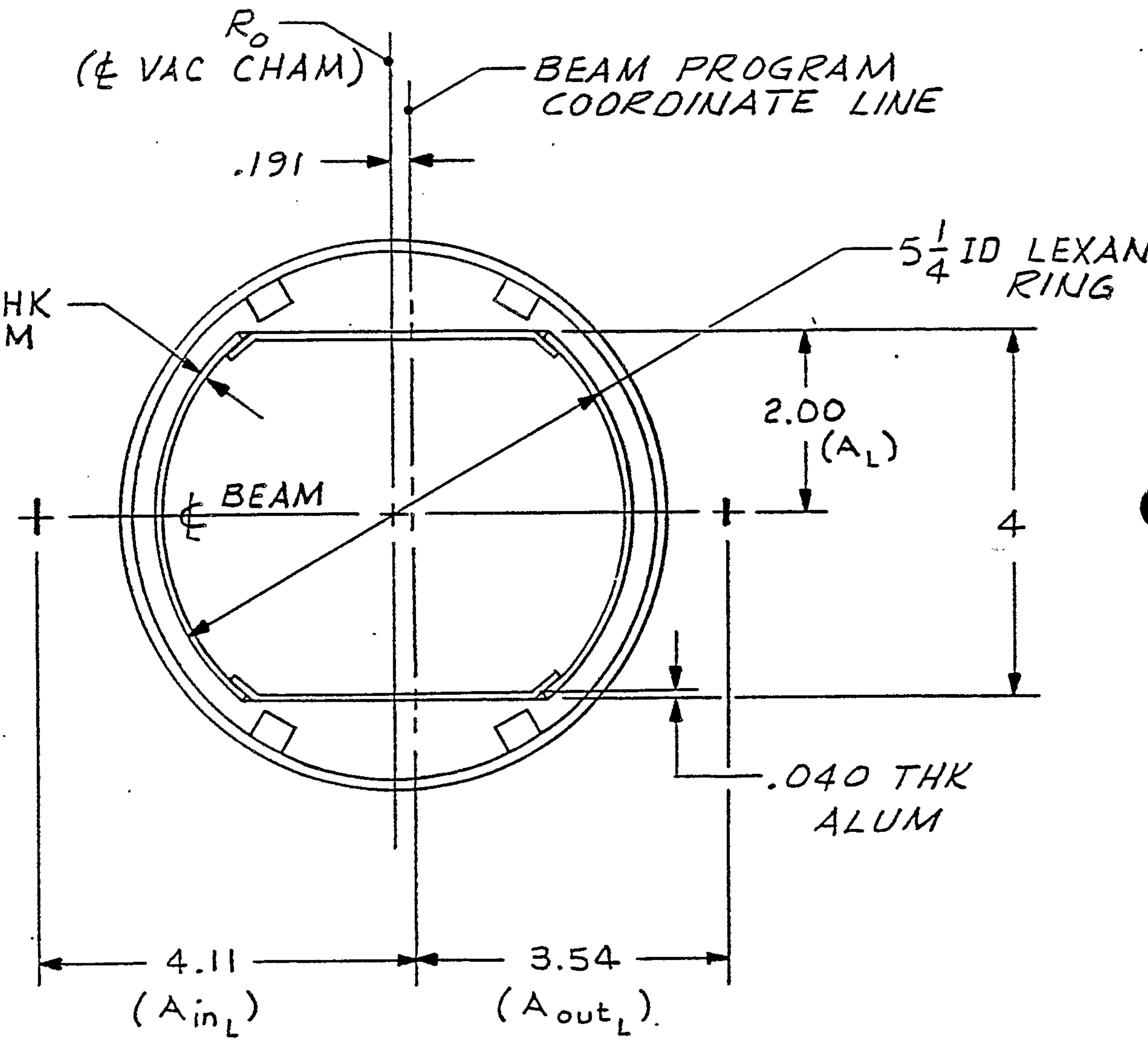

G7, J7, L7

VERTICAL PICK-UP ELECTRODE

REF DWGS: D06-M-165-4 & D06-M-254-4

SECTION THRU DOWNSTREAM END

3-20-85

VIEW LOOKING DOWNSTREAM

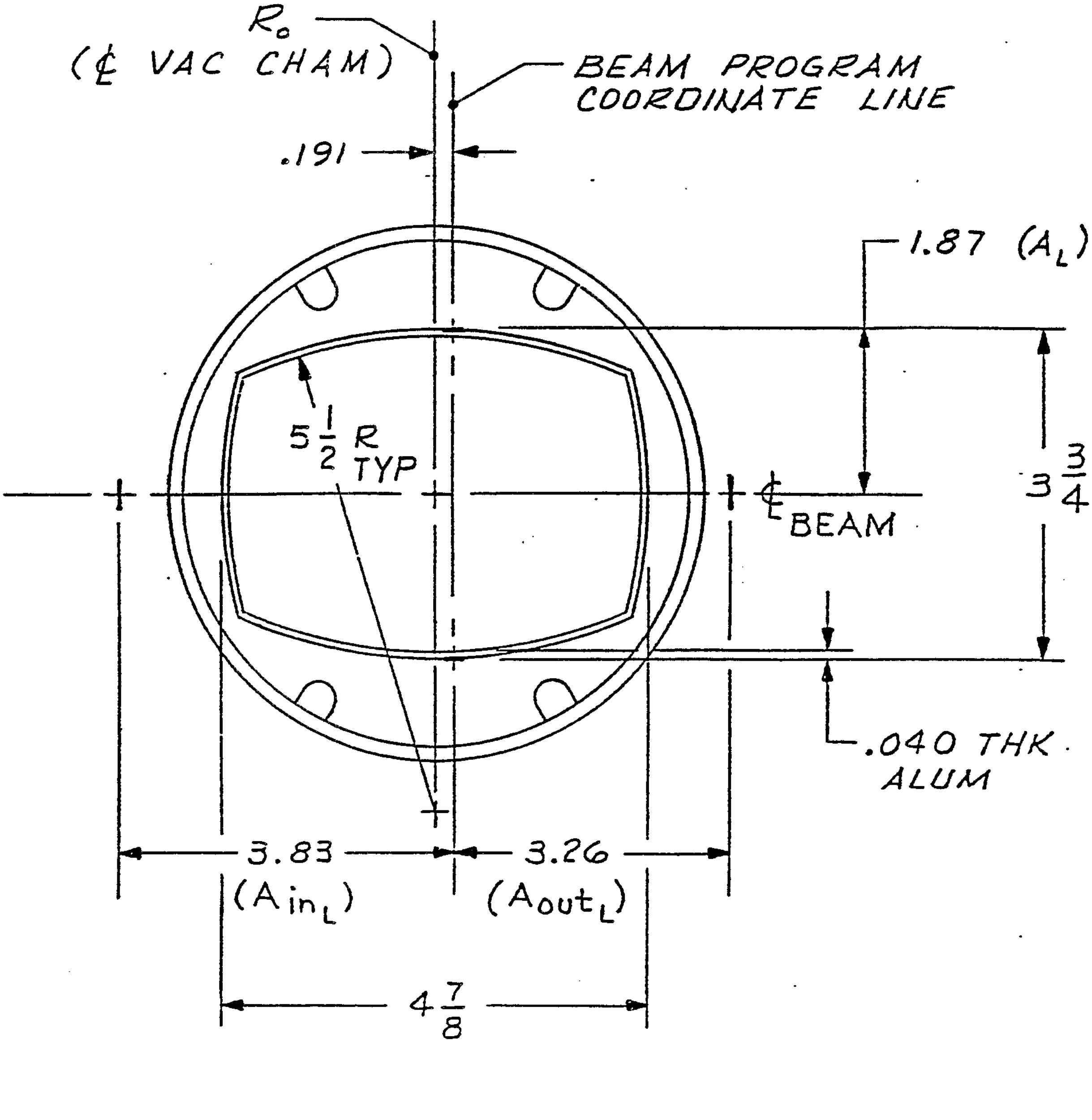

G7, J7, L7

HORIZONTAL PICK-UP ELECTRODE

REF DWGS: D06-M-254-4 & D06-M-165-4

INSERTED POSITION

VIEW LOOKING DOWNSTREAM

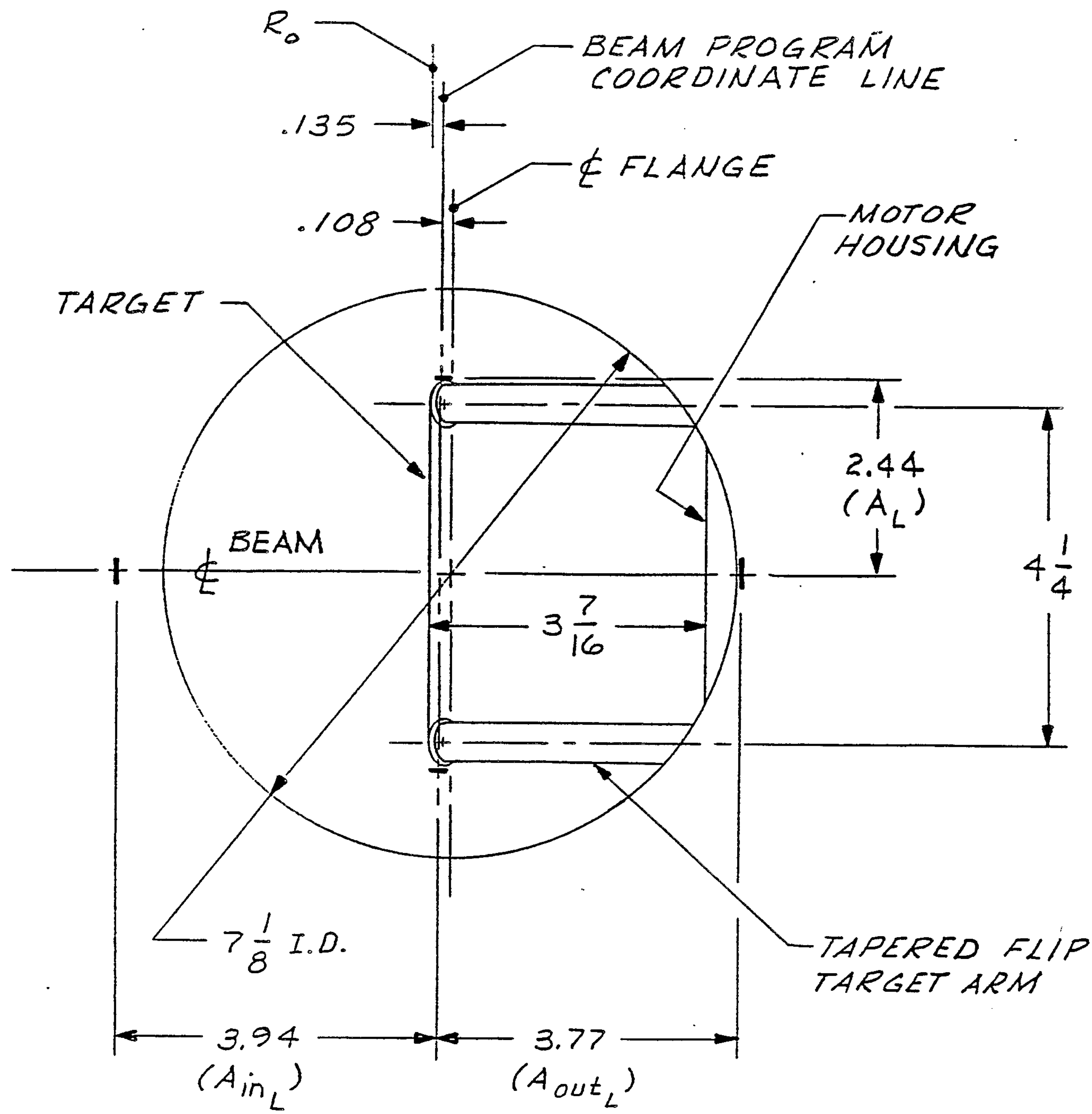

G10

POLARIMETER

REF DWGS: D11-M-11273-5 & D11-M-11282-5

UPSTREAM FLANGE (VIEW LOOKING DOWNSTREAM)

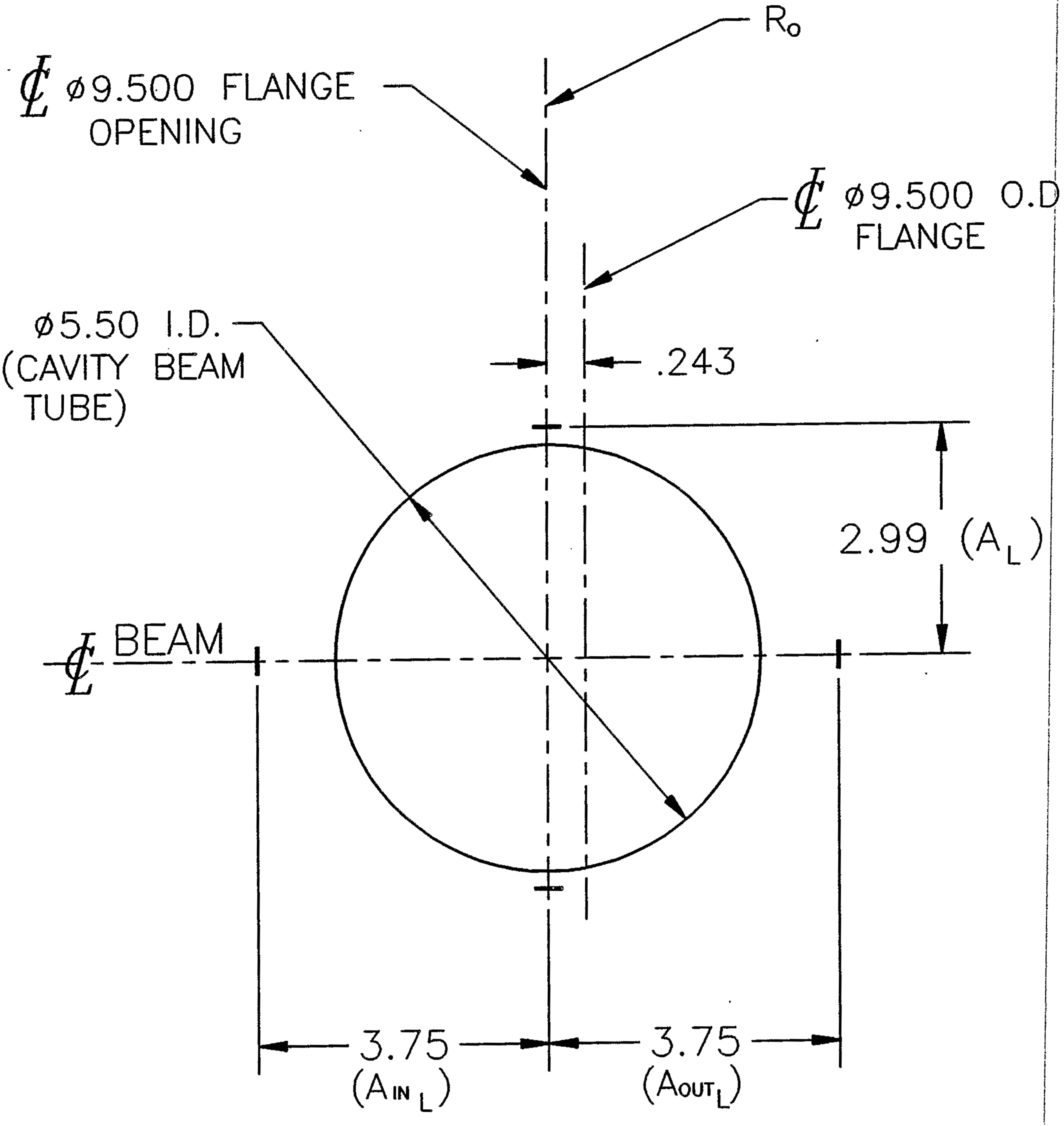

G20
VHF CAVITY

REF. DWGS.: D06-M-1411-5, D06-M-1453-5 & D06-M-1496-5

DOWNSTREAM (VIEW LOOKING DOWNSTREAM)

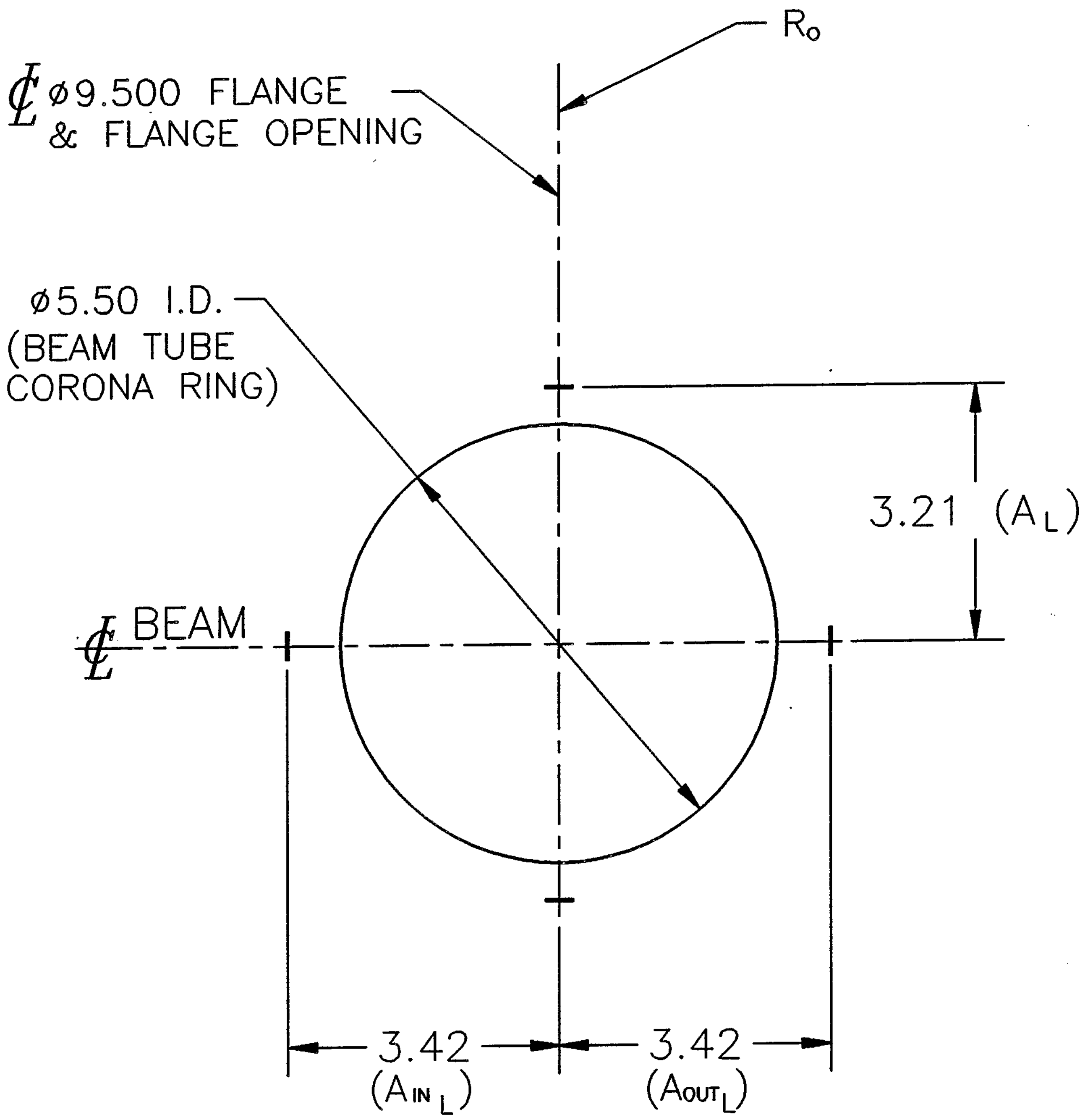

G20

VHF CAVITY

REF. DWGS.: D06-M-1411-5, D06-M-1453-5 & D06-M-1496-5

SECTION THRU UPSTREAM END
VIEW LOOKING DOWNSTREAM

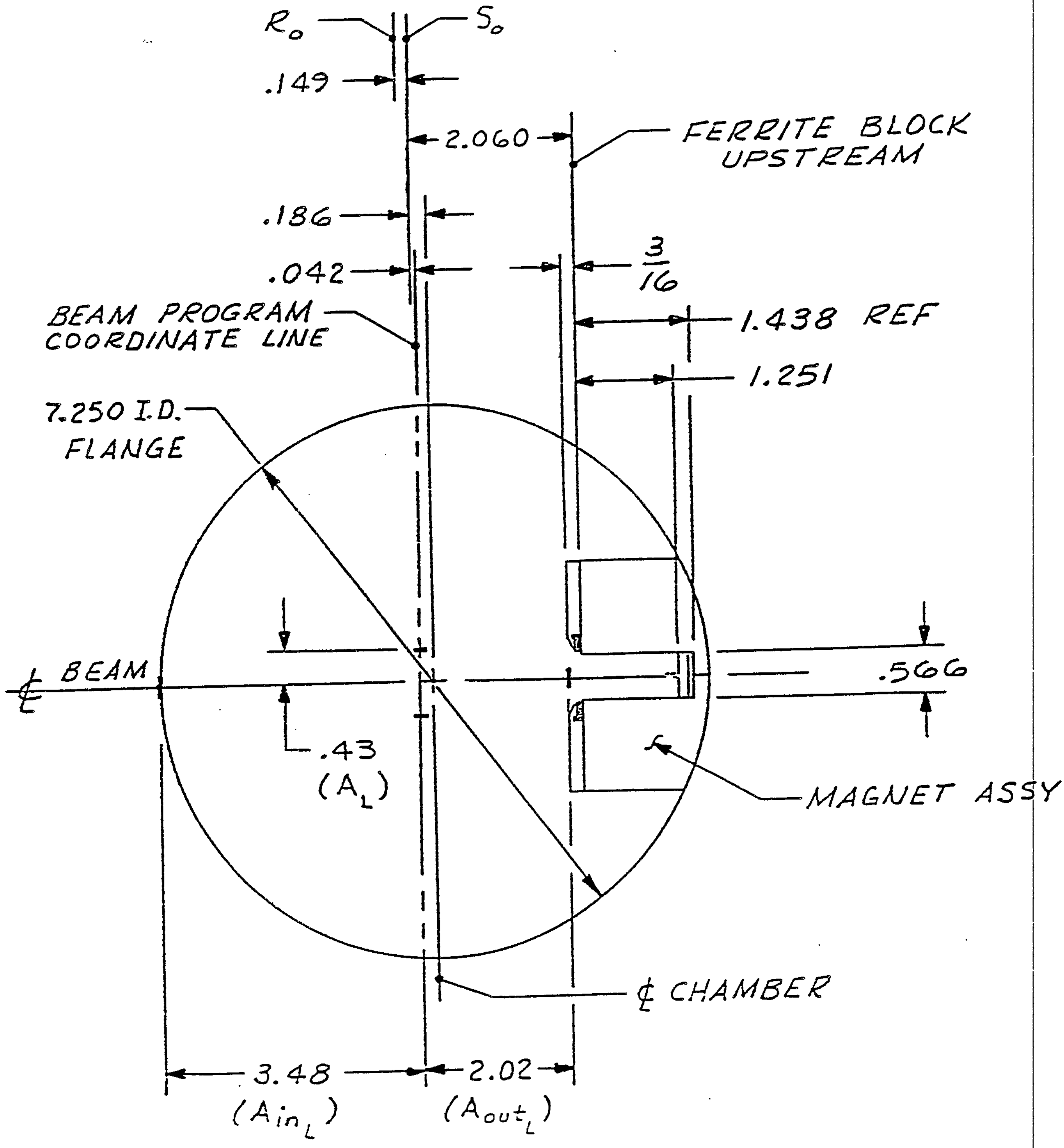

H5

CONVERTIBLE KICKER

REF DWGS: D11-M-11272-5, D11-M-11350-5 & D11-M-11271-5

3-20-85

SECTION THRU DOWNSTREAM END

VIEW LOOKING DOWNSTREAM

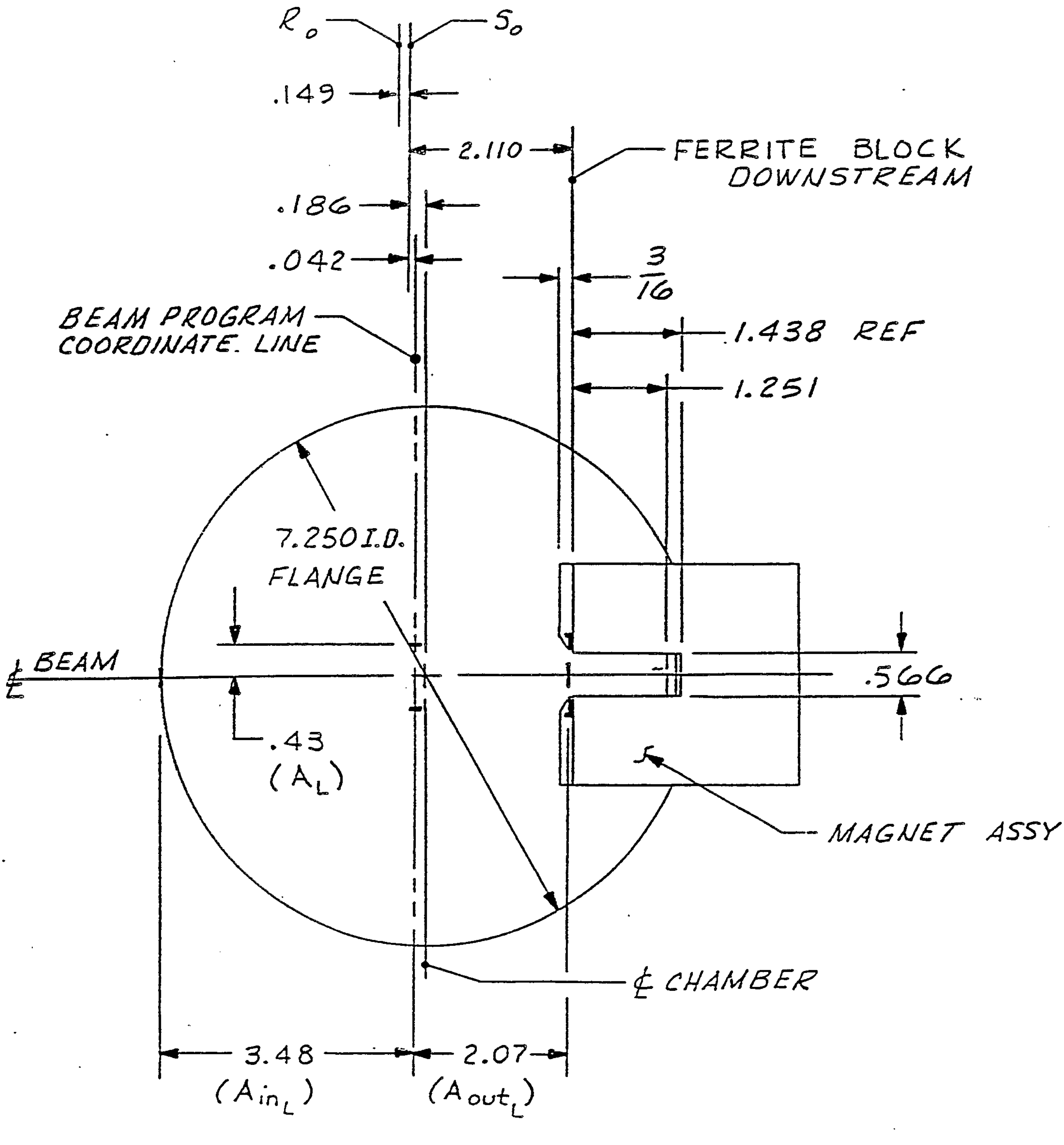

H5

CONVERTIBLE KICKER

REF DWGS: D11-M-11272-5, D11-M-11350-5 & D11-M-11271-5

SECTION THRU UPSTREAM END

VIEW LOOKING DOWNSTREAM

4-5-85

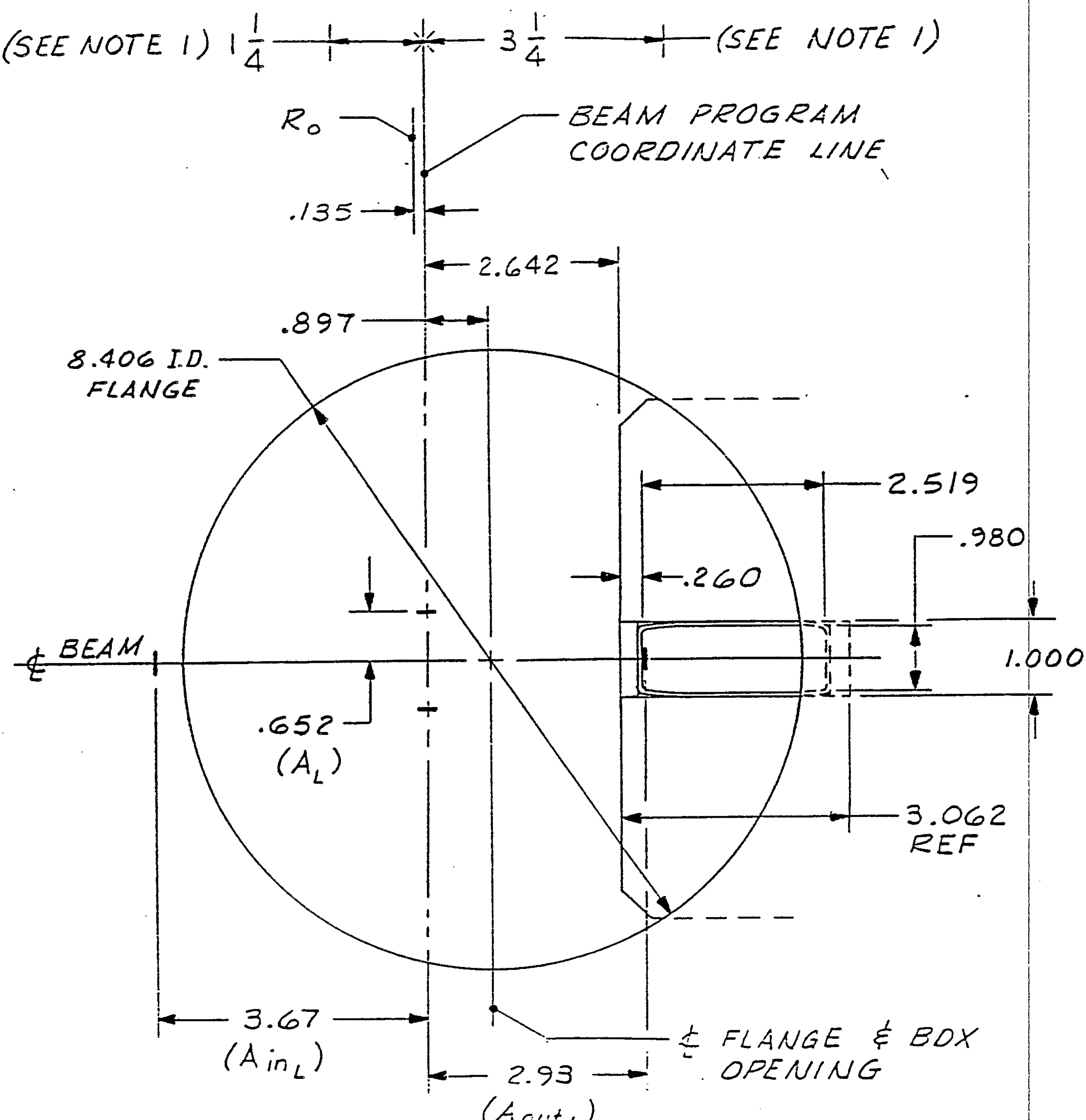

NOTE:

1. MAGNET SHOWN IN NOMINAL OPERATING POSITION. MOVEMENT IS 1¼" TO BEAM; 3¼" FROM BEAM.

H10

REF DWGS: D11-M-6959-4 & D11-M-11230-5

4-5-85

SECTION THRU DOWNSTREAM END
VIEW LOOKING DOWNSTREAM

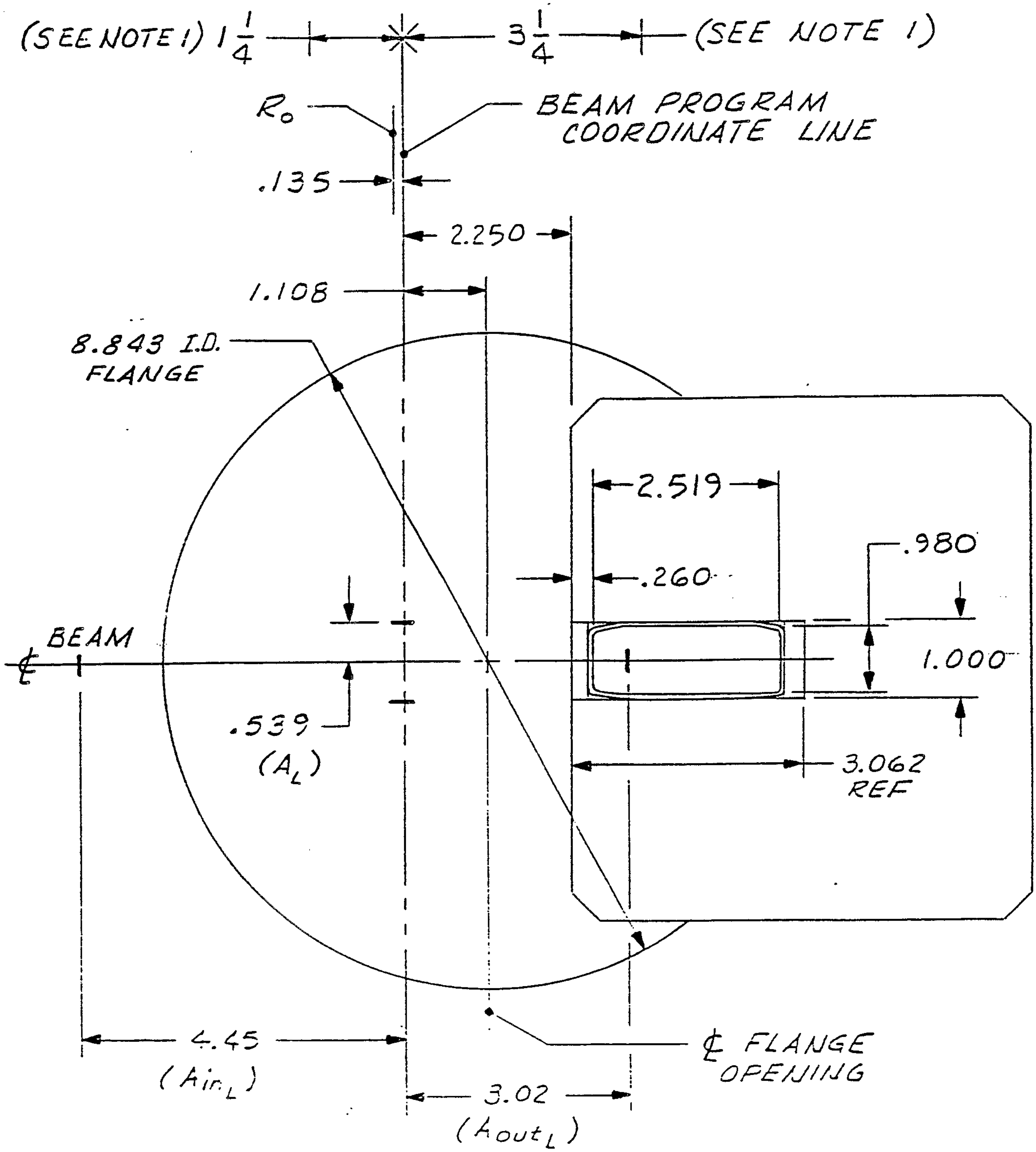

NOTE:
1. MAGNET SHOWN IN NOMINAL OPERATING POSITION. MOVEMENT IS 1 1/4" TO BEAM; 3 1/4" FROM BEAM.

H10

REF DWGS: D11-M-6959-4 & D11-M-11230-5

VIEW LOOKING DOWNSTREAM

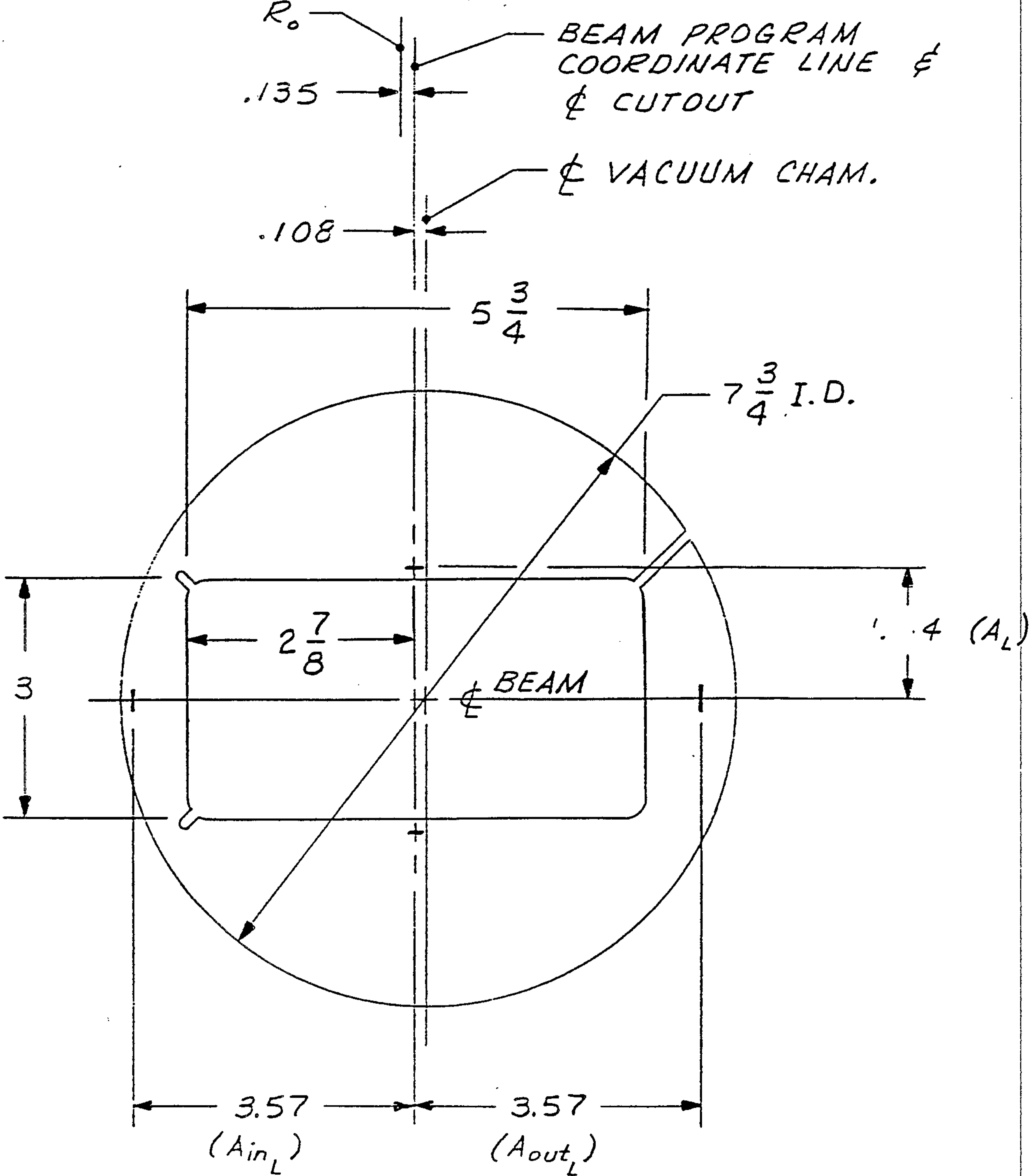

I 10
COHERENCE DAMPER

REF DWGS : D11-M-11570-5 & D11-M-11573-4

VIEW LOOKING DOWNSTREAM

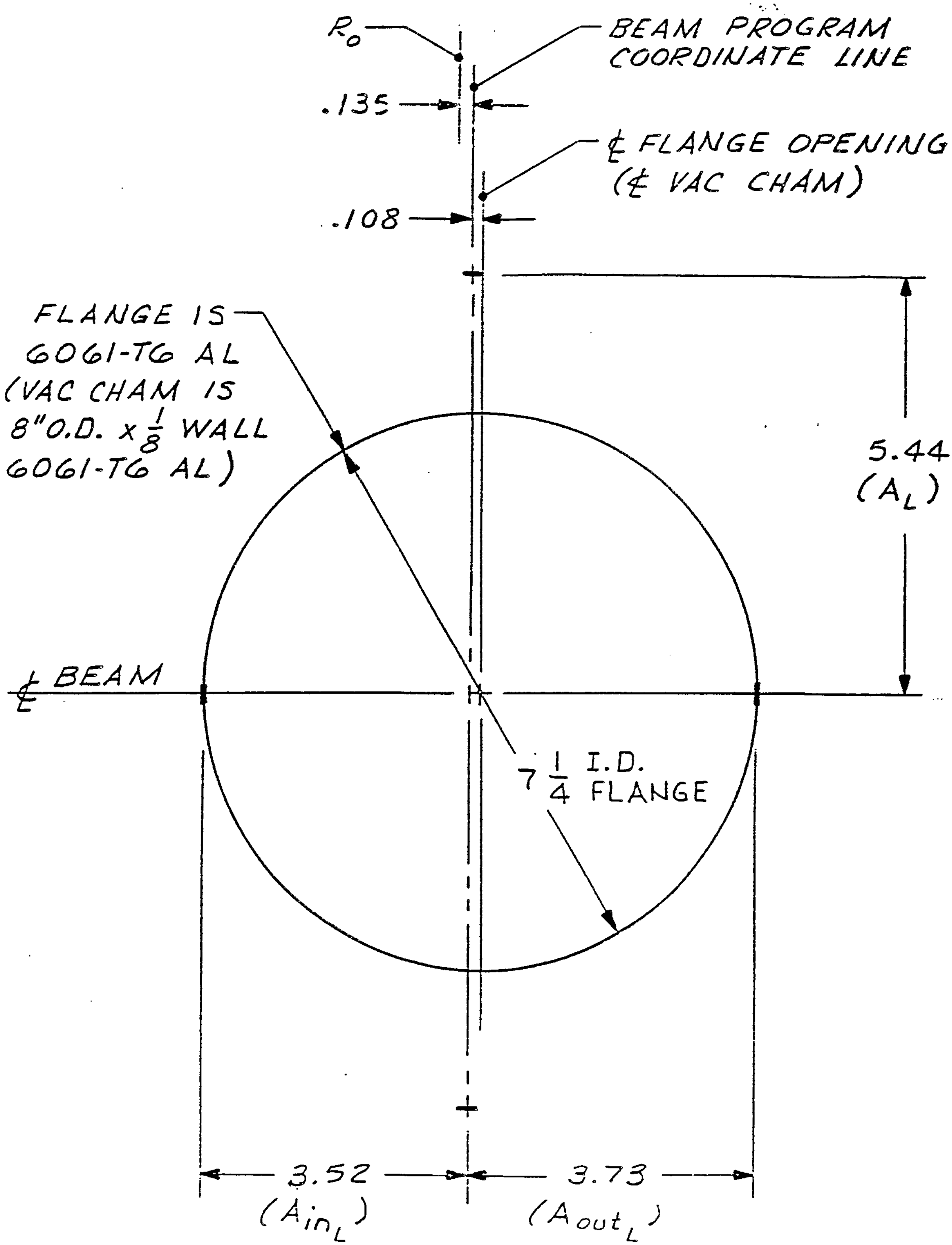

L5

REF DWG: D05-M-1701

VIEW LOOKING DOWNSTREAM

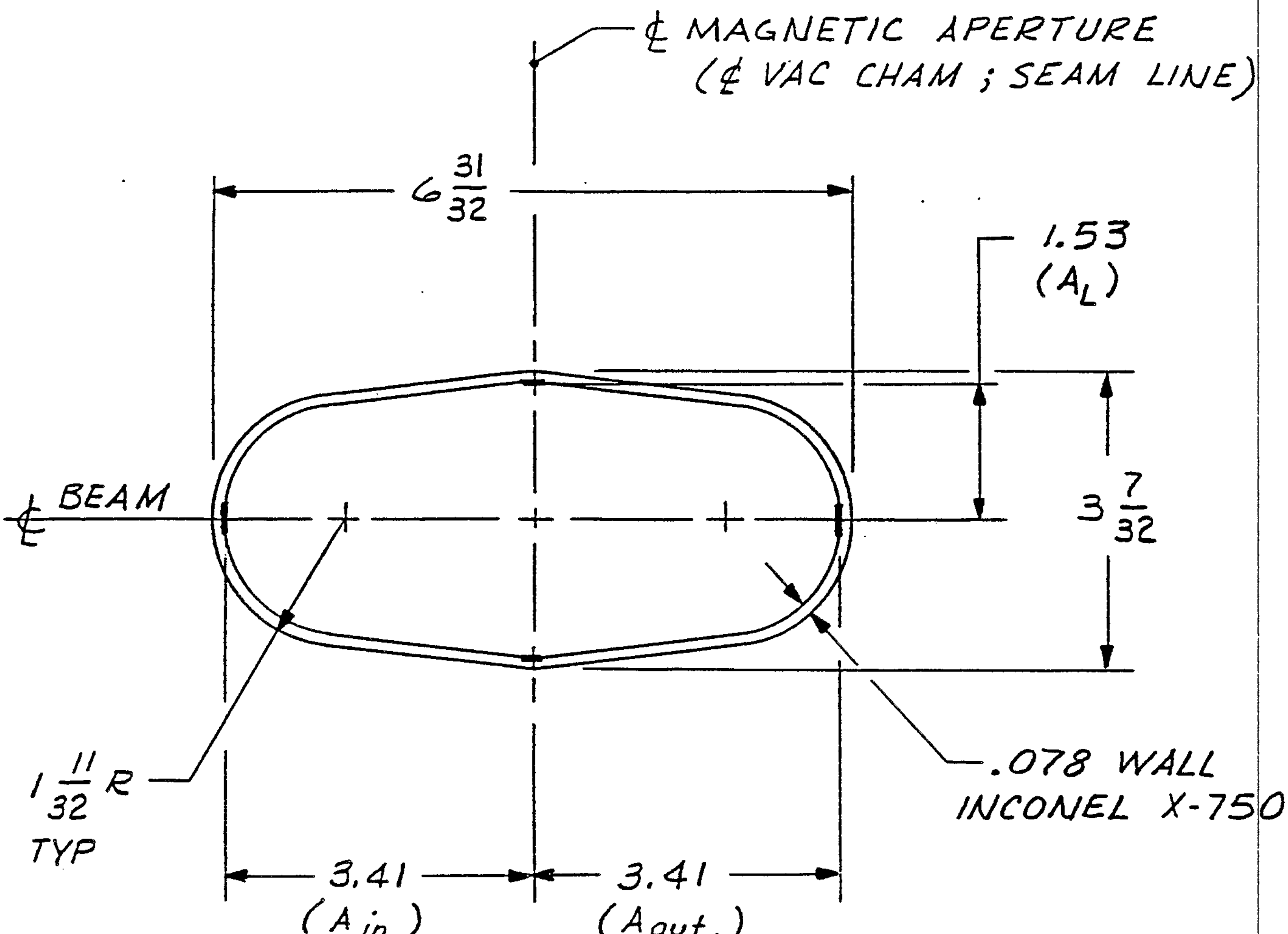

MAIN MAGNET VACUUM CHAMBER
TYPICAL SECTION

REF DWGS: D05-M-472-6